

REMARKS

Applicants wish to thank the Examiner for his careful review of this application. Please reconsider the present application in view of the above amendments and the following remarks.

Status of the claims

Claims 1 – 24 were previously canceled. Claims 25 – 44 are currently pending. Claims 26, 28, 31, 35, 36, 39, 40, 43, and 44 are withdrawn as they are directed to non-elected invention. Accordingly, claims 25, 27, 29, 30, 32 – 34, 37, 38, 41, and 42 are currently under examination. Claims 25 and 27 are independent. The remaining claims depend, directly or indirectly, from the two independent claims.

Sequence rule and objection to the specification

The Examiner objects to Table 1 on page 8 of the specification where the protein sequences listed in the table are absent sequence identifiers. Accordingly, Applicants have amended the specification to comply with sequence rules. Withdrawal of this objection is respectfully requested.

Objections to the claims

The Examiner objected to claims 25 and 27 as encompassing non-elected inventions. In response, Applicants have amended both claims to recite only elected invention.

The Examiner also objected to claim 32 as being duplicative of claim 30. In response, Applicants have canceled claim 32.

The Examiner further objected to claims 41 and 42 as being of improper dependent form. The Examiner suggested that the claims may be amended in product-by-process language. Accordingly, Applicants have amended the claims to conform to product-by-process claiming language.

Finally, Applicants have also corrected the minor typographical error in claim 37.

In view of the above, withdrawal of all outstanding objections is respectfully requested.

Claim rejections under 35 U.S.C. §101 and §112 1st paragraph

Claims 25, 27, 29, 30, 32 – 34, 37, 38, 41 and 42 stand rejected under 35 U.S.C. §101 as being unsupported by either a specific and substantial asserted utility or a well established utility. Specifically, the Examiner asserts that novel biological molecules lack an established utility and must undergo extensive experimentation to determine an appropriate specific and substantial utility. The Examiner also rejected the claims under 35 U.S.C. §112 1st paragraph as lacking enablement. Applicants will traverse these two rejections in turn below.

1. Utility rejections

With regard to independent claim 25, the claim, as amended, is directed to an isolated polypeptide comprising the sequence of SEQ ID NO: 1 or 21, which correspond to the hHSS1 polypeptide in full-length immature or mature form. The Examiner alleges that the specification does not teach any physiological ligands or functional characteristics of the hHSS1 polypeptide or the nucleic acid molecule (SEQ ID NO:5) encoding it. Applicants respectfully disagree.

Applicants respectfully call the Examiner's attention to Figure 8 in which a plot of the results from a colony forming cell (CFC) assay using hematopoietic progenitor/stem cells granulocyte, erythroid, macrophage, megakaryocyte (GEMM). In this figure, it can be seen that the addition of HSS1 can increase the number of multipotent, primitive hematopoietic GEMM colonies in a dose dependent fashion. Referring further to the Examples, the HSS1 gene was discovered by virtue of it being highly expressed, as compared to other genes, in a primitive and highly purified population of hematopoietic stem cells, further highlighting the specific effect of HSS1 to hematopoietic stem cells.

Hematopoietic stem cells are well-characterized tissue-specific stem cells that exhibit remarkable self-renewal capacity and are responsible for the life-long maintenance of the hematopoietic system. Given their hematopoietic reconstitution potency, the clinical applications for hematopoietic stem cells are enormous. However, these stem cells are rather rare. Thus, the fact that HSS1 can affect the growth of hematopoietic GEMM is of great utility in a real world context. Given the data shown in Figure 8 and the associated descriptive text in the specification, this utility will be apparent to anyone of ordinary skill in the art.

Moreover, several known association of the HSS1 gene with cancer also lends the sequences excellent diagnostic utility. For example, Figure 1 shows that the genomic location of the human HSS1 gene is at chromosome 19, locus 19q13.33. It is known in the art that tumor cells such as neuroblastomas and gliomas have common genomic deletions in the 19q13 chromosomal region (see Exhibits 1 – 4). Therefore, HSS1 gene sequences are genetic markers for at least gliomas and neuroblastomas.

In view of the foregoing, Applicants respectfully submit that the invention as recited in claim 25 has met the utility requirement of 35 U.S.C. §101. Accordingly, withdrawal of this rejection is respectfully requested.

2. Enablement rejections

Claim 25 is further rejected under 35 U.S.C. §112 1st paragraph for lacking enablement. The Examiner asserts that absent any further guidance in the specification one of ordinary skill in the art at the time of the invention would not be able to predict the outcome of any particular insertion, deletion, or replacement in a novel protein. Therefore, the specification cannot enable one of ordinary skill in the art to make and use the invention as claimed.

Applicants submit that this rejection is now moot in view of the amended claim 25, which does not recite any insertion, deletion, or replacement of amino acids/nucleotides. The amended claim now only recites the sequences specifically disclosed in the specification, which are fully enabled by the specification.

Accordingly, withdrawal of this rejection is requested.

With regard to independent claim 27, the claim has also been similar amended in this Reply and is similarly traversed as above.

With regard to dependent claim 29, the Examiner alleges that the claim was drawn to a pharmaceutical composition but the specification does not provide any teaching or guidance as to how to treat or prevent any disease or conditions by administering the pharmaceutical composition. To overcome this rejection, the Examiner suggests amending the claim to recite a "composition" as opposed to a "pharmaceutical composition".

Applicants have amended the claim as suggested by the Examiner. Accordingly, withdrawal of this rejection is requested.

To the extent that these foregoing rejections are applicable to dependent claims 30, 32, 34, 37, 38, 41, and 42, they are similarly traversed as above.

Claim rejection under 35 U.S.C. §112 1st paragraph (Written Description)

Claims 25, 27, 29, 30, 32 – 34, 37, 38, 41 and 42 stand rejected under 35 U.S.C. §112 1st paragraph as containing subject matter which was not described in the specification in such a way as to reasonably convey to one skilled in the relevant art that the inventor(s), at the time the application was filed, had possession of the claimed invention.

Specifically, the Examiner asserts that these claims are drawn broadly to a genus of isolated mammalian polypeptide comprising the sequence of SEQ ID NO:1 or SEQ ID NO:21 and variants thereof without providing adequate written description and evidence of possession of a claimed genus.

In response, Applicants have narrowed the claims to those species specifically disclosed in the specification (i.e. SEQ ID NO: 1, 21, and 5). Therefore, this rejection is now moot.

Accordingly, withdrawal of this rejection is respectfully requested.

Claim rejections under 35 U.S.C. §112 2nd paragraph

Claims 41 and 42 stand rejected under 35 U.S.C. §112 2nd paragraph as being indefinite for failing to particularly point out and distinctly claim the subject matter which applicant regards as the invention. In particular, the Examiner asserts that

the “nucleic acid sequence corresponding to the peptide” limitation in claim 41 and the “expressed polypeptide” limitation do not have sufficient antecedent basis.

Applicants note that claims 41 and 42 have been amended in this Reply which renders this rejection moot. Accordingly, withdrawal of this rejection is respectfully requested.

Claim rejection under 35 U.S.C. §102

Claim 25, 27, 29 – 30, 32 – 34, 41, and 42 are rejected under 35 U.S.C. 102(e) as being anticipated by Baker et al. (US 2003/0073129 A1). Specifically, the Examiner cites PRO1556 (SEQ ID NO: 372) disclosed in Baker *et al.* as anticipating SEQ ID NO:1 of the present invention. The Examiner alleges that because the two sequences share ~ 90% identical sequences, therefore, PRO1556 is considered to anticipate the polypeptide of SEQ ID NO:1. Applicants respectfully disagree.

It is well known in the art that the properties and characteristics of a polypeptide (or protein) is not defined by the 2D sequence, but rather, by the 3D shape that the polypeptide (or protein) folds into. Furthermore, prediction of 3D structure from 2D sequence is still an unpredictable art, hence, similarity at the sequence level is no guarantee of identify, or even similarity at the 3D level. In this case, the specification teaches that SEQ ID NO:1, which corresponds to hHSS1 (see page 2, line 17 and page 10, lines 1 – 6), is a secreted soluble polypeptide. In contrast, Baker *et al.* clearly teaches that PRO1556 (SEQ ID NO:372) is a transmembrane protein (paragraph [0258] – [0259]). Thus, despite the sequence similarity, the two polypeptides are actually chemically, functionally, and structurally distinct from each other. In other words, they are not the same.

Appl. No. 10/541,086
Amdt. Dated April 24, 2008
Reply to Office Action of January 24, 2008

Attorney Docket No. 89188.0115
Customer No.: 26021

In view of the foregoing, claims 25, 27, 29 – 30, 32 – 34, 41, and 42 are all patentable over Baker *et al.* Accordingly, withdrawal of this rejection is respectfully requested.

Conclusion

In view of the foregoing, it is respectfully submitted that the application is in condition for allowance. Reexamination and reconsideration of the application, as amended, are requested.

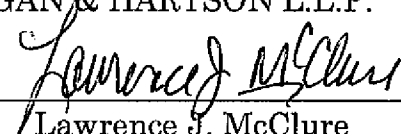
If for any reason the Examiner finds the application other than in condition for allowance, the Examiner is requested to call the undersigned attorney at the Los Angeles, California telephone number (310) 785-4600 to discuss the steps necessary for placing the application in condition for allowance.

If there are any fees due in connection with the filing of this response, please charge the fees to our Deposit Account No. 50-1314.

Respectfully submitted,
HOGAN & HARTSON L.L.P.

Date: April 24, 2008

By: _____


Lawrence J. McClure
Registration No. 44,228
Attorney for Applicant(s)

1999 Avenue of the Stars, Suite 1400
Los Angeles, California 90067
Phone: 310-785-4600
Fax: 310-785-4601

EXHIBIT 1

Lead article

Molecular cytogenetic analysis of chromosomes 1 and 19 in glioma cell lines

Mark E. Law^a, Kristen L. Templeton^a, Gaspar Kitange^a, Justin Smith^b, Anjan Misra^c,
Burt G. Feuerstein^c, Robert B. Jenkins^{a,*}^aDepartment of Laboratory Medicine and Pathology, Division of Laboratory Genetics, Mayo Clinic and Foundation,
200 First Street SW, Rochester, MN 55905^bDepartment of Neurosurgery, ^cDepartment of Laboratory Medicine, University of California, San Francisco, CA

Received 12 October 2004; received in revised form 16 November 2004; accepted 19 November 2004

Abstract

Deletions of chromosome 1p and 19q arms are frequent genetic abnormalities in primary human gliomas and are especially common in oligodendrogliomas. However, the chromosome 1p and 19q status of many glioma cell lines has not been established. Using homozygosity mapping, fluorescence in situ hybridization (FISH), and comparative genomic hybridization to arrayed BAC (CGHa), we screened 17 glioma cell lines for chromosome 1 and 19 deletions. Sequence tagged site polymorphisms were used to evaluate the cell lines for regions of chromosome 1p and 19q homozygosity. Cell lines A172, U251, TP265, U118, SW1088, U87, SW1783, and D32 contained significant regions of 19q homozygosity. In addition, A172, U87, TP483, D37, U118, MO67, and TP265 contained significant regions of 1p homozygosity. FISH probes localized to 1p36.32 and 19q13.33 as well as CGHa were used to determine which cell lines had deletions of 1p and/or 19q. Cell lines A172, U87, TP483, TP265, H4, U251, and D37 were deleted for portions of 1p. CGHa and homozygosity mapping of these cell lines define a 700-kilobase (Kb) common deletion region that is encompassed by a larger deletion region previously mapped in sporadic gliomas. This common deletion region is localized at 1p36.31 and includes *CHD5*, a putative tumor suppressor gene. Cell line A172 was observed to have a deletion between 19q13.33 and 19q13.41, while U87 was observed to have a smaller deletion of 19q13.33. Cell lines A172 and U87 contain 1p and 19q deletions similar to those found in sporadic gliomas and will be useful cellular reagents for evaluating the function of putative 1p and 19q glioma tumor suppressor genes. © 2005 Elsevier Inc. All rights reserved.

1. Introduction

Chromosome 1p and 19q arm deletions are frequent genetic abnormalities in primary gliomas, especially oligodendrogliomas. While 1p deletions are relatively common in other types of tumors, 19q deletions appear to be common only in gliomas [1]. Oligodendrogliomas with deletion of chromosome arms 1p and/or 19q have been reported to have a better survival and response to radiation therapy and chemotherapy [2–4]. Minimal deletion regions on 1p and 19q have been mapped recently using primary glioma specimens [5,6]. A comprehensive analysis of 1p and 19q alterations, however, had not been performed on the existing glioma cell lines.

The observation that 1p and 19q deletions are frequent in gliomas suggests that these two chromosomes may harbor genes responsible for the suppression of these tumors. Despite the ongoing effort in positional cloning, no credible candidate gene has yet been discovered. Thus, mapping 1p and 19q deletions in glioma cell lines may be a necessary step toward isolating these putative tumor suppressor genes. For example, the cloning of *CDKN2A* (and its relatives) and *PTEN* was facilitated by finding cell lines with loss of these specific regions, adding chromosomal material, and mapping revertants [7,8]. In addition, cell lines with deletions may be useful cellular reagents for functional studies of putative tumor suppressor genes.

We used several approaches to identify chromosome 1p and 19q alterations in glioma cell lines, including loss of heterozygosity (LOH), also referred to herein as homozygosity mapping [9], multicolor fluorescence in situ hybridization

* Corresponding author. Tel.: (507) 284-9617; fax: (507) 284-0043.
E-mail address: rjenkins@mayo.edu (R.B. Jenkins).

(M-FISH) [10], locus-specific fluorescence in situ hybridization (FISH) [11], and comparative genomic hybridization to arrayed BAC (CGHa) [12].

2. Materials and methods

2.1. Cell culture

Glioma cell lines A172, CCF, D23, D37, H4, Hs683, MO67, SW1088, SW1783, T98G, TP265, TP365, TP483, U87, U118, U251, and U373 (obtained from C. David James, Mayo Clinic, Rochester, MN) were cultured and harvested according to standard cytogenetic techniques [13]. Cells were seeded into a T75 flask and cultured in Dulbecco's modified Eagle medium supplemented with 10% fetal bovine serum (FBS)/1% penicillin-amphotericin B solution (Sigma Chemical Co., St. Louis) and incubated at 37°C in a humidified incubator with 5% O₂/5% CO₂ air. Cells were grown until they were approximately 70% confluent. Colcemid (Sigma) was added and the culture was incubated for 2–4 hours. Cells were then trypsinized with 0.5% trypsin/0.5% EDTA (Irvine Scientific, Santa Anna, CA), collected, and centrifuged at 500× *g* for 8 minutes. Then cells were resuspended in 10 mL of hypotonic solution (0.03 mol/L KCl/0.5% sodium citrate). After incubation at room temperature for 20 minutes, 5 mL of Carnoy's fixative (methanol/acetic acid 3:1) was added. Cells were again centrifuged and resuspended with 10 mL of Carnoy's fixative. This step was repeated twice using fresh fixative.

2.2. Mapping of homozygosity

LOH analysis was performed on each cell line according to a method described by Weber and May [14] using 26 STS markers on chromosome 1p, 2 STS markers on chromosome 1q, 4 STS markers on chromosome 19p, and 26 STS markers on chromosome 19q. Cell line polymerase chain reaction (PCR) amplicons were internally labeled with [α^{32} P]dCTP (New England Nuclear, Boston), electrophoresed on 6% denaturing polyacrylamide gels, and subjected to autoradiography. Homozygosity status was determined by visual inspection of the film. If there was any evidence of a second allele, the STS was scored as heterozygous.

2.3. FISH and M-FISH

Fixed cells were centrifuged and fresh fixative was added to obtain the desired cell concentrations for FISH analysis. Cell suspensions were then dropped on clean, dry slides in a CDS-5 cytogenetic drying chamber (Thermotron, Holland, MI), which was set at 25°C and 50–60% humidity [15]. The slides were then artificially aged in a 90°C convection oven for 10 minutes. After cooling down to room temperature, the slides were pretreated and denatured in a VP 2000 (Vysis, Downers Grove, IL) using the following protocol: 0.005% pepsin/0.01 N HCl at 37°C for 30–60 seconds, 100% ethanol

(EtOH) for 1 minute, 2× standard saline citrate (SSC; 1.75% NaCl, 0.88% sodium citrate, pH 7.0) at 37°C for 1 hour, then dehydrated in an EtOH series (70, 85, 100%) for 1 minute in each solution and finally in 100% EtOH for 10 minutes. Slides were dried for 5 minutes, denatured in 70% formamide/2× SSC, pH 7–7.5 at 70°C for 1 minute, EtOH series for 1 minute each solution, and then jet air-dried. Locus-specific FISH probes were made from BAC clones that were grown in antibiotic/LB media according to the manufacturers' instructions (BAC PAC Resources, Oakland, CA; Invitrogen, Carlsbad, CA). BAC DNA was extracted using the Qiagen (Valencia, CA) plasmid extraction kit and labeled using the Vysis nick translation kit. Locus-specific FISH probes for 1p and 19q were labeled with Alexa 594 dUTP (Molecular Probes, Eugene, OR) while control FISH probes were labeled with SpectrumGreen dUTP (Vysis). FISH probe hybridization solution was prepared by mixing 1- μ L of 1p or 19q locus-specific probes, 2 μ L of 1q or 19p control probes, and 7 μ L of LSI/WCP hybridization buffer (Vysis). The M-FISH probe was used straight from a ready-made solution supplied by the vendor (Vysis). Probe solutions and/or M-FISH reagents were pipetted into 200- μ L PCR reaction tube(s) and denatured in a thermocycler at 70°C for 5 minutes. The denatured probe solution was placed on the previously denatured slides, covered with glass coverslips, sealed with rubber cement, and hybridized in a humidified chamber at 37°C for at least 12 hours. After removal of the coverslips, slides were washed in 0.4× SSC at 70°C for 2 minutes, briefly rinsed in 2× SSC/0.1% NP-40 at room temperature, jet air-dried, counterstained with DAPI (100 ng 4',6'-diamidino-2-phenylindole dihydrochloride per milliliter of Vectashield antifade), and covered with glass coverslips. FISH probe signals were viewed under a fluorescent microscope equipped with a 100-watt mercury lamp and a triple-bandpass filter for DAPI, fluoroisothiocyanate (FITC), and Texas red (Chromatechnology, Battleboro, VT). Metaphase spreads (20–50) were analyzed, and the most common copy number for each probe (1p, 1q, 19p, and 19q) was recorded for each glioma cell line. Chromosomes were counted to ascertain the modal chromosome number. Cells hybridized with M-FISH reagent were viewed with a fluorescent microscope equipped with a 100-watt mercury lamp and filters for Cy5.5, Texas red, SpectrumGold, FITC, SpectrumAqua, and DAPI (Vysis). Up to five metaphase spreads were imaged and analyzed for each cell line, as described by Jalal and Law [10].

2.4. CGHa

Human BAC clones were isolated and ligation-based PCR-amplified to make the print target for array fabrication [16]. Capillary quartz print heads measuring 10 μ m in diameter were used to print the arrays in triplicate onto chromium-coated glass slides. The DNA target diameters varied from 50 to 150 μ m. The average genomic resolution of the array was less than 2 megabases (Mb). Water and normal human DNA

were used as controls. Some targets were printed in different positions of the same array as internal controls for positional effects of BAC DNA in an array. Cell line DNA and sex-matched reference DNA (normal leukocyte DNA from male or female) were labeled with Cy3 and Cy5 (Amersham Pharmacia Biotech, Piscataway, NJ), respectively, by random priming [17]. Repetitive DNA sequences were blocked with human cot-1 DNA (Invitrogen). Probes from both normal and cell line DNA were mixed and hybridized to the arrays in 2× SSC and 50% formamide with 15% dextran sulfate, pH 7.0, on a gently rocking platform for 16–40 hours [18]. Slides were washed once at 45°C for 15 minutes in 50% formamide in 2× SSC, pH 7.0, and once at room temperature for 10 minutes in 0.1 mol/L Na₂HPO₄ with 0.1% NP-40, pH 8.0, mounted with DAPI in 90% glycerol. A 16-bit charged couple device 4.0-megapixel camera was used to acquire images at 12.5-μm resolutions using a mercury arc lamp and a set of excitation and emission filters specific for DAPI, Cy3, and Cy5 [16,18]. The exposure times were typically 4–6 seconds for DAPI, 60–80 seconds for Cy3, and 120–200 seconds for Cy5. The ‘Spot’ program [19] was used to convert the array images into digital intensity values. The program fits grids of known row and column numbers over images of arrayed BAC DNA to fit each spot within one cell of the grid. It determines the center and boundary of each spot, the intensity of Cy3, Cy5, and DAPI in each pixel within the spot, as well as background intensities at pixels outside spot boundaries. Data were acceptable if background-subtracted intensity values were greater than 100 for normal (Cy5) intensity and if the correlation coefficient of (Cy3/Cy5) intensity ratios among pixels within a spot were more than 0.9. About 90–95% of spots on an array typically met these criteria. Data were normalized by dividing the raw intensity ratio (Cy3/Cy5) values by the median intensity ratio for each hybridization. In 95% or more cases, the median was close ($\pm 5\%$) to the average intensity ratio.

2.5. FISH mapping of breakpoints

Cell lines with deletions or rearrangements near the 19q critical deletion region were subjected to additional FISH tests to approximate the breakpoints within a 100-Kb range. Using the Lawrence Livermore map of chromosome 19 (Lawrence Livermore National Laboratory Cosmid/BAC Tiling Path http://www.bahama_jgi-psf.org/publicch19/html/ch19_map3.html), clones proximal and distal to the breakpoints were selected and locus-specific FISH was performed until the breakpoints were found.

3. Results

3.1. Chromosome regions 1p and 19q LOH analysis in glioma cell lines

Glioma cell lines were screened for loss of chromosome regions 1p and 19q using LOH analysis by homozygosity

mapping (Figs. 1 and 2). Sequence tagged site (STS) markers were scored by visually assessing whether there was one or two alleles present based on the polymorphic PCR amplicons. When six or more contiguous loci were homozygous, we considered the cell line to have a significant region of homozygosity. The probability of six contiguous loci to be homozygous by chance alone was less than 0.05 for the chosen 1p and 19q markers (data not shown). The homozygosity mapping results for chromosome 19 (Fig. 1) demonstrate that cell lines U118, TP265, and D32 are homozygous for all chromosome 19 markers. Significant contiguous regions of 19q homozygosity were observed in A172, SW1088, SW1783, U87, and U251 cell lines. These regions of homozygosity overlapped the minimal region of deletion on chromosome 19 that had been previously mapped in primary gliomas by Smith et al. [5,6]. Cell lines U118, A172, TP265, MO67, D37, TP483, and U87 also had significant contiguous regions of homozygosity of chromosome region 1p (Fig. 2), and these deletions overlapped a previously mapped minimal region of deletion found in sporadic gliomas [5].

3.2. Screening for 1p and 19q deletion using locus-specific FISH

The cell lines were primarily screened for 1p and 19q deletions using FISH probes for 1p36.32 (*P73*) with a control probe at 1q25.2 and 19q13.33 (*EHD2*) with a control probe at 19p13.2. These probes are contained within the minimal 1p and 19q deletion regions previously mapped in sporadic gliomas [5,6]. As shown in Table 1, cell lines A172 and U87 mimic the haploinsufficiency (1p and 19q/modal chromosome number ratios 0.56 and 0.51, respectively) commonly found in oligodendrogliomas with 1p and 19q deletions. Locus-specific FISH results revealed that A172 was hypertriploid (82 chromosomes) and had two copies of the *P73* probe, six copies of the 1q25.2 probe, four copies of 19p13.2, and two copies of the *EHD2* probe. Cell line U87 was near diploid (45 chromosomes) and had one copy of *P73*, two copies of 1q25.2, two copies of 19p13.2, and one copy of *EHD2*.

Two cell lines, TP483 and D37, had a low chromosome dosage of *P73* (0.39 and 0.62, respectively) and corresponding contiguous runs of homozygosity (Fig. 2). Cell line TP483 was hyperpentaploid (120 chromosomes) and had six copies of 1q25.2 and two copies of *P73*, while D37 was hypertriploid (75 chromosomes) and had three copies of 1q25.2 and two copies of *P73*. Cell line U251 was hyperdiploid (56 chromosomes) and had two copies of *P73* and three copies of 1q25.2.

Cell lines Hs683 and TP365 were hypertriploid (78 and 79 chromosomes, respectively) and had three normal chromosomes 19 and one chromosome 19 with a 19q deletion (by FISH) overlapping the minimal deletion region. Neither cell line, however, had a contiguous region of homozygosity in the deleted region (Fig. 1).

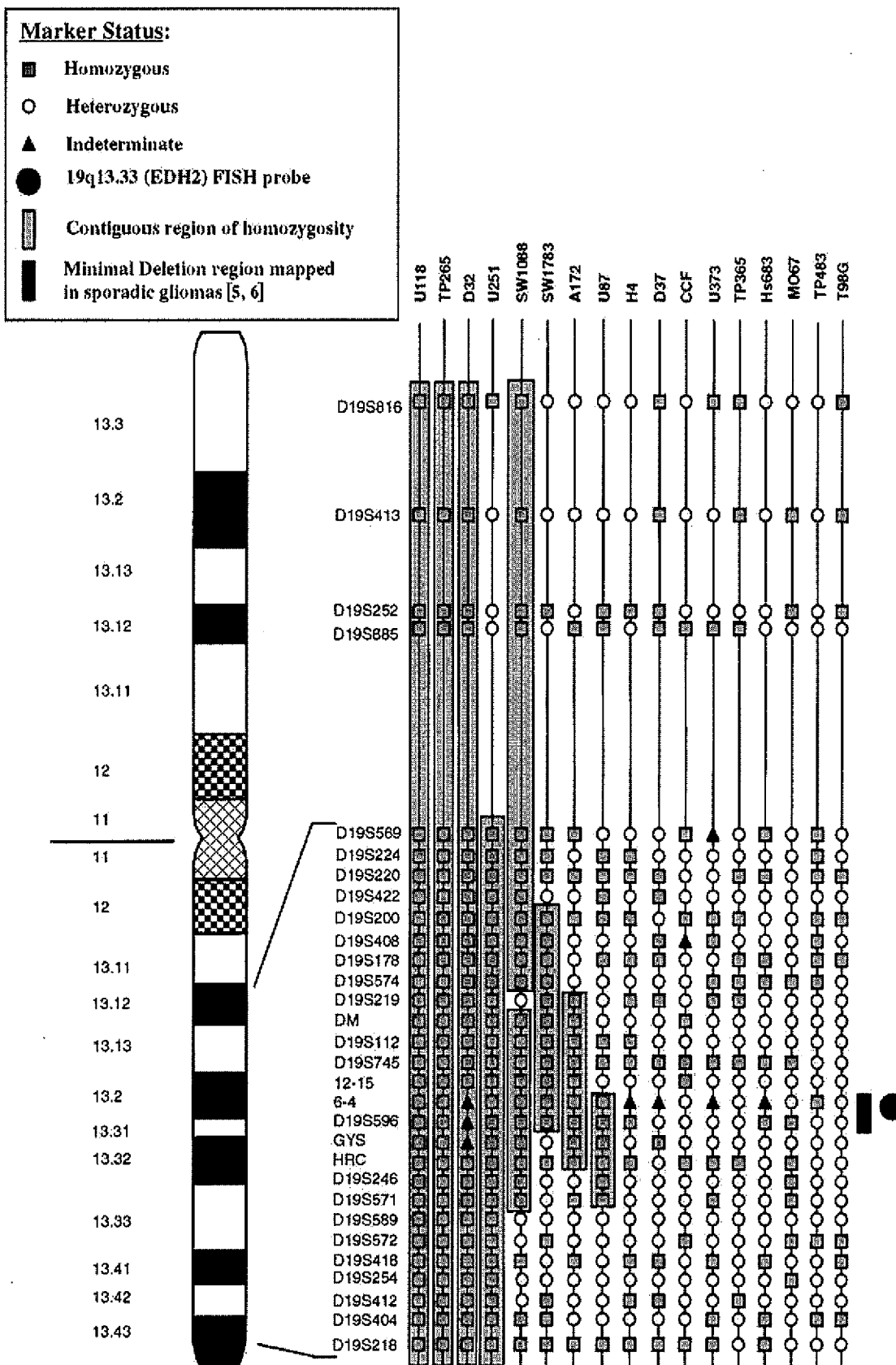


Fig. 1. Chromosome 19 LOH analysis by homozygosity mapping of glioma cell lines. LOH was performed using STS markers as described in Materials and methods. Shaded areas indicate contiguous regions of homozygosity.

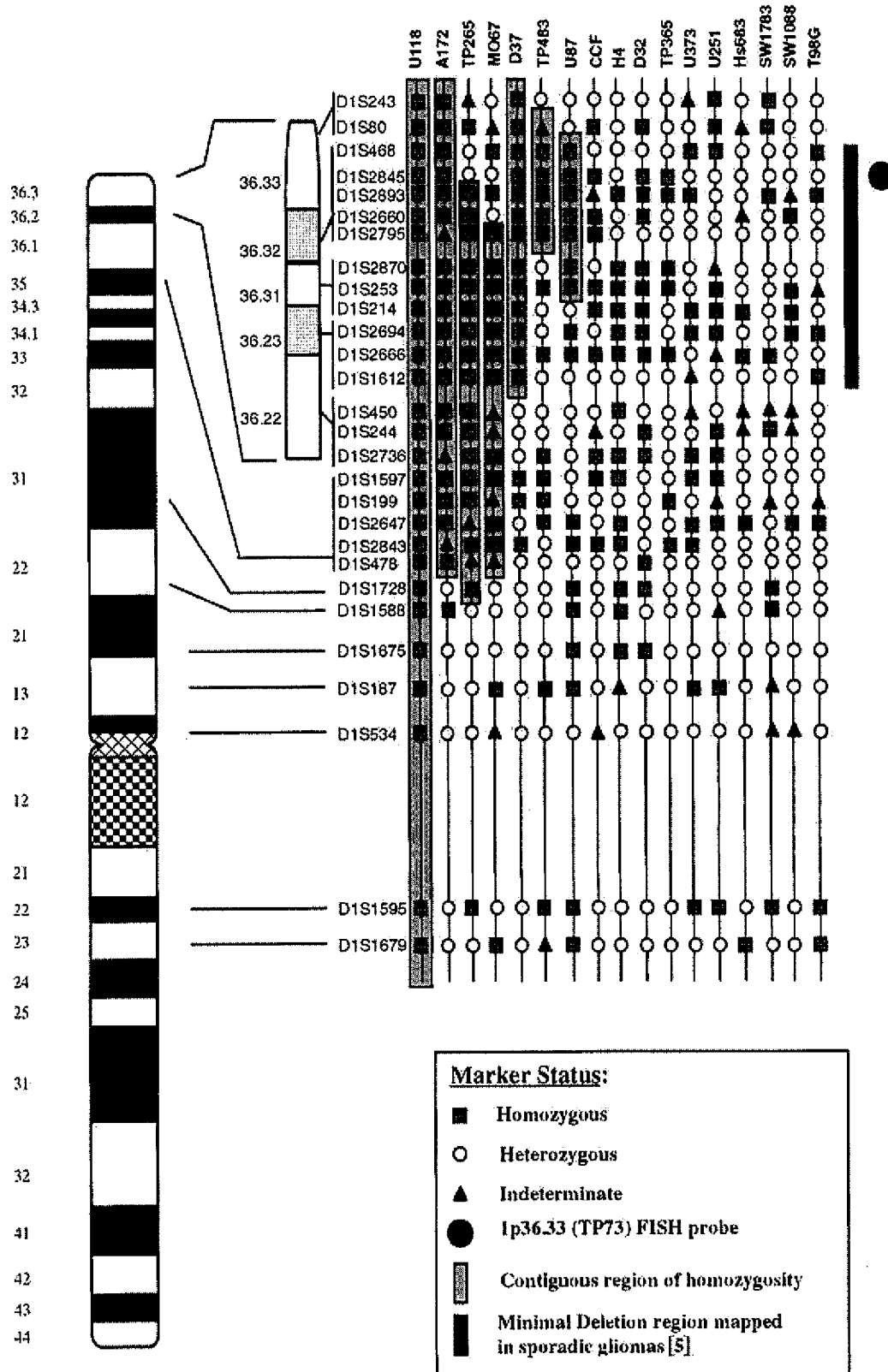


Fig. 2. Chromosome 1 LOH analysis by homozygosity mapping of glioma cell lines. LOH was performed using STS markers as described in Materials and methods. Shaded areas indicate contiguous regions of homozygosity. Chromosome region 1p36.22–p36.33 is enlarged to more accurately depict polymorphic markers used from that region.

Table 1

Summary of LOH mapping, FISH, and CGHa analysis of various glioma cell lines

| Cell line | Homozygosity ^a | | | | FISH results ^b | | | | | CGHa ^c | |
|-----------|---------------------------|-------|-------|-----|---------------------------|------------------|-----------------|----------------|----------------|-------------------|---------|
| | 19p | 19q | 1p | 1q | Modal chr no. | 19q13.33/19p13.2 | 19q13.33 dosage | 1p36.32/1q25.2 | 1p36.32 dosage | 19q13.33 | 1p36.32 |
| A172 | 1/4 | 15/26 | 19/23 | 0/2 | 82 | 2/4 | 0.56 | 2/6 | 0.56 | -0.35 | -0.45 |
| U87 | 2/4 | 14/26 | 15/26 | 2/2 | 45 | 1/2 | 0.51 | 1/2 | 0.51 | -0.39 | ND |
| TP483 | 0/4 | 6/26 | 12/25 | 1/1 | 120 | 6/6 | 1.15 | 2/6 | 0.39 | 0.27 | -0.89 |
| D37 | 4/4 | 10/25 | 16/26 | 0/2 | 75 | 3/2 | 0.94 | 2/3 | 0.62 | 0.06 | -0.54 |
| U251 | 1/4 | 26/26 | 10/22 | 1/2 | 56 | 3/3 | 1.23 | 2/3 | 0.82 | 0.07 | -0.37 |
| U118 | 4/4 | 26/26 | 26/26 | 2/2 | 82 | 4/5 | 1.11 | 5/3 | 1.39 | 0.23 | 0.28 |
| TP265 | 4/4 | 26/26 | 17/23 | 1/2 | 72 | 4/4 | 1.28 | 4/5 | 1.28 | 0.28 | 0.35 |
| D32 | 4/4 | 23/23 | 14/26 | 0/2 | 63 | 3/3 | 1.10 | 3/3 | 1.10 | 0.46 | 0.21 |
| SW1088 | 4/4 | 20/26 | 5/22 | 0/2 | 67 | 2/2 | 0.69 | 3/2 | 1.05 | -0.06 | 0.06 |
| SW1783 | 1/4 | 19/26 | 7/23 | 1/2 | 125 | 7/7 | 1.29 | 6/5 | 0.91 | ND | ND |
| MO67 | 2/4 | 8/26 | 14/20 | 1/2 | 114 | 6/6 | 1.20 | 6/4 | 1.20 | -0.03 | 0.33 |
| CCF | 1/4 | 8/25 | 10/23 | 0/2 | 83 | 4/4 | 1.11 | 4/4 | 1.11 | 0.02 | -0.06 |
| H4 | 1/4 | 12/25 | 14/25 | 0/2 | 72 | 4/3 | 1.28 | 4/4 | 1.28 | 0.33 | 0.59 |
| Hs683 | 0/4 | 9/25 | 3/22 | 1/2 | 78 | 3/4 | 0.84 | 4/3 | 1.13 | 0.04 | 0.33 |
| T98G | 3/4 | 10/26 | 5/24 | 2/2 | 94 | 4/3 | 1.00 | 4/5 | 1.00 | -0.09 | -0.05 |
| TP365 | 3/4 | 8/26 | 7/26 | 0/2 | 79 | 3/4 | 0.85 | 4/4 | 1.13 | -0.09 | 0.19 |
| U373 | 2/4 | 10/24 | 9/23 | 1/2 | 67 | 3/3 | 1.00 | 3/3 | 1.00 | 0.11 | 0.11 |

Abbreviation: ND, not determined.

Cell lines are ordered from top to bottom according to their 19q FISH deletion status, 1p FISH deletion status, and size of contiguous region of homozygosity on 19q and 1p. Cell lines with bold letters contain 19q and/or 1p chromosomal deletions. Other bold lettering denotes significant regions of contiguous homozygosity or CGHa results.

^a Homozygosity was defined as the presence of only one polymorphism in a given STS and is expressed as the number of homozygous STS per number of STS tested. Regions of six or more contiguous homozygous STS were considered significant.

^b FISH probes were considered deleted when control probe (1q or 19p) outnumbered the experimental probe (1p or 19q) by at least a 2:1 ratio. Chromosome dosage was calculated by dividing the number of FISH probe signals by the modal chromosome number and multiplying by 23.

^c CGHa results are expressed as the ratio of the log 2 fluorescence intensity cell line DNA/log 2 fluorescence intensity of control DNA of the arrayed BACs (one each on 1p and 19q) closest to the mapped deletion regions. Negative numbers denote spots with ratios smaller than the median ratio of the sample.

3.3. Comparative genomic hybridization to arrayed BAC PCR products

Because we found cell lines with contiguous regions of homozygosity but no deletion by FISH, we used CGHa to screen for other possible 1p and 19q deletions not overlapping the previously mapped deletion regions. A detailed description of the complete genomic CGHa results will be described elsewhere (Misra A, Nigro J, Feuerstein B, Jenkins R., submitted). Fig. 3 illustrates the chromosome 19 CGHa results for several cell lines. Both A172 and U87 contained deletions centered at the 53-Mb position on the UCSC July 2003 freeze of the human genome (<http://www.genome.ucsc.edu/cgi-bin/hgGateway>). Both deletions encompass the 19q minimal deletion region, as confirmed by FISH (Table 1). The CGHa tracing of A172 also showed a small deletion telomeric to the first deletion region and a gain of 19q resulting from an unbalanced translocation with chromosome 10. Cell lines Hs683 (Fig. 3) and TP365 (data not shown) each had a supernumerary chromosome 19 with a loss of 19q that included 19q13.3 (19q13.13–qter and 19q13.32–qter, respectively). Cell line TP265 contained gain of chromosome 19 (Fig. 3).

CGHa indicated 19q13.3 deletions not including the *EHD2* probe that may be present in H4 and Hs683 (Fig. 3). CGHa also suggested that U251 contained a gain of 19q13.13–q13.31 (Fig. 3). Therefore, FISH was performed

on all 17 cell lines using the BAC clones RP11-133A7, RP11-18J23, CTD-2221F12, and CTC-301O7. These clones coincide with the apparent 19q changes in dosage detected by CGHa in cell lines H4, Hs683, and U251, and were 7 Mb proximal, 6 Mb proximal, 1 Mb distal, and 2 Mb distal, respectively, to the *EHD2* probe used to initially screen all the cell lines for deletion (see arrows in Fig. 3). We found no additional deletions in any of the cell lines when using these FISH probes but did find that cell lines TP265 and U251 had duplications of BAC clones RP11-133A7 and RP11-18J23 (19q13.2). Other chromosome 19q anomalies were seen by CGHa but were not confirmed by FISH. These include a gain of 19q12–q13.13 and deletion of 19p12–q12 in H4, a deletion of 19p12–q12 in U251 (Fig. 3), and a gain of 19q12 in D37 (data not shown).

CGHa detected 1p36.3 deletions in cell lines A172, TP483, D37, and U251 (Fig. 4). FISH analysis using the *P73* probe confirmed all four deletions (Table 1). Cell line H4 was observed to have three 1p deletions: 1p36.2, 1p13, and 1p22–p31. The latter deletion overlapped a second deletion in A172 (Fig. 4). Cell line TP265 was observed to have extra copies of chromosome 1 and two 1p deletions, 1p36.1–p36.3 and 1p22–p34.2 (data not shown). The *P73* probe was not deleted in H4 or TP265. To confirm these deletions, FISH was performed using a probe for 1p36.2 (*CAMTA1*). Cell lines H4, TP265, D37, and A172 showed

Chr. 19 CGHa of Selected Glioma Cell Lines

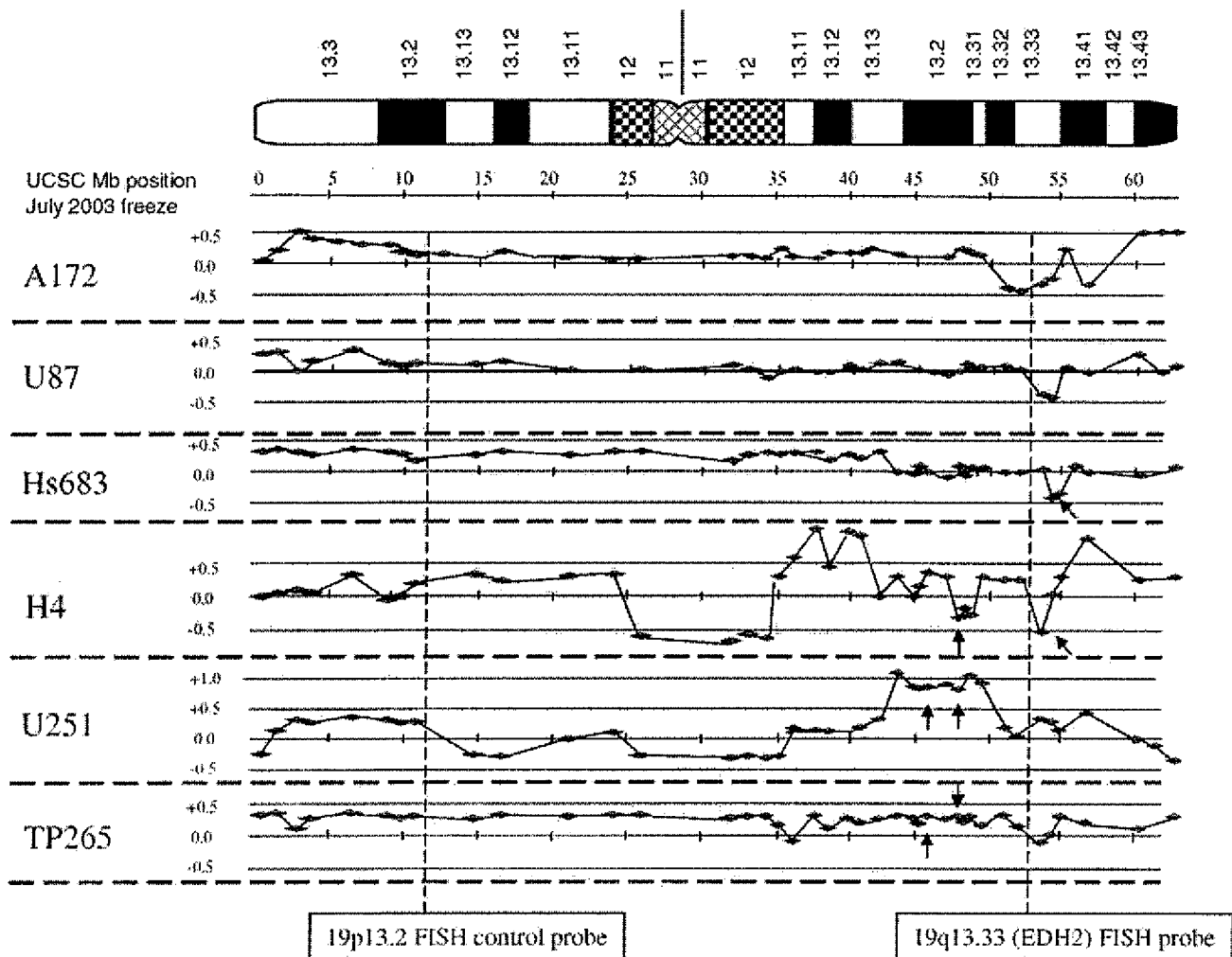


Fig. 3. Chromosome 19 CGHa of selected glioma cell lines. The CGHa tracing is scaled to the July 2003 freeze of the UCSC database (<http://www.genome.ucsc.edu/cgi-bin/hgGateway>). BAC used to confirm aberrations indicated by CGHa are denoted by arrows (see text).

deletion of *CAMTA1*. CGHa, in conjunction with homozygosity data, show a possible overlap of the 1p deletions contained in cell lines A172, TP483, D37, H4, U87, and TP265 (Fig. 5). This common deletion was confirmed in these cell lines using a FISH probe that mapped to position 5.7 Mb on the July 2003 freeze of the UCSC database (Fig. 5).

Single BAC deletions occurred at 1p36.1 and 1p21 in cell lines MO67, Hs683, CCF (data not shown), D37, and TP483 (Fig. 5). These deletions were not tested by FISH. Gains within the 1p arm were detected in cell lines MO67, U118, TP365, T98G, D37, and H4. CGHa indicated gain of the entire 1p arm in cell lines MO67 and U118, gain of 1p34.4~p36.3 in TP365 (data not shown), gain of 1p36.3~pter and 1p31~p34.3 in H4 (Fig. 4), gain of 1p22~p34.3 in T98G (data not shown), and gain of 1p34.1~p34.3 in D37 (Fig. 4). The gains involving 1p36.33 (P73) were confirmed by FISH (Table 1).

3.4. FISH mapping of chromosome 19 deletion breakpoints in cell lines A172 and U87

A comparison of chromosome 19 LOH, CGHa, and locus-specific FISH results for cell lines A172 and U87 is shown in Fig. 6. The results from FISH mapping the breakpoints in glioma cell lines A172 and U87 are summarized in Fig. 7. In A172, the two abnormal copies of chromosome 19 have two regions of deletion and a translocation with chromosome 10. The centromeric deletion is approximately 5 Mb and encompasses the previously described 19q minimal deletion region [5,6]. The proximal breakpoint is located near Mb 50.2 and the distal breakpoint is telomeric to Mb 55.1 in the July 2003 freeze of the UCSC database. The telomeric deletion is 4 Mb from the previously described minimal deletion region in gliomas [5,6], and the translocation involving chromosome 10 [20] is approximately 800 kb

Chr. 1 CGHa of selected Glioma Cell Lines

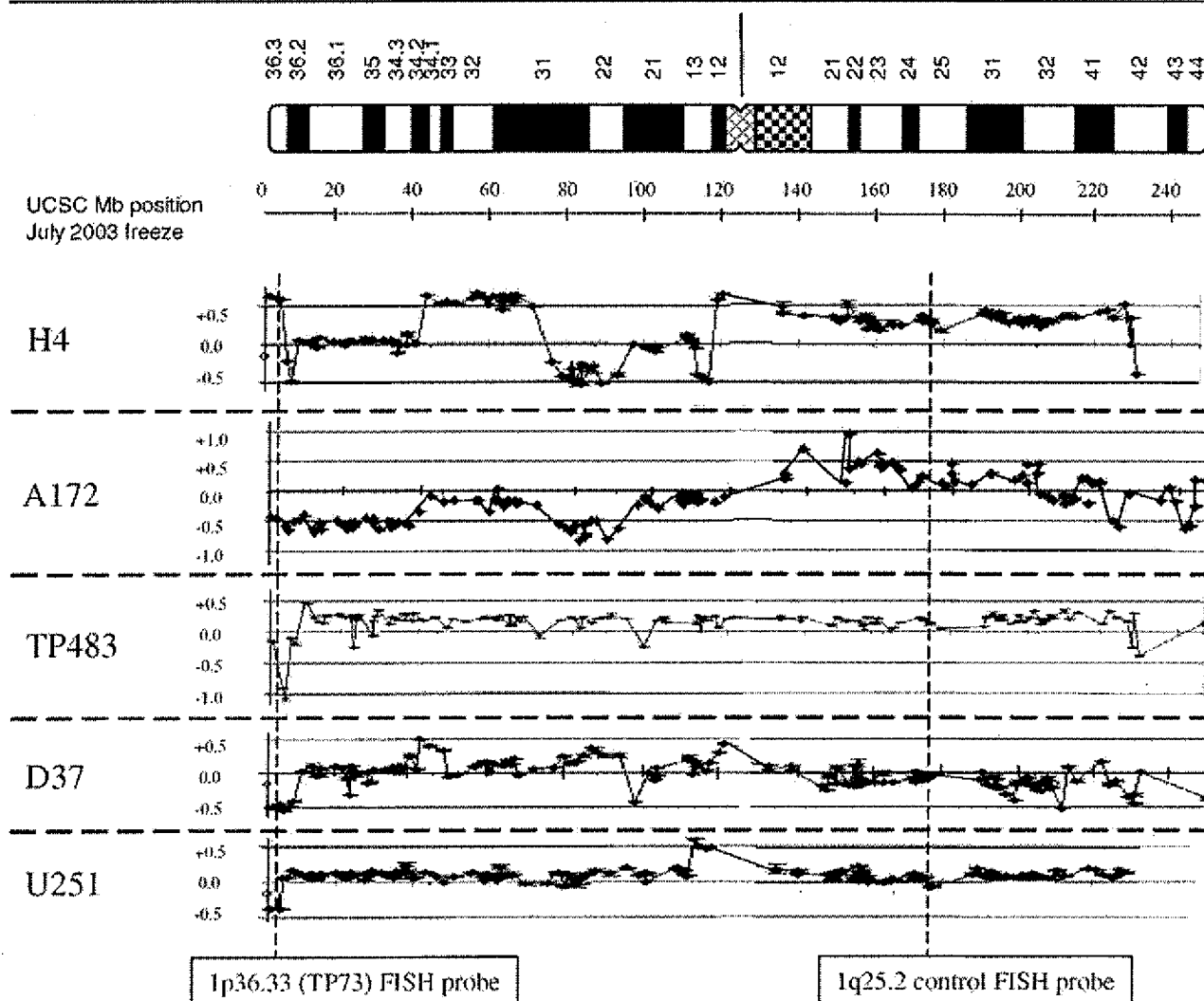


Fig. 4. Chromosome 1 CGHa of selected glioma cell lines. The CGHa tracing is scaled to the July 2003 freeze of the UCSC database.

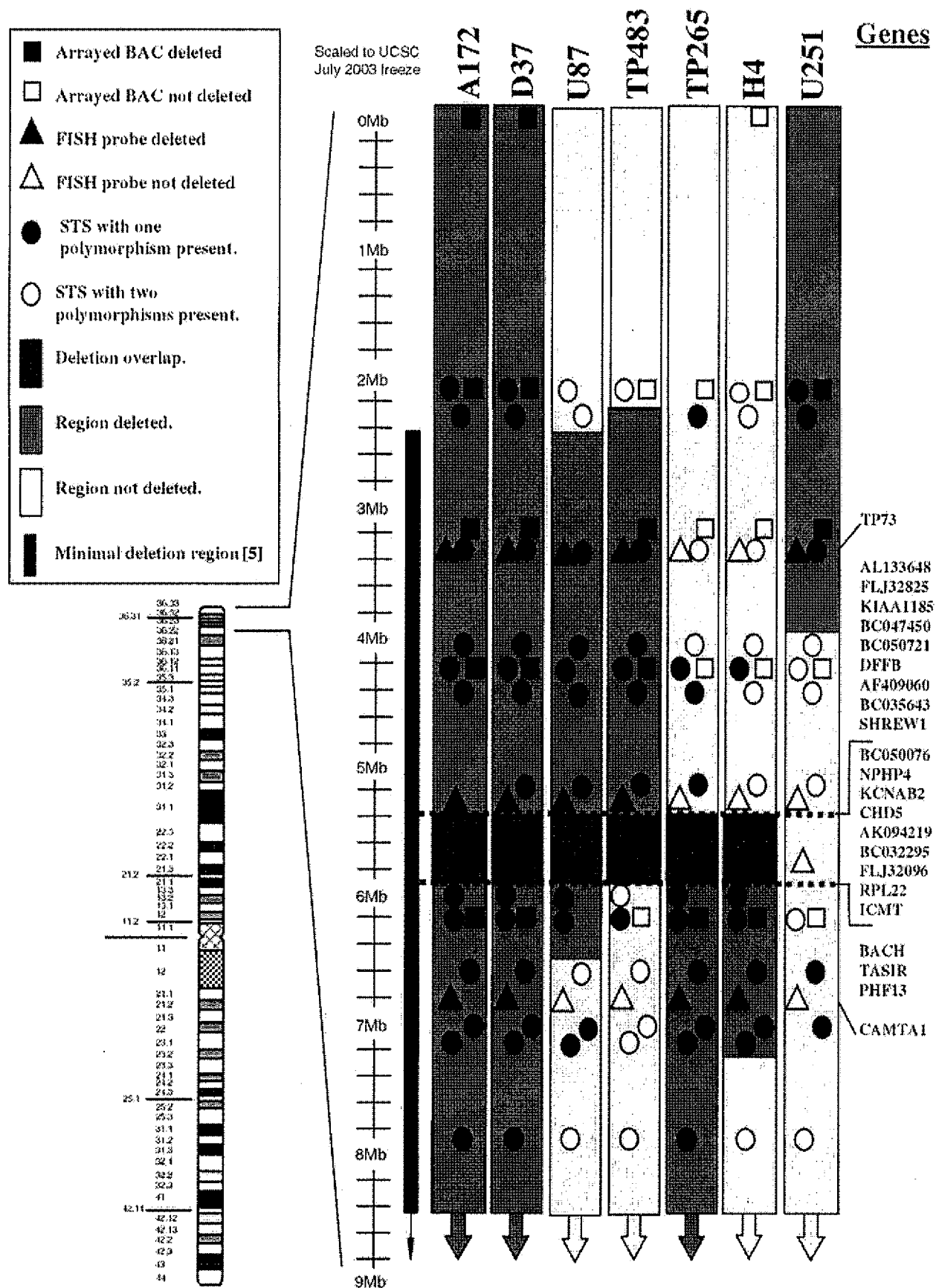
distal to this second deletion (Fig. 7). The chromosome 19 deletion in cell line U87 is approximately 2.1 Mb in size and is completely encompassed by the A172 deletion region. The distal breakpoints of the nested U87 and A172 deletions are separated by less than 200 kb (Fig. 7).

3.5. Cytogenetic karyotyping by M-FISH

Metaphase cells from each cell line were analyzed by M-FISH and up to five karyotypes were prepared. All the cell lines were found to have complex karyotypes with numerous structural and numeric abnormalities. For several cell lines, the anomalies were relatively homogeneous across the karyotypes. For example, in cell line A172, four of the five metaphases karyotyped were cytogenetically identical and the fifth was missing one derivative marker. Cell lines U87, U251, and D32 were similarly homogeneous (data not

shown). Conversely, some of the cell lines were heterogeneous, having multiple cells with significant karyotype variation. For instance, while the five karyotypes from H4 had 18 common markers, each also had up to 10 dissimilar anomalies. Cell lines MO67, SW1783, TP265, and U118 were similarly heterogeneous (data not shown). Importantly, the chromosome 1 and 19 abnormalities were consistent between karyotypes for each cell line. We focused on the

Fig. 5. A cartoon displaying the chromosome 1p36 deletion map. Chromosome region 1p36.23~1pter is enlarged. Cell lines with regions of homozygosity and deletions indicated by CGHa of 1p36 were mapped. Arrows indicate deletions extending beyond the map. Dotted horizontal lines indicate the breakpoint of the common 1p deletion region. Genes found within the common deletion region mapped in gliomas [5] is indicated by a vertical blue line. Base position is scaled to the July 2003 freeze of the UCSC database.



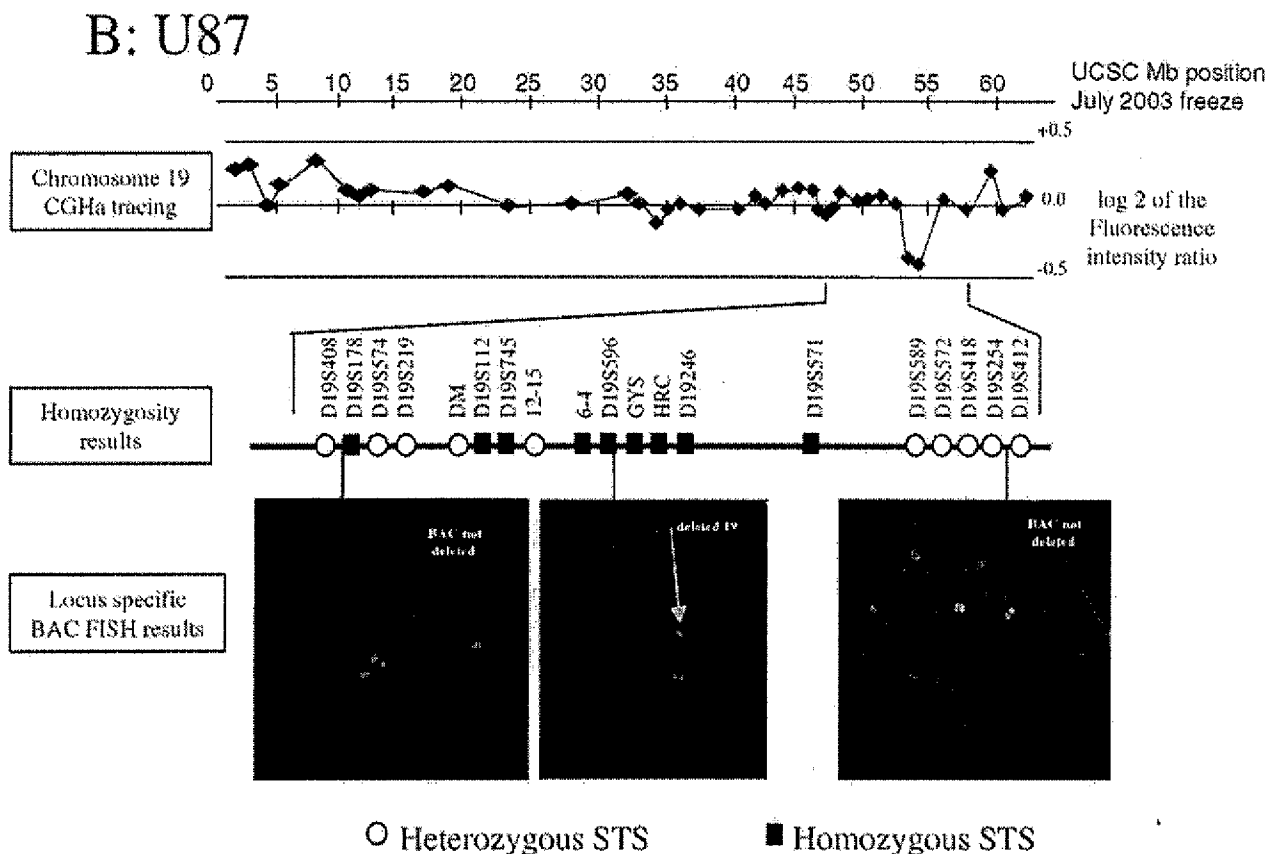
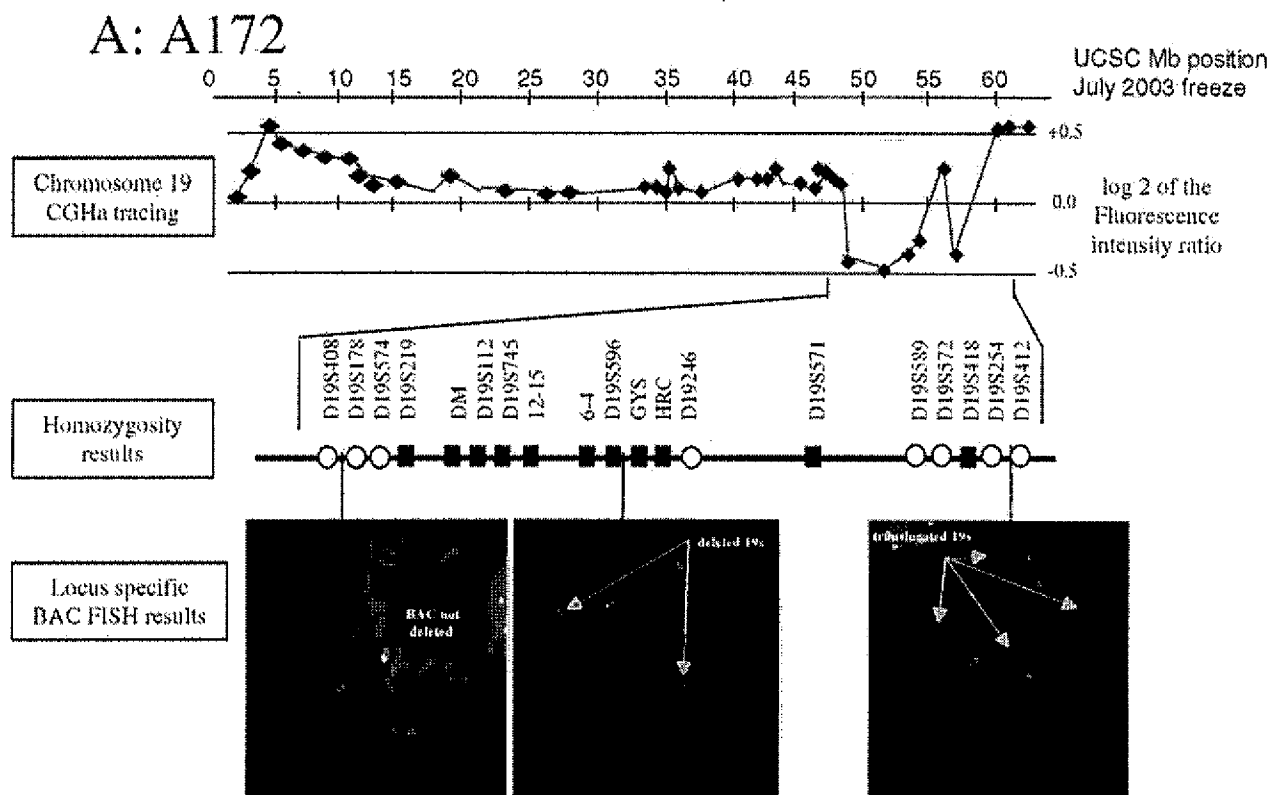


Fig. 6. Chromosome 19q deletion mapping by LOH, FISH, and CGHa (A) in A172 and (B) U87 cells. BAC used for locus-specific FISH and CGHa arrays are indicated in Materials and methods. The contiguous regions of homozygosity detected by LOH (middle panels) agrees with the deletion of 19q detected by CGHa (top panels) and FISH (bottom panels), respectively.

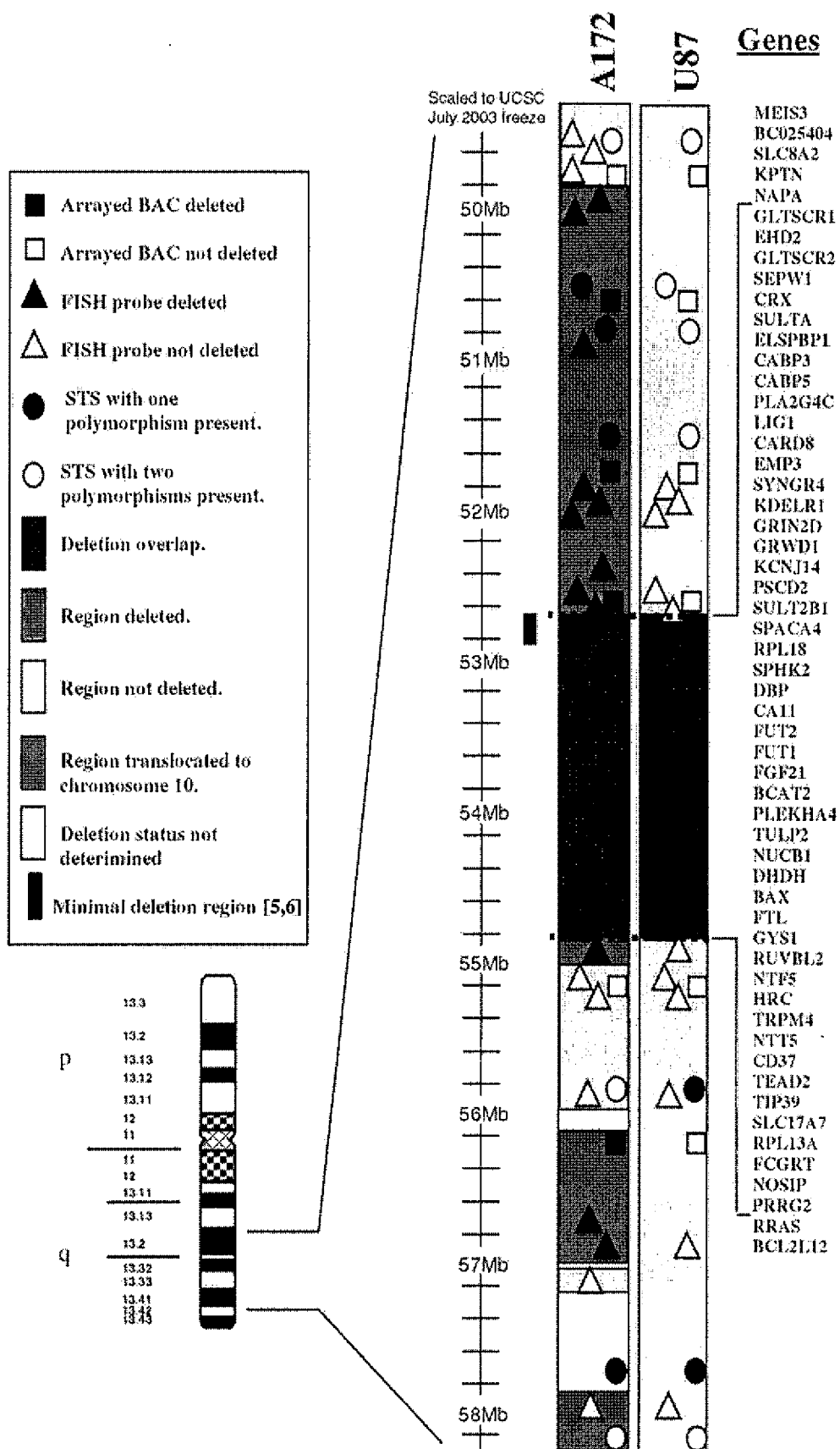


Fig. 7. A cartoon displaying a map of 19q deletions in cell lines A172 and U87. Chromosome region 19q13.2–q13.42 is enlarged to show base position (Mb) and BAC contig based on Lawrence Livermore National Laboratory chromosome 19 map (http://www.bahama_jgi-psf.org/publicch19/html/ch19.map3.htm). Dotted horizontal lines indicate the breakpoint of the 19q deletion. Genes found within the common deletion are listed to the right. The minimal deletion region mapped in gliomas [5,6] is indicated by a vertical blue line. Base position is scaled to the July 2003 freeze of the UCSC database.

Table 2

Summary of cytogenetic abnormalities involving chromosomes 1 found in glioma cell lines

| Cell line | Description of structurally abnormal chromosomes 1 |
|-----------|---|
| A172 | t(1;14)(p22;q13)x2,ider(1)t(X;1)(q26;q42), der(11)t(1;11)(p32;q23),der(11)t(1;11)(p32;q11), der[1]t(1;18)[(de1(1)(p34);18)[q42;q21] |
| D32 | der(1)t(1;3)(q25;?) |
| D37 | der(1)t(1;5)(p36.2;?),der(14)t(1;14)(q?;q?) |
| H4 | t(1;2)(?;?),der(14)t(1;14)(p?;q?),der(1;23)(?;?) |
| Hs683 | der(1)t(1;21)(q11;p11) |
| MO67 | der(1)t(1;6)(q11;?)x2 |
| SW1088 | der(1)t(1;4)(?;?) |
| SW1783 | der(1)ins(4;1)(?;?),der(2)t(1;2)(p;?) |
| T98G | der(1)t(1;7)(p34.2;?) |
| TP265 | der[4]t(4;1;11)(?;q;?) |
| TP483 | der(1)t(1;3)x2,del(1)(p36.3)x4 |
| U87 | der(20)t(1;14;20)(p11p36;q22;p11),der[1]t(1;del(13)(q22)) [p11;p11]x2,der(16)t(1;16)(p22;p13.1) |
| U118 | der(1)t(1;6)(q11;q11),der(7)t(1;7)(p11;q11),der(8)t(1;8)(p11;?) |
| U251 | der(1)t(1;13)(p36.3;p11) |

The partial karyotype descriptions summarize the available M-FISH, locus-specific FISH, GTL banding, and CGHa results.

most common clones (with respect to their M-FISH result) in each glioma cell line and analyzed their chromosomes 1 and 19. Fourteen cell lines had at least one structurally abnormal chromosome 1 (Table 2) and 13 cell lines had at least one structurally abnormal chromosome 19 (Table 3).

Table 3

Summary of cytogenetic abnormalities found in glioma cell lines involving the q arm of chromosome 19

| Cell line | Description of structurally abnormal chromosomes 19 |
|-----------|---|
| A172 | der(19)t(10;del(19)(q13.3q13.3))[q13.2q13.3] {q25;q13.4}x2 |
| D37 | der(5)t(5;16;18;19)(q31;q22;q21;q13.1),der(6)t(6;19)(q21;p13.1), der(13)t(13;19)(p12;p13.2),der(14)t(14;19)(q32;q13.1), der(15)ins(19;15)(q13.1q13.4;q22) |
| H4 | der(13)t(13;19)(p11;p11),der[16]t(16;19)(q12;q13.1);19[p11;q13.1], der(19)t(10;17;19)(p13;?;p13.3) |
| Hs683 | r(19)(pterq13.1) |
| SW1088 | der(19)t(X;16;19)(q22;q13q24;q13.4) |
| SW1783 | t(19;21)(q13.1q22;19;22)(q13.1;q13) |
| T98 | t(10;19)(q24;q13.1)x3,ins[19;del(10)(q24)][p13.2p13.3;q11.2] |
| TP265 | dup[19][dup(19)(q13.1q13.2)q13.2] |
| TP365 | del(19)(q13.2) |
| TP483 | t(19;20)(p13.1;p11.2)x3,i(19)(q10) |
| U87 | del(19)(q13.3q13.3) |
| U118 | der(10)t(10;19)(p11.2;q11.2),der(14)t(14;19)(q32;p11.2), der(15)t(15;19)(p11;p11) |
| U251 | der[19]ins[4;inv[invdup(19)(q13.2q13.3)][p13.2q13.3] {?;p13.1} |

The partial karyotype descriptions summarize the available M-FISH, locus-specific FISH, GTL banding, and CGHa results.

The most common translocation partner with chromosome 1 was chromosome 14 (5 out of 31 chromosome 1 abnormalities), and with chromosome 19 it was chromosome 10 (8 out of 29 chromosome 19 abnormalities). None of these translocations appeared to have common breakpoints even though there were multiple copies of some abnormal chromosomes within a cell line. Combined data from CGHa, locus-specific FISH, and M-FISH analysis revealed that cell lines A172, D32, D37, H4, Hs683, MO67, SW1088, SW1783, T98G, TP265, TP483, U87, U118, and U251 each have at least one 1p structural anomaly (Table 2), and that cell lines A172, D37, H4, Hs683, SW1088, SW1783, T98G, TP265, TP365, TP483, U118, U87, and U251 each have at least one 19q structural anomaly (Table 3).

4. Discussion

Deletions of 1p and 19q are particularly common in oligodendrogliomas [5]. Thus 1p and/or 19q have been hypothesized to harbor tumor suppressor gene(s) important for glioma formation. Despite the effort of many investigators, no credible candidate gene has been yet discovered in these chromosomal regions. These efforts have been hampered by a lack of appropriate cellular reagents. This is particularly true for oligodendrogliomas, a tumor type from which no bona-fide cell line has been established. Because 1p and 19q deletions are also seen in a subset of astrocytic tumors [4], it was likely that cell lines established from astrocytoma patients would also harbor these deletions. While glioma cell lines have been characterized cytogenetically by Sallinen et al. [21], no study has comprehensively screened the available glioma cell lines for 1p and 19q deletions. Thus, we screened glioma cell lines for deletions using homozygosity mapping, FISH, and CGHa. Cell lines A172 and U87 were observed by all three methods to have deletions of 1p and 19q (Figs. 5 and 6). The 2.1-Mb 19q deletion in U87 is completely encompassed by the larger A172 deletion, and these 1p and 19q deletions overlap the minimal deletion regions previously mapped in sporadic gliomas [5,6].

Cell lines A172, TP483, D37, U87, U251, TP265, and H4 were found to have deletion of 1p36.3 or 1p36.2 by LOH, CGHa, and FISH. Of the seven cell lines containing 1p deletion, six (A172, D37, U87, TP483, TP265, and H4) had deletion regions that overlapped. The extent of this common deletion is from position 5.3 to 6.0 Mb on the July 2003 freeze of the UCSC database (chromosome band 1p36.31). Interestingly, the gene *CHD5* is localized within this region (position 5.87–5.94 Mb) and was recently hypothesized as being a candidate tumor suppressor gene in neuroblastomas [22]. All six glioma cell lines with the 1p36.2–p36.3 deletion could negatively affect this gene. U251 has three chromosomes 1, one of which contains a terminal 1p36.3 deletion, including *P73*. Because the 1p deletion found in cell line U251 did not overlap the minimal deletion region nor was it deleted for the FISH probe at

5.7 Mb, we suspect that this deletion is a secondary random event (see later). A second common region of 1p deletion was found in cell lines TP265, A172, and H4 at 1p22–p31. The CGHa tracings of the deletions in A172 and H4 show identical breakpoints and are encompassed by the deletion in TP265, suggesting that these deletions may have biologic significance.

The homozygosity mapping results showed regions of homozygosity on 1p and 19q in cell lines A172, U87, U118, and TP265 (Figs. 1 and 2). In fact, U118 was homozygous for all STS markers tested, so it may have been derived from a haploid or near-haploid tumor. All 19q STS markers tested in TP265 and D32 were homozygous and may be the result of uniparental disomy or loss of a chromosome 19 and the duplication of its homologue during tumorigenesis. Smaller regions of 19q homozygosity were found in cell lines SW1088 and SW1783. Cell lines TP265 and MO67 had a region of homozygosity on 1p. These regions overlapped, at least in part; the previously mapped 1p and 19q minimal deletion regions [5,6].

Although the 1p and 19q deletions we observed in A172 and U87 cell lines were similar to those seen in sporadic gliomas, it is possible that these deletions were not present in the tumor of origin and instead were merely a result of cultural artifacts. If such deletions occurred as cultural artifacts, however, the prevalence of 1p and 19q deletions in the cell lines might be expected to be higher than the prevalence seen in the gliomas these cell lines were derived from. Only 2 of 17 (11%) cell lines have both 1p and 19q deletions, which is similar to the incidence of 1p and 19q deletions seen in sporadic astrocytic tumors [4].

In contrast to the deletions, translocations involving chromosomes 1 and 19 appear to result from cultural artifacts because they were numerous and the breakpoints were randomly distributed, involving a wide range of cytogenetic bands and partner chromosomes. In the 17 glioma cell lines we studied, M-FISH and CGHa data showed that 14 of them had chromosome 1 translocations or inversions (Table 2) and 10 of them had chromosome 19 translocations or inversions (Table 3). Given such a high number of these anomalies, we investigated whether chromosomes 1 and 19 were more inclined to rearrange than the other chromosomes. Therefore, we calculated a normalized prevalence of translocations and inversions by chromosome number and size. For example, the number of chromosomes 1 that had structural anomalies was divided by the total number of chromosomes 1 in all the glioma cell lines and by the current postulated size of chromosome 1 (using the UCSC database). The same calculation was done with all autosomes (chromosomes 1–22). The prevalence of structurally rearranged chromosomes 1 and 19, normalized to chromosome size, was not significantly different than the mean incidence of anomalies (data not shown). We conclude that the rate of instability for chromosomes 1 and 19 is similar to that of other chromosomes.

In addition to 1p and 19q deletions, other notable genetic characteristics of cell line A172 include homozygous deletion of *P16* (CGHa, data not shown), homozygous deletion

of *PTEN* [2] (CGHa, data not shown), and wild-type and mutant copies of *P53* [24]. Cell line U87 also had homozygous deletion of *P16* (CGHa, data not shown) and homozygous deletion of *PTEN* [23] but no *P53* mutations [24]. Both cell lines are reportedly derived from glioblastomas [25,26]. A172 and U87, however, also have characteristics of oligodendrogliomas. Like oligodendrogliomas, they have 1p and 19q deletions. In addition, Ecsedy et al. [27] and Joshi and Mishra [28] demonstrated that U87 xenografts stain positively for galactocerebroside, a marker of oligodendroglial lineage. The presence of *P16* and *PTEN* deletions does not exclude an oligodendroglial origin of A172 and U87 because a subset of anaplastic oligodendrogliomas has homozygous deletions of *P16* and *PTEN* [29]. Primary oligodendrogliomas, however, typically have larger 1p and 19q deletions than those observed in astrocytic tumors. Since 1p and 19q deletions in these cell lines overlap a region of deletion previously mapped with common breakpoints in oligodendrogliomas and astrocytomas [5,6], the presence of both 1p and 19q deletions in these cell lines can not be used as proof of their cellular origin.

Gain of chromosome 19 is also a common chromosomal alteration in gliomas [30], and patients with this abnormality tend to have a shorter survival than those with 1p and 19q deletions [31]. Two glioma cell lines in our study, TP265 and U251, were found to have regions of 19q13 duplication. Cell line TP265 has a duplication that includes 19q13.2 (BACs RP11-133A7 and RP11-18J23). CGHa did not detect this duplication, so its extent is unknown. Cell line U251 has a pericentric inversion and duplication involving 19q13.2–q13.32. Therefore, these cell lines might be useful reagents for the delineation of a common minimal region of chromosome 19 gain and the subsequent cloning of possible oncogenes important for the development of high-grade astrocytic gliomas. In a recent study, Beghini et al. [32] reported the *MARK4* gene at 19q13.32 is upregulated and overexpressed in human gliomas and in a subset of glioblastoma cell lines.

Several glioma-related tumor suppressor genes were discovered by somatic cell genetic experiments. For example, both Pershouse et al. [8] and England et al. [7] used glioma cell lines to ascertain the *PTEN* and *P16* tumor suppressor genes on chromosome 10q and 9p, respectively. Thus, cell lines A172 and U87 may be used in similar experiments to search for putative tumor suppressor gene(s) in 1p and 19q. In addition, these cell lines may be useful for the functional characterization of the 1p and 19q candidate tumor suppressor genes.

Acknowledgments

This work was funded in part by National Institutes of Health grant CA85799 to B.G. Feuerstein and R. B. Jenkins.

References

- [1] Mitelman F, Johansson B, Mertens F. Mitelman database of chromosome aberrations in cancer 2002. Available at: <http://www.cgap.nci.nih.gov/Chromosomes/Mitelman>. Accessed May 2003.
- [2] Cairncross JG, Ueki K, Zlatescu C, Lisle DK, Finkelstein DM, Hammond RR, Silver JS, Stark PC, Macdonald DR, Ino Y, Ramsay DA, Louis DN. Specific genetic predictor of chemotherapeutic response and survival in patients with anaplastic oligodendrogliomas. *J Natl Cancer Inst* 1998;90:1473–9.
- [3] Ino Y, Zlatescu MC, Sasaki H, Macdonald DR, Stemmer-Rachamimov AO, Jhung S, Ramsay DA, von Deimling A, Louis DN, Cairncross JG. Long survival and therapeutic responses in patients with histologically disparate high grade gliomas demonstrating chromosome 1p loss. *J Neurosurg* 2000;92:983–90.
- [4] Smith JS, Perry A, Borell TJ, Lee HK, O'Fallon J, Hosek SM, Kimmel D, Yates A, Burger PC, Scheithauer BW, Jenkins RB. Alterations of chromosome arms 1p and 19q as predictors of survival in oligodendrogliomas, astrocytomas, and mixed oligoastrocytomas. *J Clin Oncol* 2000;18:636–45.
- [5] Smith JS, Alderete B, Miun Y, Borell TJ, Perry A, Mohapatra G, Hosek S, Kimmel D, O'Fallon J, Yates A, Feuerstein BG, Burger PC, Scheithauer BW, Jenkins RB. Localization of common deletion regions on 1p and 19q in human gliomas and their association with histological subtype. *Oncogene* 1999;18:4144–52.
- [6] Smith JS, Tachibana I, Lee HK, Qian J, Pohl U, Mohrenweiser HW, Borell TJ, Soderberg CL, von Deimling A, Perry A, Scheithauer BW, Louis DN, Jenkins RB. Mapping of the chromosome 19q-arm glioma tumor suppressor gene using fluorescence in situ hybridization and novel microsatellite markers. *Genes Chromosomes Cancer* 2000;29:16–26.
- [7] England NL, Cuthbert AP, Trott DA, Jezzard S, Nobori T, Carson DA, Newbold RF. Identification of human tumour suppressor genes by monochromosome transfer: rapid growth-arrest response mapped to 9p21 is mediated by the cyclin-D-dependant kinase inhibitor gene, *CDKB2A (P16INK4A)*. *Carcinogenesis* 1996;17:1567–75.
- [8] Pershouse MA, Stubblefield E, Hadi A, Killary AM, Yung WK, Steck PA. Analysis of the functional role of chromosome 10 loss in human glioblastomas. *Cancer Res* 1993;53:5043–50.
- [9] Ransom DT, Ritland SR, Kimmel DW, Moertel CA, Dahl RJ, Scheithauer BW, Kelly PJ, Jenkins RJ. Cytogenetic and loss of heterozygosity studies in ependymomas, pilocytic astrocytomas, and oligodendrogliomas. *Genes Chromosomes Cancer* 1992;5:348–56.
- [10] Jalal SM, Law ME. Utility of multicolor fluorescent in situ hybridization in clinical cytogenetics. *Genetic Medicine* 1999;471:181–6.
- [11] Thompson CT, Gray JW. Cytogenetic profiling using in situ hybridization (FISH) and comparative genomic hybridization (CGH). *J Cell Biochem Suppl* 1993;17G:139–43.
- [12] Albertson DG. Profiling breast cancer by array CGH. *Breast Cancer Res Treat* 2003;78:289–98.
- [13] Rooney DE, Czepulkowski BH. Human cytogenetics a practical approach, volume 1. Constitutional analysis, 2nd edition. New York: University Press, 1992, pp. 71–3.
- [14] Weber JL, May PE. Abundant class of human DNA polymorphisms which can be typed using the polymerase chain reaction. *Am J Hum Genet* 1989;44:388–96.
- [15] Spurbeck JL, Zinsmeister AR, Meyer KJ, Jalal SM. Dynamics of chromosome spreading. *Am J Med Genetics* 1996;61:387–93.
- [16] Snijders AM, Nowak N, Seagraves R, Blackwood S, Brown N, Conroy J, Hamilton G, Hindle AK, Huey B, Kimura K, Law S, Myambo K, Palmer J, Ylstra B, Yue JP, Gray JW, Jain AN, Pinkel D, Albertson DG. Assembly of microarrays for genome-wide measurement of DNA copy number. *Nat Genet* 2001;29:263–4.
- [17] Sambrook J, Fritsch EF, Maniatis T. Molecular Cloning, 2nd edition. Cold Spring Harbor, NY: Cold Spring Harbor Laboratory Press, 1989, pp. e3–4, 10.8–10.10, 10.14–10.15.
- [18] Pinkel D, Seagraves R, Sudar D, Clark S, Poole I, Kowbel D, Collins C, Kuo WL, Chen C, Zhai Y, Dairkee SH, Ljung BM, Gray JW, Albertson DG. High resolution analysis of DNA copy number variation using comparative genomic hybridization to microarrays. *Nat Genet* 1998;20:207–11.
- [19] Jain AN, Tokuyasu TA, Snijders AM, Seagraves R, Albertson DG, Pinkel D. Fully automatic quantification of microarray image data. *Genome Res* 2002;12:325–32.
- [20] Chernova OB, Hunyadi A, Malaj I, Pan H, Crooks C, Roe B, Cowell JK. A novel member of the WD-repeat family, *WDR11*, maps to the 10q26 region and is disrupted by a chromosome translocation in human glioblastoma cells. *Oncogene* 2001;20:5378–92.
- [21] Sallinen SL, Sallinen P, Ahlstedt-Soini M, Haapasalo H, Helin H, Isola J, Karhu R. Arm-specific multicolor fluorescence in situ hybridization reveals widespread chromosomal instability in glioma cell lines. *Cancer Genetics Cytogenetics* 2003;144:52–60.
- [22] Thompson PM, Gotoh T, Kok M, White PS, Brodeur GM. CHD5, a new member of the chromodomain gene family, is preferentially expressed in the nervous system. *Oncogene* 2003;22:1002–11.
- [23] Adachi J, Ohbayashi K, Suzuki T, Sasaki T. Cell cycle arrest and astrocytic differentiation results from *PTEN* expression in glioma cells. *J Neurosurg* 1999;91:822–30.
- [24] Prasad G, Wang H, Agrawal S, Zhang R. Antisense anti-MDM2 oligonucleotides as a novel approach to the treatment of glioblastoma multiforme. *Anticancer Res* 2002;22:107–16.
- [25] Giard DJ, Aaronson SA, Todaro GJ, Arnstein P, Kersey JH, Dosik H, Parks WP. In vitro cultivation of human tumors: establishment of cell line from a series of solid tumors. *J Natl Cancer Inst* 1973;51:1417–23.
- [26] Ponten J, Macintyre EH. Long-term culture of normal and neoplastic human glia. *Acta Pathol Microbiol Scand* 1968;74:465–86.
- [27] Ecsedy JA, Holthaus KA, Yohe HC, Seyfried TN. Expression of mouse sialic acid on gangliosides of a human glioma grown as a xenograft in SCID mice. *J Neurochem* 1999;73:254–9.
- [28] Joshi PG, Mishra S. Galactocerebroside mediates Ca^{2+} signaling in cultured glioma cells. *Brain Res* 1992;597:108–13.
- [29] Reifenberger G, Louis DN. Oligodendroglioma: toward molecular definitions in diagnostic neuro-oncology. *J Neuropathol Exp Neurol* 2003;62:111–26.
- [30] Bigner SH, Mark J, Burger PC, Mahaley MS Jr, Bullard DE, Muhlbaier LH, Bigner DD. Specific chromosomal abnormalities in malignant human gliomas. *Cancer Res* 1988;48:405–11.
- [31] Burton EC, Lamborn KR, Feuerstein BG, Prados M, Scott J, Forsyth P, Passe S, Jenkins RJ, Aldape KD. Genetic aberrations defined by comparative genomic hybridization distinguish long-term from typical survivors of glioblastoma. *Cancer Res* 2002;62:6201–10.
- [32] Beghini A, Magnani I, Roversi G, Piepoli T, Di Terlizzi S, Moroni RF, Pollo B, Fuhman Conti AM, Cowell JK, Finocchiaro G, Larizza L. The neural progenitor-restricted isoform of the *MARK4* gene in 19q13.2 is upregulated in human gliomas and overexpressed in a subset of glioblastoma cell lines. *Oncogene* 2003;22:2581–91.

EXHIBIT 2

p190-A, a human tumor suppressor gene, maps to the chromosomal region 19q13.3 that is reportedly deleted in some gliomas

Anjali Tikoo ^a, Suzanne Czekay ^b, Carrie Viars ^b, Sara White ^a, Joan K. Heath ^a,
Karen Arden ^{b,c}, Hiroshi Maruta ^{a,*}

^a Ludwig Institute for Cancer Research, P.O. Box 2008, Royal Melbourne Hospital, Parkville, Melbourne 3050, Australia

^b Ludwig Institute for Cancer Research, University of California (UCSD), 9500 Gilman Drive, La Jolla, CA 92093-0660, USA

^c Department of Medicine, University of California (UCSD), 9500 Gilman Drive, La Jolla, CA 92093-0660, USA

Received 12 June 2000; received in revised form 10 August 2000; accepted 24 August 2000

Received by T. Sekiya

Abstract

To date, two distinct genes coding for Ras GAP-binding phosphoproteins of 190 kDa, p190-A and p190-B, have been cloned from mammalian cells. Rat p190-A of 1513 amino acids shares 50% sequence identity with human p190-B of 1499 amino acids. We have previously demonstrated, using rat p190-A cDNA, that full-length p190-A is a tumor suppressor, reversing v-Ha-Ras-induced malignancy of NIH 3T3 cells through both the N-terminal GTPase (residues 1–251) and the C-terminal Rho GAP (residues 1168–1441) domains. Here we report the cloning of the full-length human p190-A cDNA and its first exon covering more than 80% of this protein, as well as its chromosomal mapping. Human p190-A encodes a protein of 1514 amino acids, and shares overall 97% sequence identity with rat p190-A. Like the p190-B exon, the first exon of p190-A is extremely large (3.7 kb in length), encoding both the GTPase and middle domains (residues 1–1228), but not the remaining GAP domain, suggesting a high conservation of genomic structure between two p190 genes. Using a well characterized monochromosome somatic cell hybrid panel, fluorescent in situ hybridization (FISH) and other complementary approaches, we have mapped the p190-A gene between the markers D19S241E and STD (500 kb region) of human chromosome 19q13.3. Interestingly, this chromosomal region is known to be rearranged in a variety of human solid tumors including pancreatic carcinomas and gliomas. Moreover, at least 40% glioblastoma/astrocytoma cases with breakpoints in this region were previously reported to show loss of the chromosomal region encompassing p190-A, suggesting the possibility that loss or mutations of this gene might be in part responsible for the development of these tumors. © 2000 Elsevier Science B.V. All rights reserved.

Keywords: p190-A; Tumor suppressor; 19q13.3; Gliomas; Rho GAP; GTPase

1. Introduction

p190-A and p190-B belong to a family of large G proteins/GAPs (GTPase activating proteins) which contain both the N-terminal GTPase domain and the C-terminal GAP domain for Rho family GTPases

(Settleman et al., 1992; Morii et al., 1993; Burbelo et al., 1995). The rat p190-A of 1513 amino acids shares 50% sequence identity with the human p190-B of 1499 amino acids (Settleman et al., 1992; Burbelo et al., 1995). Both p190-A and p190-B bind the SH2 domain of a Ras GAP of 120 kDa when they are phosphorylated on Tyr (Ellis et al., 1990). Thus, Ras GTPases can link to Rho family GTPases through these two GAPs (Ras GAP of 120 kDa and p190). Interestingly, Ras requires Rho family GTPases (Rho, Rac and CDC42) for malignant transformation (Qiu et al., 1995; Lebowitz et al., 1995; Qiu et al., 1997; Maruta et al., 1999; Nur-E-Kamal et al., 1999). However, although Ras GAP of 120 kDa appears to be an oncogenic effector of Ras (Chang et al., 1995), rat p190-A is not oncogenic, but instead has anti-oncogenic effects, i.e. it can suppress Ras-induced malignancy (Wang et al., 1997). Expression of an anti-sense

Abbreviations: FISH, fluorescent in situ hybridization; GAP, GTPase activating protein; GRF-1, glucocorticoid receptor repression factor 1; GTS, glioma tumor suppressor; LOD (logarithm of the odds) score, measure of the likelihood of genetic linkage between loci; LOH, loss of heterozygosity; NCBI, National Center for Biotechnology Information; PCR, polymerase chain reaction; RT, reverse transcriptase; STS, sequence tagged site.

* Corresponding author. Tel.: +613-9341-3155; fax: +613-9341-3104.

E-mail addresses: karden@ucsd.edu (K. Arden), hiroshi.maruta@ludwig.edu.au (H. Maruta)

p190-A RNA causes malignant transformation in normal NIH 3T3 fibroblasts (Wang et al., 1997). Furthermore, the tumor suppressor p190-A contains two distinct anti-oncogenic domains, the N-terminal GTPase domain (residues 1–251) and the C-terminal GAP domain (residues 1167–1513), and overexpression of each domain suppresses Ras transformation (Wang et al., 1997). The C-terminal GAP domain blocks the Ras signal by attenuating Rho, Rac and CDC42, which are essential for the transformation. The mechanism underlying the suppression by the N-terminal GTPase domain still remains to be clarified.

To use these p190-A DNA fragments for gene therapy of Ras-associated cancer or p190-A deficient cancers, we have cloned the full-length human p190 A cDNA, as well as several genomic p190-A DNA fragments. Furthermore, we have localized p190 A to human chromosome 19q13.3, a region known to have aberrations or deletions in a variety of human solid tumors including glioblastomas and astrocytomas (Heim and Mitelman, 1995; Rosenberg et al., 1996; Smith et al., 1999, 2000), suggesting that deletion or mutations of the tumor suppressor p190-A may contribute to tumorigenesis in human.

2. Materials and methods

2.1. Cloning and sequencing of human p190-A cDNA

The cloning of human p190-A cDNA fragments was performed by RT-PCR using total RNA isolated from the human breast cancer cell line MCF-7. Total RNA from MCF-7 cells was isolated as described previously (Chomczynski and Sacchi, 1987). 2 µg of total RNA was then used as a template for RT-PCR to generate three distinct cDNA fragments of human p190-A, as described previously (Tikoo et al., 1994). Briefly, the 1.2 kb cDNA fragment A encoding the first 400 amino acids of p190-A, including the N-terminal GTPase domain (residues 1–251), was generated using a pair of PCR primers derived from the 5' end of the rat p190-A cDNA (sense) 1 (CAG GAT GTT TCG AAG ATG ATG ATG) and human GRF-1 cDNA (anti-sense) 2 (TTC GTT TTC CAT GTT GTC AAT GTG ACT) encompassing the middle region of human p190-A cDNA (LeClerc et al., 1991; Settleman et al., 1992).

The 0.93 kb cDNA fragment B encoding the 308 amino acids of the C-terminal GAP domain (residues 1145–1452) of p190-A was generated with PCR primers 3 (GAG CGA GGG CGC AAG GTT) and 4 (GGG AGC TGG GCC TGG), both derived from the human GRF-1 cDNA sequence which is similar to the rat p190-A cDNA (LeClerc et al., 1991; Settleman et al., 1992). The 0.26 kb cDNA fragment C encoding the remaining C-terminal end (residues 1431–1514) of human p190-A was generated with a third pair of PCR primers 5 (CAG TGC CCC TTC TTC TTC TAC) and

6 (CTC CTA GTG TTC CTT TGT TTG) derived from human GRF-1 cDNA (sense) and the consensus sequence (anti-sense) of two overlapping human cDNA fragments (GenBank accession numbers AA010526 and AA010440) that partially overlap the human GRF-1 cDNA. These three RT-PCR DNA fragments were then subcloned into the EcoRI site of a cloning vector using the TA cloning kit (Invitrogen) and sequenced by an automated DNA sequencer (Applied Biosystems).

2.2. Cloning of human p190-A genomic DNA fragments encoding the GTPase domain

A human placental genomic library in lambda phage (Stratagene) was probed with the 1.2 kb human p190-A cDNA fragment A. The probe was labeled with [α^{32} P-ATP] using Megaprime random primer extension kit (Amersham). Sac I digestion of seven positive clones (numbered 1–7) revealed four distinct genomic clones called 2, 3/4, 5/6 and 1/7, ranging from 15.3 to 20.9 kb in size. Southern blot analysis of the Sac I digested clones using the probe 190-A cDNA fragment A confirmed the identity of all four clones. Each clone was next digested by Not I, and subcloned into the vector pBS (KS+) (Stratagene) for sequence analysis.

2.3. Southern blot analysis for chromosomal mapping

DNA from the (human × hamster) and (human × mouse) hybrids containing various combinations of human chromosomes were used in blot hybridization (Southern, 1975) as described below. The hybrids designated with GM were obtained from the Human Genetic Mutant Cell Repository (Camden, NJ). The human chromosome content of each somatic cell hybrid was established by the Human Genetic Mutant Cell Repository.

Genomic DNA was isolated from each cell line, digested with EcoRI, fractionated by electrophoresis through 0.8% agarose gels at 1 V/cm and transferred to a nylon membrane by previously described methods (James et al., 1988). The 1.2 kb full-length cDNA clone for p190-A was labeled by random primer extension (Freiberg and Vogelstein, 1983) using [α^{32} P]-dCTP and hybridization was performed at 65°C for at least 16 h in 0.5 M NaPO₄, 7% SDS, 10 mM EDTA and 0.1 mg/ml heterologous DNA. Filters were washed twice in 2 × SSC, 0.1% SDS and in 0.1 × SSC, 0.1% SDS at room temperature for 30 min and once in 0.1 × SSC, 0.1% SDS at 42°C for 10 min. Autoradiography was performed at –80°C for 3–10 days using Kodak BioMax MR film.

2.4. PCR analysis of the Stanford G3 radiation hybrid mapping panel

The G3 radiation hybrid panel (Stewart et al., 1997) containing 83 radiation hybrid DNAs, as well as human

and hamster control DNAs, was obtained from Research Genetics, Inc. (Huntsville, AL). The human chromosome content of each somatic cell hybrid was established by Stanford Human Genome Center using more than 10000 STSs derived from random genomic DNA sequences, previously mapped genetic markers and expressed sequences (<http://www.shgc.stanford.edu/Mapping/rh/>).

PCR reactions were carried out in a 50 µl reaction containing 25 ng DNA template, 200 µM deoxynucleotide triphosphates, 100 pmol of each oligonucleotide primer and 2.5 U of Taq DNA polymerase, 2.5 mM MgCl₂, 50 mM KCl, 10 mM Tris-HCl (pH 8.3). The nucleotide sequence from clone 6 was used to generate PCR primers: p190-A1F (5'-CAT GGG AAT GTG TTT TTA-3') and p190-A1R (5'-CT CCC AAT CAA GAC TGT T-3'). 35 cycles of PCR were performed with each cycle consisting of denaturation at 95°C for 60 s, annealing at 55°C for 60 s and extension at 72°C for 60 s. PCR was initiated by a 3 min incubation at 95°C and terminated with a 72°C final extension for 10 min. Amplified products were electrophoresed through 2% agarose gels and visualized by ethidium bromide staining. The resulting PCR product was a 185 bp human p190-A-specific fragment. The presence or absence of this product was scored for each of the somatic cell hybrids. The results were submitted to the Stanford Radiation Hybrid server via the Internet (<http://www.shgc.stanford.edu>) and the computed data were returned to us.

2.5. Fluorescence in situ hybridization (FISH)

2.5.1. Human p190-A clone

A human p190-A genomic clone 2 (p190-A-2) was used for fluorescence in situ hybridization in two independent experiments. In each case the entire p190-A-2 clone was nick translated using Biotin-14 dATP and Biotin-14 dCTP (Gibco BRL) and hybridized to normal human metaphase spreads.

2.5.2. Chromosome preparations

Chromosome preparations were obtained from phytohemagglutinin (PHA)-stimulated normal peripheral blood lymphocytes cultured for 72 h. To induce R-banding, some of the cultures were synchronized with thymidine after 48 h, incubated overnight at 37°C and treated with 5-bromodeoxyuridine (BrdU) the next morning, during the final late S-phase, and harvested 6 h later (Jacky, 1991). Cytogenetic harvests and slide preparations were performed using standard methods. The slides were stored at -80°C before use.

2.5.3. Fluorescence in situ hybridization

Fluorescence in situ hybridization to metaphase chromosomes was performed as described previously (Pinkel

et al., 1986). Briefly, the biotin-labeled probe (200 ng) was dissolved in DenHyb (Sigma) hybridization buffer with 10 µg of COT-1 DNA, denatured at 72°C for 10 min and re-annealed at 37°C for 2 h to allow the COT-1 DNA to anneal to repetitive sequences in the probe. The probe mixture was then applied to the slide and co-denatured with the metaphase spreads for 10 min at 82°C on a slide warmer. Hybridization was allowed to proceed for a minimum of 24 h in a 37°C incubator. The slides were washed at 37°C in 50% formamide/2 × SSC for 15 min and in 2 × SSC for 8 min. Biotin-labeled probe detection was accomplished by incubation with the FITC-avidin conjugate (Oncor).

2.5.4. Chromosome arm identification

Chromosome arm identification was performed by simultaneous hybridization with a 19q telomere probe (Vysis Spectrum Orange) as described previously (Lemieux et al., 1992), and the metaphases were counter-stained with DAPI (0.05 µg/ml). Slides were examined and photographed using a Zeiss Axiophot microscope and appropriate UV filter combinations. The 35 mm slides were scanned using a Nikon Coolscan, processed using Adobe Photoshop 4.0 and printed using a Fujix Pictography 3000.

3. Results and discussion

3.1. Cloning of human p190-A cDNA

A comparison of the nucleotide sequence of a human cDNA known as glucocorticoid receptor repression factor 1 (GRF-1), previously cloned from a cDNA expression library of the human breast cancer cell line MCF-7 (LeClerc et al., 1991), with that of the rat p190-A cDNA (Settleman et al., 1992) revealed that the GRF-1 appears to encode a fragment of human p190-A, but clearly lacks the first 388 codons encoding the GTPase domain, as well as the last 60–70 codons encoding the C-terminal tail following the GAP domain. Furthermore, the published nucleotide sequence for GRF-1 contains a few insertions and deletions that result in frameshifts downstream of the codon 1166, where the GAP domain should start. It is now well accepted that these alterations are simply due to the sequencing errors.

To determine the full-length coding sequence of human p190-A, we cloned cDNA fragments generated by RT-PCR using total RNA isolated from MCF-7 cells as template and primers derived from the rat p190-A cDNA sequence and the human GRF-1 cDNA sequence (LeClerc et al., 1991), based on the assumption that GRF-1 is a truncated form of the human homologue of rat p190-A cDNA (see Fig. 1A). GRF-1 shares 95 and 45% sequence identity with the corresponding domains

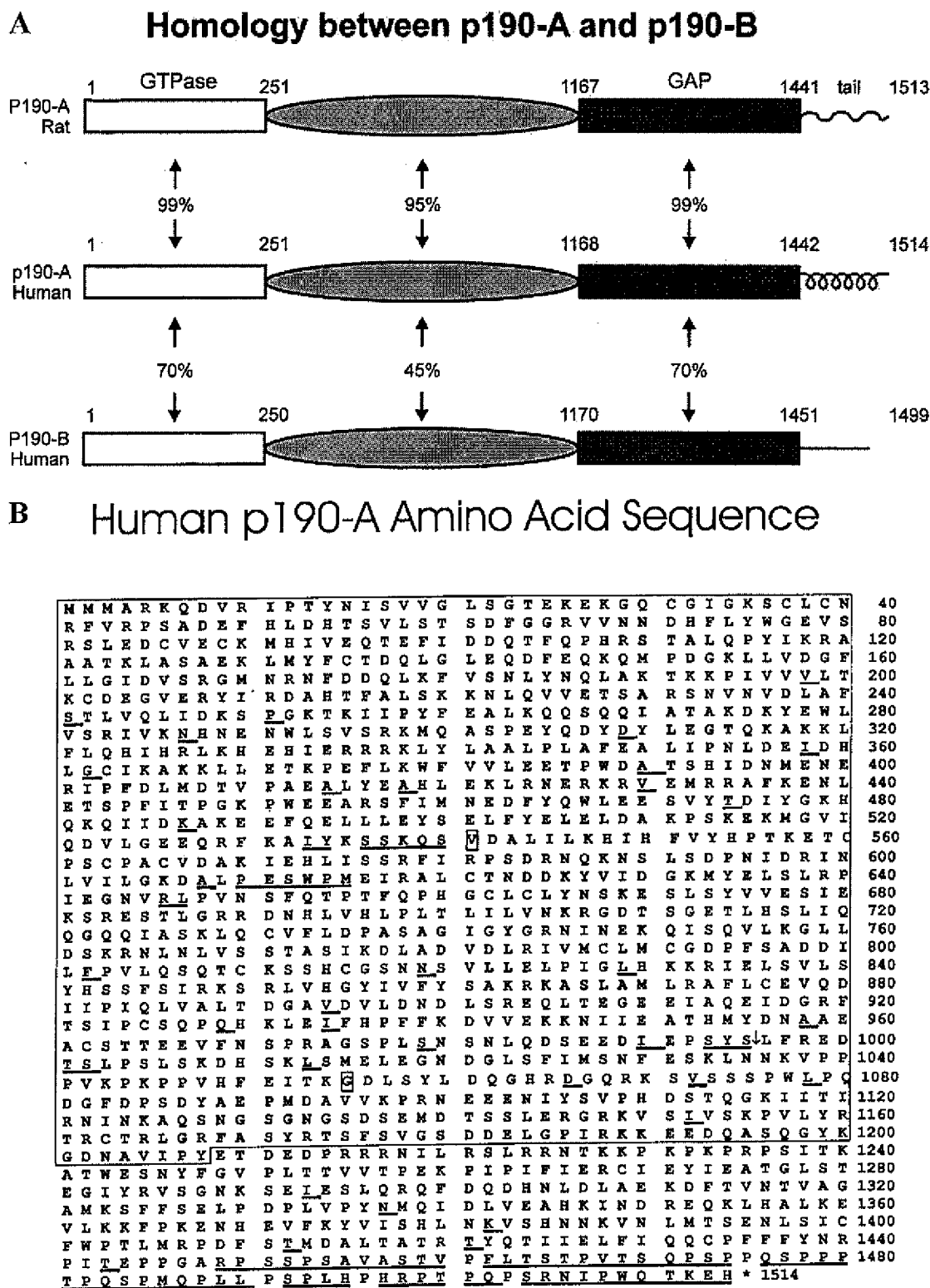


Fig. 1. The cloning and sequencing of full-length human p190-A cDNA. (A) Homology between rat 190-A, human 190-A and 190-B. The amino acid sequence identity in different domains between the three molecules is indicated in percentages. The human cDNA called GRF-1 (LeClerc et al., 1991) corresponds to codons 389 to 1442 of the human p190-A cDNA (for detail, see B). (B) The deduced amino acid sequence of full-length human p190-A based on the sequences of cloned cDNAs and genomic DNAs. The number indicates codon number, and the asterisk symbolizes the termination. Residues 1–1228 in the large box are encoded by the first exon. The underlined residues differ from those of rat p190-A, and the two residues in the small boxes are V541 and G1055 present in human p190-A but absent in rat p190-A, while the arrow indicates the additional His residue present only in the rat p190-A. The GenBank accession number of human p190-A cDNA is AF159851.

of rat p190-A and human p190-B, respectively (Settleman et al., 1992; Burbelo et al., 1995).

Nucleotide sequence analysis of the 1.2 kb RT-PCR generated fragment A, corresponding to the first 400 codons of the human p190-A, has confirmed that the codon 389 of p190-A corresponds to the codon 2 of GRF-1, and that the previously reported GRF-1 sequence missed a 'G' (nucleotide 1164 of the p190-A).

In an attempt to clone a cDNA encoding the C-terminal domain starting at codon 1145 of human p190-A, we first used the sense primer corresponding to the codons 758–763 (identical to codons 1145–1150 of rat p190-A cDNA) and the anti-sense primer corresponding to the last seven codons of rat p190-A cDNA (as no nucleotide sequence for human p190-A cDNA downstream of codon 1452 was available). However, we failed to obtain a RT-PCR product (data not shown), suggesting that the 3' end of the human p190-A coding region differs significantly from that of the rat p190-A cDNA. We next tried using the same sense primer and an anti-sense primer corresponding to codons 1431–1437 of the rat p190-A cDNA (which is identical to the corresponding sequence of GRF-1) and then a further downstream anti-sense primer corresponding to the last seven codons of GRF-1 (codons 1446–1452 of human p190-A), and successfully generated the 0.93 kb cDNA fragment B encoding the 308 amino acids of the C-terminal GAP domain (residues 1145–1452). The nucleotide sequence of fragment B revealed that the previously reported GRF-1 sequence misses a 'G' at nucleotide 3501 and a 'C' at nucleotide 4002 of the p190-A, and contains an extra 'C' around codon 1241 of the p190-A. Most importantly, the GRF-1 sequence misses a 'G' around the codon 1167 of human p190-A, causing a frameshift of the following 55 codons and

subsequently leading to a premature termination. That is why GRF-1 appears to be a truncated p190-A, which lacks the C-terminal GAP domain, as well as the N-terminal GTPase domain.

Generation of the RT-PCR fragment C encoding the last 84 amino acids of human p190-A (residues 1431–1514) became possible after a search of the National Center for Biotechnology Information (NCBI) database (<http://www.ncbi.nlm.nih.gov/>) led to the discovery of two small overlapping human cDNA fragments (accession numbers AA010440 and AA010526) which share sequence homology with rat p190-A cDNA. AA010440, but not AA010526, contains the termination codon TAG at the 3' end. Using the 3' end of the consensus sequence of these two small fragments as the anti-sense primer and the sense primer corresponding to codons 1432–1438 of human p190-A (1431–1437 of rat p190-A), the 0.26 kb RT-PCR fragment C was generated and sequenced. Sequence analysis revealed that the last 66 amino acids of human p190-A share basically no homology with those (65 amino acids) of rat p190-A (see Fig. 1B). This is due in part to the presence of an extra 'A' in the human p190-A cDNA at the gap between codons 1447 (GCT for Ala) and 1448 (GCG for Ala) of rat p190-A (see Fig. 2). This appears very unlikely to be a result of either a sequencing error or an insertional mutation unique to the MCF-7 breast cancer cell line, as the p190-A cDNA from all other human cell lines (both normal and malignant) sequenced to date, as well as a genomic human p190-A clone which encodes this C-terminal tail (HumGenome-BLAST.hmt), also contain this extra base at this position.

However, from a point of view on gene evolution, it is of interest to note that if this extra base were omitted, the sequence homology between human and rat p190-A

| 1447 | | | | | | | | | | | | | | | 1448 | | | | | | | | | | | | | | |
|----------|----------|-----|----------|----------|----------|----------|-----|----------|----------|-----|----------|----------|----------|----------|----------|------------|------------|----------|-------|--|--|--|--|--|--|--|--|--|--|
| I | S | E | P | P | G | A | . | A | L | A | P | L | Q | P | W | H | P | L | Rat | | | | | | | | | | |
| ATC | AGT | GAG | CCA | CCG | GGG | GCT | . | GCG | CTG | GCT | CCC | CTT | CAG | CCA | TGG | CAC | CCA | CTG | | | | | | | | | | | |
| ATC | ACC | GAG | CCC | CCC | GGC | GCC | A | GGC | CCA | GCT | CCC | CCT | CTG | CCG | TGG | CTT | CCA | CCG | | | | | | | | | | | |
| I | T | E | P | P | G | A | . | G | P | A | P | E | L | P | W | L | P | P | Human | | | | | | | | | | |
| | | | | | | | | | | | | | | | | | | | | | | | | | | | | | |
| S | P | S | S | P | L | H | L | L | P | V | S | H | H | L | P | S | H | L | Rat | | | | | | | | | | |
| TCC | CCT | TCC | TCA | CCT | CTA | CAC | CTG | CTA | CCA | GTC | AGC | CAT | CAC | CTC | CCC | AGT | CAC | CTC | | | | | | | | | | | |
| TCC | CCT | TCC | TCA | CTT | CCA | CGC | CTG | TCA | CAA | GTC | AGC | CGT | CGC | CCC | CAC | AGT | CGC | CTC | | | | | | | | | | | |
| S | P | S | S | <u>L</u> | <u>P</u> | <u>R</u> | L | <u>S</u> | <u>Q</u> | V | S | <u>R</u> | <u>R</u> | <u>P</u> | <u>H</u> | S | <u>R</u> | L | Human | | | | | | | | | | |
| | | | | | | | | | | | | | | | | | | | | | | | | | | | | | |
| L | Q | P | L | S | P | Q | C | S | H | C | S | P | L | S | S | K | P | N | Rat | | | | | | | | | | |
| CTC | CAA | CCC | CTC | AGT | CCC | CAA | TGC | AGC | CAT | TGC | TCT | CCT | CTC | AGC | TCC | AAG | CCG | AAC | | | | | | | | | | | |
| CAC | CCA | CCC | CCC | AGT | CCC | CAA | TGC | AGC | CAC | TGC | TTC | CCT | CCC | CGC | TTC | ATC | CCC | ACC | | | | | | | | | | | |
| <u>H</u> | <u>P</u> | P | <u>E</u> | S | P | Q | C | S | H | C | <u>E</u> | P | <u>P</u> | <u>R</u> | <u>F</u> | <u>I</u> | P | <u>T</u> | Human | | | | | | | | | | |
| | | | | | | | | | | | | | | | | | | | | | | | | | | | | | |
| T | R | C | E | P | P | Q | P | R | K | Q | E | N | Q | L | S | S | 1513 Rat | | | | | | | | | | | | |
| ACA | CGC | TGT | GAG | CCA | CCA | CAG | CCC | AGG | AAG | CAG | GAA | AAT | CAG | TTG | TCT | TCT | <u>TGA</u> | | | | | | | | | | | | |
| GTC | CCA | CTC | CAC | AGC | CTT | CCC | GAA | ACA | TTC | CCT | GGC | AAA | CAA | AGG | AAC | <u>ACT</u> | <u>AGG</u> | AG. | | | | | | | | | | | |
| V | P | L | H | S | L | P | E | T | F | P | G | K | Q | R | N | T | <u>R</u> | Human | | | | | | | | | | | |

Fig. 2. Sequence alignment of human and rat p190-A cDNAs encoding the C-terminal tail regions after deletion of the extra base A (boxed) inserted into the human sequence. The underlined amino acid residues differ between rat and human sequences. The underlined triplets are 'termination' codons for each gene.

would have been extended further to codon 1490, although the latter frameshifted human sequence (more matched to the rat sequence) would carry no termination codon in frame (see Fig. 2). It is also worth noting that human p190-A and p190-B, which share 70% sequence identity in both the GTPase and GAP domains, share no sequence homology downstream of codons 1447–1448, suggesting that this DNA region is highly susceptible to mutations during their evolution from a common ancestral gene. Nevertheless, the overall amino acid sequence identity between human and rat p190-A is as high as 97%. Moreover, in both GTPase and GAP domains they share 99% sequence identity.

3.2. Cloning of genomic human p190-A DNAs

It has been reported that (i) the mouse p190-B gene maps to chromosome 12 which corresponds to human chromosome 14 and (ii) a single exon of 3.9 kb contains 80% of the coding region of the mouse p190-B (codons 1–1238) which encodes both the N-terminal GTPase domain and the middle domain of unknown function, but not either the GAP domain or the C-terminal tail (Burbelo et al., 1998).

To determine the chromosomal locus for the human p190-A gene, four distinct genomic human p190-A DNA fragments of 15–21 kb were cloned, using the 1.2 kb cDNA fragment A as a hybridization probe. Interestingly, the 1.2 kb p190-A cDNA contains two EcoRI sites, at codons 10 and 374, and therefore the EcoRI digestion of this cDNA fragment would be expected to produce a 1.1 kb fragment, as observed in Fig. 3, suggesting that at least the codons 10–374 of human p190-A are encoded by a single exon. The further sequencing of all four genomic clones has confirmed that (i) there is no intron between the codons 1 and 1228 of the human p190-A gene, indicating that the exon 1 of 3.7 kb encodes the GTPase domain (codons 1–251) and the following 977 codons of the middle-domain (see Fig. 1) and (ii) the intron between exons 1 and 2 is longer than 16 kb (data not shown), indicating that the genomic structures of p190-A and p190-B are very similar.

3.3. Mapping of human p190-A gene to the chromosome 19

The preliminary chromosomal localization of the p190-A gene was established by Southern blot analysis of DNA samples isolated from a panel of hamster/human or mouse/human somatic cell hybrids. The 1.2 kb p190-A cDNA probe hybridized to a single EcoRI fragment of 1.1 kb in human genomic DNA (Fig. 3). Cross hybridization to both mouse (10.0 kb) and hamster (7.4 kb) DNA suggests the presence of homologous genes in these species. Segregation of the p190-A locus correlated with the distribution of human

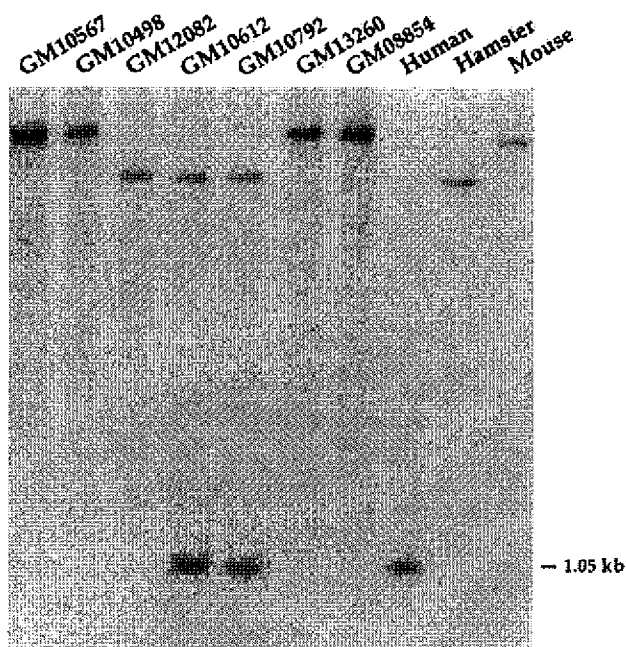


Fig. 3. Southern blot analysis of EcoRI digests of genomic DNAs from hamster, mouse, human and a subset of the somatic cell hybrid cell lines, using the same human p190-A cDNA probe. From left to right: lane 1, cell line GM10567 containing only human chromosome 16; lane 2, cell line GM10498 containing human chromosome 17; lane 3, cell line GM12082 containing only human chromosome 18; lane 4, cell line GM10612 containing only human chromosome 19; lane 5, cell line GM10792 containing only human chromosomes 12 and 19; lane 6, cell line GM13260 containing only human chromosome 20; lane 7, cell line GM08854 containing only human chromosome 21; lane 8, human DNA; lane 9, hamster DNA; lane 10, mouse DNA.

chromosome 19 in the hybrid cell lines. These data as well as the human chromosomal content of the somatic cell hybrids are summarized in Table 1.

In short, among the 25 distinct human/mouse or human/hamster hybrid cell lines, only two cell lines (GM10612 and 10792) contain human chromosome 19. However, GM10792 contains human chromosome 12 as well. As shown in Fig. 3, the human p190-A probe hybridized only with these two cell lines, and not any other cell lines including GM10868 which contains human chromosome 12. These data together suggest that p190-A gene is localized only in chromosome 19.

3.4. FISH analysis and radiation hybrid mapping of the human p190-A gene locus

The chromosomal localization of the human p190-A locus obtained by somatic cell hybrid mapping was independently confirmed and refined by FISH. In two separate experiments we scored a total of 150 metaphase spreads from normal lymphocytes for specific signals. We considered signals to be specific only if they were detected on both chromatids of a single chromosome. Specific signals were seen in 85 of the 150 metaphases

Table 1
Segregation of p-190 with human chromosomes in human × hybrid cell lines^a

| Hybrid | p-190 | Human chromosome | | | | | | | | | | | | | | | | | | | | | | |
|------------------------------|-------|------------------|----|----|----|----|----|----|----|----|----|----|----|----|----|----|----|----|----|----|----|----|----|----|
| | | 1 | 2 | 3 | 4 | 5 | 6 | 7 | 8 | 9 | 10 | 11 | 12 | 13 | 14 | 15 | 16 | 17 | 18 | 19 | 20 | 21 | 22 | X |
| GM13139 | + | + | + | + | + | + | + | + | + | + | + | + | + | + | + | + | + | + | + | + | + | + | + | + |
| GM11686 | + | + | + | + | + | + | + | + | + | + | + | + | + | + | + | + | + | + | + | + | + | + | + | + |
| GM10253 | + | + | + | + | + | + | + | + | + | + | + | + | + | + | + | + | + | + | + | + | + | + | + | + |
| GM11687A | + | + | + | + | + | + | + | + | + | + | + | + | + | + | + | + | + | + | + | + | + | + | + | + |
| GM10114 | + | + | + | + | + | + | + | + | + | + | + | + | + | + | + | + | + | + | + | + | + | + | + | + |
| GM11580 | + | + | + | + | + | + | + | + | + | + | + | + | + | + | + | + | + | + | + | + | + | + | + | + |
| GM10791 | + | + | + | + | + | + | + | + | + | + | + | + | + | + | + | + | + | + | + | + | + | + | + | + |
| GM10156B | + | + | + | + | + | + | + | + | + | + | + | + | + | + | + | + | + | + | + | + | + | + | + | + |
| GM10611 | + | + | + | + | + | + | + | + | + | + | + | + | + | + | + | + | + | + | + | + | + | + | + | + |
| GM11688A | + | + | + | + | + | + | + | + | + | + | + | + | + | + | + | + | + | + | + | + | + | + | + | + |
| GM10927 | + | + | + | + | + | + | + | + | + | + | + | + | + | + | + | + | + | + | + | + | + | + | + | + |
| GM10868 | + | + | + | + | + | + | + | + | + | + | + | + | + | + | + | + | + | + | + | + | + | + | + | + |
| GM11689 | + | + | + | + | + | + | + | + | + | + | + | + | + | + | + | + | + | + | + | + | + | + | + | + |
| GM11535 | + | + | + | + | + | + | + | + | + | + | + | + | + | + | + | + | + | + | + | + | + | + | + | + |
| GM11715 | + | + | + | + | + | + | + | + | + | + | + | + | + | + | + | + | + | + | + | + | + | + | + | + |
| GM10567 | + | + | + | + | + | + | + | + | + | + | + | + | + | + | + | + | + | + | + | + | + | + | + | + |
| GM10498 | + | + | + | + | + | + | + | + | + | + | + | + | + | + | + | + | + | + | + | + | + | + | + | + |
| GM12082 | + | + | + | + | + | + | + | + | + | + | + | + | + | + | + | + | + | + | + | + | + | + | + | + |
| GM10612 | + | + | + | + | + | + | + | + | + | + | + | + | + | + | + | + | + | + | + | + | + | + | + | + |
| GM10792 | + | + | + | + | + | + | + | + | + | + | + | + | + | + | + | + | + | + | + | + | + | + | + | + |
| GM13260 | + | + | + | + | + | + | + | + | + | + | + | + | + | + | + | + | + | + | + | + | + | + | + | + |
| GM3854 | + | + | + | + | + | + | + | + | + | + | + | + | + | + | + | + | + | + | + | + | + | + | + | + |
| GM10888 | + | + | + | + | + | + | + | + | + | + | + | + | + | + | + | + | + | + | + | + | + | + | + | + |
| GM06318B | + | + | + | + | + | + | + | + | + | + | + | + | + | + | + | + | + | + | + | + | + | + | + | + |
| GM06317 | + | + | + | + | + | + | + | + | + | + | + | + | + | + | + | + | + | + | + | + | + | + | + | + |
| Number of concordant hybrids | (+/+) | 0 | 0 | 0 | 0 | 0 | 0 | 0 | 0 | 0 | 0 | 1 | 0 | 0 | 0 | 0 | 0 | 0 | 0 | 2 | 0 | 0 | 0 | 0 |
| Number of discordant hybrids | (-/-) | 22 | 22 | 22 | 21 | 22 | 22 | 22 | 22 | 22 | 22 | 22 | 22 | 22 | 22 | 22 | 22 | 22 | 22 | 23 | 23 | 22 | 22 | 22 |
| Percentage discordancy | (+/-) | 2 | 2 | 2 | 2 | 2 | 2 | 2 | 2 | 2 | 2 | 2 | 1 | 2 | 2 | 2 | 2 | 2 | 2 | 0 | 2 | 2 | 2 | 2 |
| | (-/+) | 1 | 1 | 1 | 2 | 1 | 1 | 1 | 1 | 1 | 1 | 1 | 1 | 1 | 1 | 1 | 1 | 1 | 1 | 0 | 1 | 1 | 1 | 1 |
| | | 12 | 12 | 12 | 16 | 12 | 12 | 12 | 12 | 12 | 12 | 8 | 12 | 12 | 12 | 12 | 12 | 12 | 12 | 0 | 12 | 12 | 12 | 12 |

^a + = chromosome present; -- = chromosome absent.



Fig. 4. Localization of the p190-A gene by fluorescence in situ hybridization. Partial metaphase spread counterstained with DAPI showing co-hybridization of both a chromosome 19q-specific telomere probe at the tip of the q arm (red) and the p190-A probe (green) demonstrating p190-A-specific signals in 19q13.2–q13.4.

examined (53%). In each case the hybridization signals were located in the distal region of chromosome 19, 19q13.2–q13.4 (see Fig. 4).

Flanking markers for p190-A were determined by PCR analysis of the Stanford G3 radiation hybrid mapping panel. The localization of p190-A on human chromosome 19 was confirmed, p190-A was linked to the ordered marker D19S851 with a LOD score of 12.32 flanked proximally by marker D19S985 (5 cR) and distally by marker D19S1057 (5 cR) (data not shown). This confirms its localization to the long arm of chromosome 19 and places p190-A within the context of established maps. Furthermore, both marker D19S412, 21 cR (approximately 441 kb) proximal to the D19S851 and marker D19S987 distal to D19S1057 have been mapped to 19q13.3 (for detail, see Fig. 5A). Mapping of the p190-A gene to 19q13.3 using the Stanford G3 radiation hybrid mapping panel is consistent with our FISH localization of the p190-A gene to 19q13.2–q13.4.

A search of human genome databases using the p190-A nucleotide sequence revealed homology to a 111 bp STS, WI-9140, which has been localized to chromosome 19 between D19S219 and D19S418, within the 69–97 cM interval on chromosome 19, 305.3 cR from the top of the chromosome 19 linkage group by WICGR using the GB4 panel (Thomas Hudson, unpublished data found at <http://www.ncbi.nlm.nih.gov/cgi-bin/Schuler/irx2html/dbdtd>) supporting our chromosomal localization.

3.5. Possible deletion of the p190-A gene in human tumors

Interestingly, it has been reported previously that the aberrations at 19q13.3 locus are often found in a variety

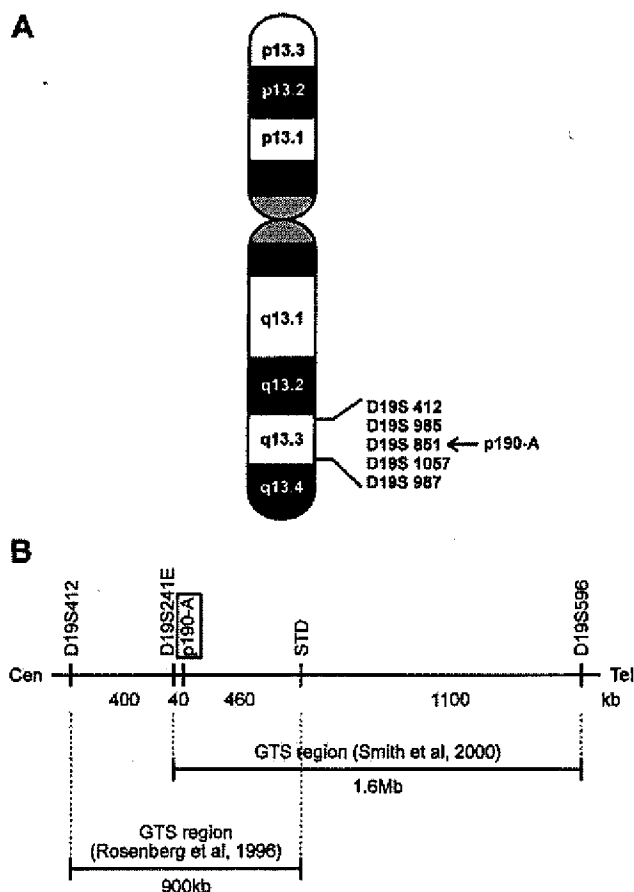


Fig. 5. Mapping of p190-A gene to human chromosomal locus 19q13.3. (A) p190-A in 19q13.3. p190-A gene is linked to the DNA marker D19S851 which is flanked by the markers D19S985 and D19S1057 that have been mapped to the chromosomal locus 19q13.3. (B) p190-A within a common glioma tumor suppressor (GTS) region. p190-A gene is mapped within a common GTS region of 500 kb flanked by markers D19S241E and STD in 19q13.3. The estimated gap between p190-A gene (larger than 21 kb) and D19S241E (Smith et al., 2000) is around 40 kb.

of human solid tumors such as pancreatic carcinomas, gliomas, ovarian cancers and thyroid tumors (Heim and Mitelman, 1995). Furthermore, a glioma tumor suppressor (GTS) gene has also been mapped to 19q13.3, in a 900 kb interval flanked by the two markers D19S412 and STD (Rosenberg et al., 1996; Smith et al., 1999). More recently, a GTS gene has been mapped in a 1.6 Mb region between the new markers D19S241E and D19S596 which flank STD (Smith et al., 2000). In either case, however, the identity of the GTS gene(s) still remains to be determined. As summarized in Fig. 5B, these two GTS gene regions share a common 500 kb interval flanked by D19S241E and STD, and p190-A maps right within this common GTS gene interval. The estimated distance between the marker D19S241E and p190-A (around 40 kb) and the size of p190-A gene (larger than 21 kb) suggest that p190-A gene maps very close to this new marker. Moreover, at least three out

of eight glioblastoma/astrocytoma cases (40%) with break-points in the 19q13.3 locus demonstrate LOH (loss of heterozygosity) of several gene markers including both D19S412 and STD which flank the p190-A gene (Rosenberg et al., 1996), strongly suggesting that the tumor suppressor p190-A is deleted at least in these tumors.

To obtain further, more direct evidence that the p190-A also serves as a tumor suppressor in human as it does in mice (Wang et al., 1997), we are currently screening for some established glioma or other cancer cell lines of human origin in which p190-A gene is deleted, mutated or underexpressed. Once such a human cell line(s) is identified, by overexpressing the wild-type human p190-A gene in these cells, we are able to test whether restoring p190-A gene is sufficient for the reversion of their malignant phenotype in vitro and in vivo. Furthermore, we are developing a p190-A-deficient mouse model to determine which tissues are susceptible to tumorigenesis by the deletion of this gene, and also whether the dysfunction of this gene results in any other phenotypic abnormality during embryonic development.

Acknowledgements

We are grateful to Guo-Fen Tu for her DNA sequencing, Christine Roeder for her technical assistance during the cloning of p190-A genomic DNAs, and Dr. Manjapra Govindan for his information on GRF-1 cDNA and genomic DNAs.

References

- Burbelo, P., Miyamoto, S., Utani, A., Brill, S., Yamada, K., Hall, A., Yamada, Y., 1995. p190-B, a new member of the Rho GAP family, and Rho are induced to cluster after integrin cross-linking. *J. Biol. Chem.* 270, 30919–30926.
- Burbelo, P., Finegold, A., Kozak, C., Yamada, Y., Takami, H., 1998. Cloning, genomic organization and chromosomal assignment of the mouse p190-B gene. *Biochim. Biophys. Acta* 1443, 203–210.
- Chang, J.S., Kobayashi, M., Wang, D., Maruta, H., Iwashita, S., 1995. Two regions with differential growth-modulating activity in the N-terminal domain of RAS GAP: Src homology and Gly-Ala-Pro-rich regions. *Eur. J. Biochem.* 232, 691–699.
- Chomczynski, P., Sacchi, N., 1987. Single-step method of RNA isolation by acid guanidinium thiocyanate-phenol-chloroform extraction. *Anal. Biochem.* 162, 156–159.
- Ellis, C., Moran, M., McCormick, F., Pawson, T., 1990. Phosphorylation of GAP and GAP-associated proteins by transforming and mitogenic Tyr kinases. *Nature* 343, 377–381.
- Freiberg, A., Vogelstein, B., 1983. A technique for radiolabeling DNA restriction endonuclease fragments to high specific activity. *Anal. Biochem.* 132, 6–13.
- Heim, S., Mitelman, F., 1995. *Cancer Cytogenetics: Chromosomal and Molecular Genetic Aberrations of Tumor Cells*. Wiley, New York.
- Jacky, P., 1991. In: Barch, M. (Ed.), *The ACT Cytogenetics Laboratory Manual*. Raven Press, New York, p. 89.
- James, C., Carlsson, E., Dumanski, J., Hansen, M., Nordenskjold, M., Collins, V., Cavence, W., 1988. Clonal genomic alterations in glioma malignancy stages. *Cancer Res.* 48, 5546–5551.
- Lebowitz, P., Davide, J., Prendergast, G., 1995. Evidence that farnesyltransferase inhibitors suppress RAS transformation by interfering with Rho activity. *Mol. Cell Biol.* 15, 6613–6622.
- LeClerc, S., Palaniswami, D., Xie, B., Govindan, M.V., 1991. Molecular cloning and characterization of a factor that binds the human glucocorticoid receptor gene and represses its expression. *J. Biol. Chem.* 266, 17333–17340.
- Lemieux, N., Durillaux, B., Viegas-Pequignot, E., 1992. A simple method for simultaneous R- or G-banding and fluorescence in situ hybridization of small single copy gene. *Cytogenet. Cell Genet.* 59, 311–312.
- Maruta, H., He, H., Tikoo, A., Nur-E-Kamal, M.S.A., 1999. Cytoskeletal tumor suppressors that block oncogenic RAS signaling. *Ann. N. Y. Acad. Sci.* 886, 48–57.
- Morii, N., Kumagai, N., Nur-E-Kamal, M.S.A., Narumiya, S., Maruta, H., 1993. Rho GAP of 28 kDa (GAP2), but not of 190 kDa (p190-A), requires Asp 65 and Asp 67 of Rho GTPase for its activation. *J. Biol. Chem.* 268, 27160–27163.
- Nur-E-Kamal, M.S.A., Kamal, J., Qureshi, M., Maruta, H., 1999. The CDC42-specific inhibitor derived from ACK-1 blocks v-Ha-RAS-induced transformation. *Oncogene* 18, 7787–7793.
- Pinkel, D., Straume, T., Gray, J., 1986. Cytogenetic analysis using quantitative, high-sensitivity fluorescence hybridization. *Proc. Natl. Acad. Sci. USA* 83, 2934–2938.
- Qiu, R.G., Che, J., Kim, D., McCormick, F., Symons, M., 1995. An essential role for Rac in RAS transformation. *Nature* 374, 457–459.
- Qiu, R.G., Abo, A., McCormick, F., Symons, M., 1997. CDC42 regulates anchorage-independent growth and is necessary for RAS transformation. *Mol. Cell Biol.* 17, 3449–3458.
- Rosenberg, J., Lisle, D., Burwick, J., Ueki, K., von Deimling, A., Mohrenweiser, H., Louis, D., 1996. Refined deletion mapping of the chromosomal 19q glioma tumor suppressor gene to the D19S412–STD interval. *Oncogene* 13, 2483–2485.
- Settleman, J., Narasimhan, V., Foster, L., Weinberg, R., 1992. Molecular cloning of cDNAs encoding the GAP-associated protein p190: implications for a signaling pathway from RAS to the nucleus. *Cell* 69, 539–549.
- Smith, J., Alderete, B., Minn, Y., Borell, T., Perry, A., Mohapatra, G., Hosek, S., Kimmel, D., O'Fallon, J., Yates, A., Feuerstein, B., Burger, P., Scheithauer, B., Jenkins, R., 1999. Localization of common deletions on 1p and 19q in human gliomas and their association with histological subtype. *Oncogene* 18, 4144–4152.
- Smith, J., Tachibana, I., Pohl, U., Lee, H.K., Thanarajasingam, U., Portier, B., Ueki, K., Ramaswamy, S., Billings, S., Mohrenweiser, H., Louis, D., Jenkins, R., 2000. A transcript map of the chromosome 19q-arm glioma tumor suppressor region. *Genomics* 64, 44–50.
- Southern, E.M., 1975. Detection of specific sequences among DNA fragments separated by gel electrophoresis. *J. Mol. Biol.* 98, 503–517.
- Stewart, E., McKusick, K., Aggarwal, A., Bajorek, E., Brady, S., et al., 1997. An STS-based radiation hybrid map of the human genome. *Genome Res.* 7, 422–433.
- Tikoo, A., Varga, M., Ramesh, V., Gusella, J., Maruta, H., 1994. An Anti-RAS function of neurofibromatosis type 2 gene product (NF2/Merlin). *J. Biol. Chem.* 269, 23387–23390.
- Wang, D.Z.M., Nur-E-Kamal, M.S.A., Tikoo, A., Montague, W., Maruta, H., 1997. The GTPase and Rho GAP domain of p190-A, a tumor suppressor that binds the RAS GAP of 120 kDa, independently function as anti-RAS tumor suppressors. *Cancer Res.* 57, 2478–2484.

EXHIBIT 3

EMP3, a Myelin-Related Gene Located in the Critical 19q13.3 Region, Is Epigenetically Silenced and Exhibits Features of a Candidate Tumor Suppressor in Glioma and Neuroblastoma

Miguel Alaminos,^{1,2} Verónica Dávalos,¹ Santiago Ropero,¹ Fernando Setién,¹ Maria F. Paz,¹ Michel Herranz,¹ Mario F. Fraga,¹ Jaume Mora,³ Nai-Kong V. Cheung,⁴ William L. Gerald,⁵ and Manel Esteller¹

¹Cancer Epigenetics Laboratory, Molecular Pathology Programme, Spanish National Cancer Centre, Madrid, Spain;

²Department of Histology, Unidad Mixta de Investigaciones Médicas, University Hospital San Cecilio, Granada, Spain;

³Department of Oncology, Hospital Sant Joan de Deu, Barcelona, Spain; and Departments of ⁴Pediatrics and

⁵Pathology, Memorial Sloan-Kettering Cancer Center, New York, New York

Abstract

The presence of common genomic deletions in the 19q13 chromosomal region in neuroblastomas and gliomas strongly suggests the presence of a putative tumor suppressor gene for these neoplasms in this region that, despite much effort, has not yet been identified. In an attempt to address this issue, we compared the expression profile of 89 neuroblastoma tumors with that of benign ganglioneuromas by microarray analysis. Probe sets (637 of 62,839) were significantly down-regulated in neuroblastoma tumors, including, most importantly, a gene located at 19q13.3: the epithelial membrane protein 3 (*EMP3*), a myelin-related gene involved in cell proliferation and cell-cell interactions. We found that *EMP3* undergoes hypermethylation-mediated transcriptional silencing in neuroblastoma and glioma cancer cell lines, whereas the use of the demethylating agent 5-aza-2-deoxycytidine restores *EMP3* gene expression. Furthermore, the reintroduction of *EMP3* into neuroblastoma cell lines displaying methylation-dependent silencing of *EMP3* induces tumor suppressor-like features, such as reduced colony formation density and tumor growth in nude mouse xenograft models. Screening a large collection of human primary neuroblastomas ($n = 116$) and gliomas ($n = 41$), we observed that *EMP3* CpG island hypermethylation was present in 24% and 39% of these tumor types, respectively. Furthermore, the detection of *EMP3* hypermethylation in neuroblastoma could be clinically relevant because it was associated with poor survival after the first 2 years of onset of the disease (Kaplan-Meier; $P = 0.03$) and death of disease (Kendall τ , $P = 0.03$; $r = 0.19$). Thus, *EMP3* is a good candidate for being the long-sought tumor suppressor gene located at 19q13 in gliomas and neuroblastomas. (Cancer Res 2005; 65(7): 2565-71)

Introduction

The most prevalent tumors of the nervous system are gliomas and neuroblastomas. Neuroblastoma, a tumor arising from precursor cells of the peripheral sympathetic nervous system, is the most common extracranial malignant solid tumor of childhood (1, 2), whereas gliomas affect the central nervous system,

particularly in adults, usually with a poor prognosis (3). It is thought that both neuroblastomas and gliomas might arise from neuroectodermal precursor cells (4).

With an overall survival rate of <50%, the prognosis of neuroblastoma patients is highly variable and is associated with many biological and clinical features, including the stage of the disease (5), patient age, tumor ploidy (6), and a series of genetic and epigenetic molecular features of the tumor, such as MYCN amplification (5), 1p deletions, 17q gains, and HOXA9 and RARB2 CpG island hypermethylation (7). Children (>12 months old at diagnosis) with stage IV or stage III tumors with amplification of the oncogene MYCN are at high risk of mortality (>60%), whereas infants (<12 months at diagnosis) with stage IVS disease have the highest survival (nearly 100%) even without treatment (8, 9). On the other hand, gliomas are heterogeneous central nervous system neoplasms. The major subtypes of glioma are astrocytomas and oligodendrogliomas; each subtype has characteristic histologic features and different clinical behaviors. Collectively, these lesions are the most common central nervous system tumors of adults, with nearly 15,000 diagnosed annually in the United States and a mortality approaching 80% within 1 year following diagnosis (10).

One of the common genetic aberrations found in neuroblastoma and glioma is 19q13 loss of heterozygosity (3, 9, 11-16). The heterozygous deletion of 19q13 is particularly characteristic of aggressive neuroblastoma, especially in local-regional recurrent neuroblastoma (9). For gliomas, 19q13 deletions are the only known common genetic alterations shared by all pathologic types (11, 13); gross deletions occur in ~75% of oligodendrogliomas, 45% of mixed oligoastrocytomas, and 40% of astrocytomas (15). Furthermore, 19q13 allelic loss is associated with malignant progression and a poorer prognosis in astrocytomas (14, 16).

All these observations suggest that 19q13 harbors at least one tumor suppressor gene that is important for the development of human primary gliomas and neuroblastomas. However, this putative tumor suppressor gene (or genes) remains unidentified. In this study, we have found that the myelin-related gene epithelial membrane protein 3 (*EMP3*), located in the critical 19q13.3 region, undergoes CpG island promoter-associated silencing in neuroblastomas and gliomas and that their reintroduction into cancer-deficient cell lines has growth inhibitory effects. Furthermore, the presence of *EMP3* CpG island hypermethylation in human primary neuroblastomas is associated with a poor prognosis in these patients. Thus, our findings imply that *EMP3* is a likely candidate for the long-sought tumor suppressor gene in the 19q13 chromosomal region.

Requests for reprints: Manel Esteller, Cancer Epigenetics Laboratory, Spanish National Cancer Centre, Melchor Fernandez Almagro 3, 28029 Madrid, Spain. Phone: 34-917328000; Fax: 34-912246923; E-mail: mesteller@cnio.es.

©2005 American Association for Cancer Research.

Materials and Methods

Cell lines and tumor samples. Nine neuroblastoma, one glioma, and one medulloblastoma cancer cell lines were studied. The neuroblastoma lines used were: LAI-5S (MYCN amplified, S type), LAI-55N (MYCN amplified, N type), LAN-1 (MYCN amplified, N type), SHIN (MYCN nonamplified, I type), SH-EP1 (MYCN nonamplified, S type), and SK-N-BE(2)C (a I-type, MYCN-amplified variant of neuroblastoma established from a relapse tumor sample) kindly provided by R. Ross and B. Spengler of Fordham University (Fordham, NY); SK-N-JD (MYCN amplified, I type) derived in one of our laboratories (Nai-Kong V. Cheung, Memorial Sloan-Kettering Cancer Center, New York, NY), and finally, SK-N-AS (MYCN nonamplified, S type, derived from a bone marrow metastasis) and IMR-32 (N-type and MYCN-amplified, derived from a primary tumor) were purchased from the American Type Culture Collection (Manassas, VA). "N," "I," and "S" stands for neuroblastic, undifferentiated, and Schwannian cell types, respectively. The glioma cell line used was U-87 and the medulloblastoma cell line D283 was also analyzed. Cells were cultured and passaged in RPMI or DME-HG with 10% FCS.

For human primary tumors, we first analyzed 89 neuroblastoma tumors (4 INSS stage I, 13 stage II, 10 stage III, 52 stage IV, and 10 stage IVS) and 10 benign ganglioneuromas by using Affymetrix Genechip Human Genome U95 Set oligonucleotide arrays (62,839 probe sets). For the EMP3 methylation studies, we used DNA from samples corresponding to 116 neuroblastic primary tumors and 41 gliomas obtained at the time of surgery and immediately frozen in liquid nitrogen. The Institutional Review Boards at the Memorial Sloan-Kettering Cancer Center and the Spanish National Cancer Centre approved this research. The neuroblastic tumors corresponded to five ganglioneuromas, six stage IVS, seven stage I, 16 stage II, 16 stage III, and 66 stage IV neuroblastoma tumors. At the mean follow-up time of 76.5 months, 73 patients were alive and 43 patients had died of the disease. Histologic sections of the frozen samples were reviewed by a pathologist, and the areas of high tumor content (>70%) were manually dissected.

Microarray gene expression analysis. Total RNA corresponding to the tumors and cell lines was extracted by using TRIzol reagent (Life Technologies, Inc., Gaithersburg, MD) and purified with the Qiagen RNeasy System (Qiagen, Mississauga, Ontario, Canada), according to the manufacturer's recommendations. Quality and integrity of the RNAs was verified by checking 28S and 18S rRNA after ethidium bromide staining of total RNA samples on 1.2% agarose gel electrophoresis. Total cDNA was synthesized with a T7-polyT primer and a reverse transcriptase (Superscript II, Life Technologies, Inc., Carlsbad, CA), and labeled cRNA were synthesized by *in vitro* transcription with biotinylated UTP and CTP (Enzo Diagnostics, Farmingdale, NY). Labeled nucleic acid target quality was assessed by test 2 arrays and hybridized (45°C for 16 hours) to Affymetrix Human U95 oligonucleotide arrays. After automated washing and staining, absolute values of expression were calculated and normalized from the scanned array by using Affymetrix Microarray Suite (version 5.0). To identify candidate genes that could be silenced in neuroblastoma tumors, we selected genes down-regulated in malignant neuroblastoma and up-regulated in benign ganglioneuroma. The following three gene selection criteria, all of which had to be fulfilled, were used: (a) genes with >3-fold change in expression in comparisons of ganglioneuroma versus neuroblastoma; (b) genes giving a significant probability in a Mann-Whitney test ($P < 0.01$) for comparisons of ganglioneuroma versus neuroblastoma; (c) genes with previously characterized sequences that map at 19q13.3 and have a CpG island associated with their promoter region.

Analysis of EMP3 promoter-associated CpG island methylation status. We determined EMP3 CpG island methylation status by PCR analysis of bisulfite-modified genomic DNA, which induces chemical conversion of unmethylated, but not methylated, cytosine to uracil, using two procedures.

First, methylation status was analyzed by bisulfite genomic sequencing of both strands of the EMP3 CpG island. The primers used were 5'-TAGTATATATTGAGAGGAGAG-3' (sense) and 5'-CTTCCAACTACATATCCCA-3' (antisense), encompassing the transcription start site

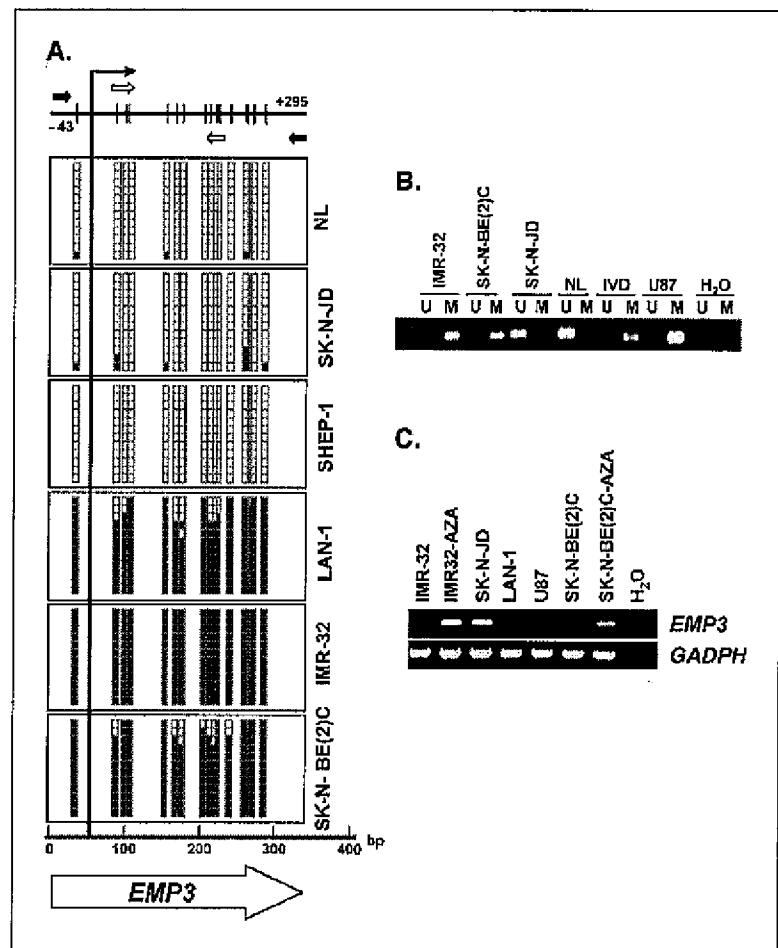
(Fig. 1A). The second analysis used methylation-specific PCR with primers specific for either the methylated or modified unmethylated DNA (17). Primer sequences of EMP3 for the unmethylated reaction were 5'-GAAGAGATGTAGAAGGAGAGTGTAGT-3' (sense) and 5'-CTTATCCCTCAC-TCAAACCTCCATA-3' (antisense) and for the methylated reaction 5'-GACGTAGAAGGAGAGCGAGC-3' (sense) and 5'-CCTCGCTCGAACCTCCGTA-3' (antisense). Primers were located encompassing the transcription start site (Fig. 1A). The annealing temperature for both unmethylated and methylated reactions was 58°C. DNA from normal lymphocytes treated *in vitro* with SssI methyltransferase was used as a positive control for methylated alleles. DNA samples from normal lymphocytes and adrenal medulla were used as a positive control for unmethylated alleles. PCR products were loaded onto nondenaturing 3% polyacrylamide gels, stained with ethidium bromide, and visualized under a UV-transilluminator.

EMP3 reverse transcriptase-PCR and treatment with the demethylating agent 5-aza-2-deoxycytidine. RNA was isolated using TRIzol (Life Technologies, Gaithersburg, MD). Two micrograms of RNA were reverse transcribed using SuperScript II reverse transcriptase (Life Technologies, Gaithersburg, MD) and amplified using specific primers for EMP3 5'-CTTATCTGCTTTTCGTGGCCAC-3' (forward) and 5'-GATGAAGGAGAGACAGCAGAGAATGAG-3' (reverse). PCR was done for 35 cycles (94°C for 30 seconds, 57°C for 30 seconds, and 72°C for 30 seconds) in a final volume of 25 μ L containing 1 \times PCR buffer (Life Technologies, Gaithersburg, MD), 1.5 mmol/L MgCl₂, 0.3 mmol/L deoxynucleotide triphosphate, 0.25 mmol/L of each primer, and 2 units Taq polymerase (Life Technologies, Gaithersburg, MD). Reverse transcriptase-PCR (RT-PCR) primers were designed between exons 1 and 3, encompassing large introns to avoid any amplification of genomic DNA. Glyceraldehyde-3-phosphate dehydrogenase was used as an internal control to ensure cDNA quality and loading accuracy. The amplification products were resolved by 2% agarose gel electrophoresis and visualized by ethidium bromide staining. The cell lines were treated with 2 μ mol/L 5-aza-2'-deoxycytidine (Sigma, St. Louis, MO) for 3 days to achieve demethylation, as previously described (18).

EMP3 transfection and colony formation assay. The EMP3 expression vector pCMV-EMP3 was constructed by cloning the cDNA corresponding to the gene *EMP3* in pCMVtag3A vectors (Stratagene, La Jolla, CA) under the control of a cytomegalovirus (CMV) immediate-early promoter. Primers used for amplification of the four exons of the *EMP3* gene from total RNA of the EMP3-expressing neuroblastoma cell line SK-N-AS were 5'-GCGGATCCGATGTCACCTCTTGCTG-3' and 5'-CAGAATCTTTTGGAGGACGC GCGGCA-3'. The pCMV-EMP3 expression vector was transfected into the IMR-32 cells by lipofection. Briefly, cells were seeded in a 6-well plate 1 day before transfection at a density of 2×10^5 cells per well. Two milligrams of purified plasmid DNA were transfected with LipofectAMINE Plus reagent, according to the manufacturer's recommendations. The experiment was repeated thrice. Twenty-four hours after transfection, β -gal activity was measured in the cells carrying the control vector using a β -gal activity kit. Clones expressing the transfected proteins were selected in complete medium supplemented with 1 mg/mL G418, 48 hours post-transfection. Stable clones were maintained in complete medium with G418 (800 mg/mL). Total RNA from individual clones was extracted and RT-PCR was done to confirm that the clones were expressing the transfected genes. IMR-32 cells were also transfected with the vector containing no inserts, and stable clones were isolated. As a positive control we transfected wild-type *p16^{INK4a}* (pLPC-hp16 wt-HA-puromycin provided by Dr. Manuel Serrano, Molecular Oncology Program, Spanish National Cancer Centre, Madrid, Spain), a well known tumor suppressor gene that is lost in IMR-32 cells, and as a negative control we transfected a mutant *p16^{INK4a}*, a form without tumor suppressor growth activity (pLPC-hp16 mut-HA-M53L-puromycin, also provided by Dr. Manuel Serrano). After ~16 days of selection, stable G418-resistant colonies were fixed, stained with 2% methylene blue in 60% methanol, and the average number of colonies present in each well was determined.

Mouse xenograft model. Six-week-old female athymic nude mice *nu/nu* (Harlan Sprague-Dawley, Indianapolis, IN), housed under specific pathogen-free conditions (Institutional Animal Welfare Committee Agreement), were used for LAN-1 tumor xenografts. Five specimens were used. Both flanks of each animal were injected s.c. with 10^6 cells in a total volume of 200 μ L of PBS.

Figure 1. A, analysis of EMP3 CpG island promoter methylation status in human cancer cell lines. Top, schematic depiction of the EMP3 CpG island around the transcription start sites (long black arrows). CpG dinucleotides (short vertical lines). Location of bisulfite genomic sequencing PCR primers (black arrows) and methylation-specific PCR primers (white arrows). Results of bisulfite genomic sequencing of 12 individual clones for five human cancer cell lines and normal lymphocytes (NL). Presence of a methylated cytosine (black square) and presence of an unmethylated cytosines (white square). B, methylation-specific PCR for the EMP3 gene in cancer cell lines. Lane M, methylated genes; lane U, unmethylated genes. Normal lymphocytes (NL) and *in vitro* methylated DNA (IVD) are used as negative and positive control for unmethylated and methylated genes, respectively. C, EMP3 CpG island methylation is associated with EMP3 gene silencing. RT-PCR analysis of EMP3 expression. The EMP3 hypermethylated cell lines IMR-32, LAN-1, U-87, and SK-N-BE(2)C do not express the EMP3 transcript. The treatment with the demethylating agent reactivates *EXT1* gene expression (lanes IMR-32-AZA and SK-N-BE(2)C-AZA). EMP3 unmethylated cell line SK-N-JD as a positive control for EMP3 expression. GAPDH expression as loading control.



The right flank was always used for EMP3-transfected LAN-1 cells and the left for empty vector LAN-1 control cells. Tumor development at the site of injection was evaluated daily. Animals were sacrificed at 30 days. The tumors were then excised and weighed.

Statistical analysis. For the analysis of the microarray data, average expression corresponding to neuroblastomas or ganglioneuromas was calculated for each probe set. The mean expression ratio was then calculated by dividing the mean expression of ganglioneuroma by that of neuroblastoma. The Mann-Whitney test was used to identify probe sets that were differentially expressed in the compared groups. Fisher's exact test was used to examine the association of EMP3 CpG island methylation and clinical subgroups. The Kaplan-Meier log-rank test was used to determine the association between methylation and survival in primary tumors. Correlation between the methylation status of EMP3 and survival was estimated by Kendall's τ . Values of $P < 0.05$ were considered significant for all tests.

Results

EMP3 gene expression is down-regulated in primary neuroblastoma tumors. Our goal was to find a candidate gene located in the neuroblastoma and glioma critical 19q13 region undergoing methylation-associated silencing. To this end, we first studied the microarray expression pattern of 89 neuroblastoma tumors (4 INSS stage I, 13 stage II, 10 stage III, 52 stage IV, and 10 stage IVS) and 10 ganglioneuromas by using Affymetrix Genechip Human Genome U95 Set oligonucleotide arrays (62,839 probe sets), looking for underexpressed genes in the neuroblastoma tumors located at the 19q13 chromosomal hotspot. The analysis of the microarray data

revealed 637 transcripts in neuroblastoma that were significantly down-regulated relative to benign tumor ganglioneuromas. Of these underexpressed sequence genes, only six were located at the 19q13 chromosomal locus: *EMP3*, related ras viral oncogene homologue (*RRAS*), Fc fragment of the IgG receptor transporter (*FCGRT*), *NRIH1*, nucleobindin 1 (*NUCB1*), nuclear receptor subfamily 1 group H member 2 (*NRIH2*), and selenoprotein W1 (*SEPW1*). Most importantly, the *EMP3* gene was the only one with over 3-fold down-regulation that contained a CpG island. The *EMP3* gene is a member of the peripheral myelin protein 22 family (19), encoding a four-transmembrane domain protein involved in cell proliferation and cell-cell interactions (19, 20) and has been mapped at the critical region 19q13.3 (21).

EMP3 CpG island hypermethylation in neuroblastoma and glioma cell lines and its association with transcriptional gene silencing. *EMP3* is a candidate gene for hypermethylation-associated inactivation in human cancer because a 5'-CpG island is located around the transcription start site of each gene (Fig. 1A). To analyze the methylation status of the promoter-associated CpG island of *EMP3*, we screened nine neuroblastoma and two glioma cell lines using bisulfite genomic sequencing and methylation-specific PCR targeted to the area surrounding its transcription start site, as described in Materials and Methods. *EMP3* CpG island promoter hypermethylation was found in three neuroblastoma cell lines, SK-N-BE(2)C, IMR-32, and LAN-1 and one glioma cell line, U-87. The remaining neuroblastoma and medulloblastoma cell lines, LAI-5S, LAI-55N, SHIN, SH-EP1, SK-N-JD, SK-N-AS, and D283,

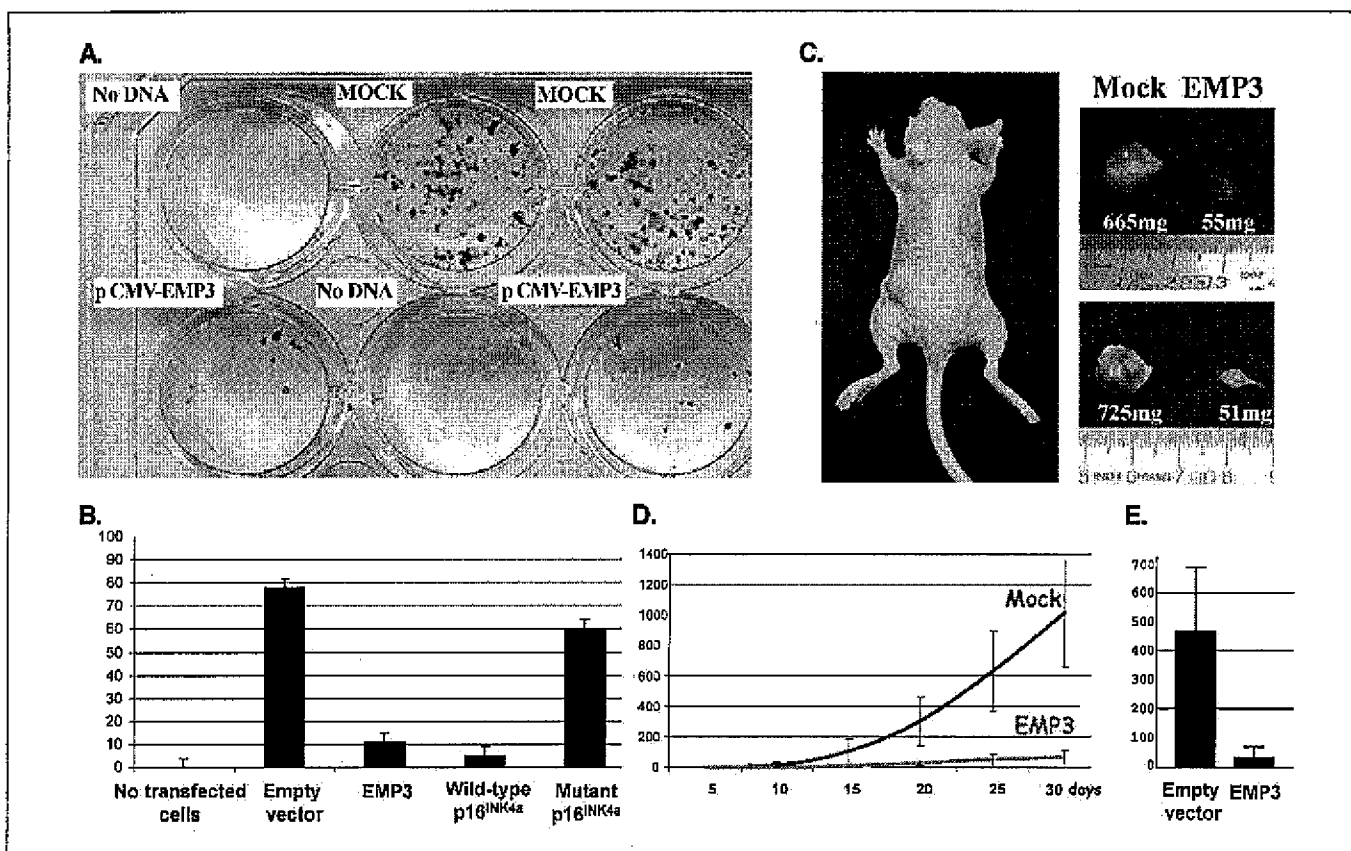


Figure 2. Tumor suppressor-like properties of EMP3 reintroduction. **A**, example of colony focus assay in IMR-32 neuroblastoma cells after a 2-week selection of G418 and staining with methylene blue. **B**, quantitation of the number of G418-selected IMR-32 colonies using no transfected empty vector (mock), EMP3, wild-type p16^{INK4a}, and mutant p16^{INK4a}. Average of three independent experiments. **C**, female athymic nude mice 30 days after injection of 10⁶ LAN-1 cells (left). Note the large tumor on the left flank, corresponding to empty vector-LAN-1 cells and the small tumor on the opposite flank, corresponding to EMP3-LAN-1 cell injection. Tumors were excised cautiously to avoid skin contamination and then weighed. Tumor detail in cm and weight in mg. **D**, effect of EMP3 transfection on the *in vivo* growth of LAN-1 cells. Tumor size was monitored over time and size in mm³. **E**, tumoral weight data at 30 days from empty vector and EMP3 transfected LAN-1 xenografts. Columns, means; bars, \pm SD.

were unmethylated at the EMP3 CpG island. All normal tissues analyzed, including lymphocytes and adrenal medulla, were completely unmethylated at the EMP3 CpG island promoter. These results were confirmed by bisulfite genomic sequencing and methylation-specific PCR (Fig. 1A and B).

Having noted EMP3 promoter hypermethylation in the described cancer cell lines, we assessed the association between this epigenetic aberration and the putative transcriptional inactivation of the EMP3 gene at the RNA level. The neuroblastoma and glioma cell lines SK-N-BE(2)C, IMR-32, LAN-1, and U-87, hypermethylated at the EMP3 CpG island, did not express any EMP3 RNA transcript, as determined by RT-PCR (Fig. 1C). However, the remaining neuroblastoma and glioma cell lines and normal lymphocytes, unmethylated at the EMP3 promoter, strongly expressed EMP3 (Fig. 1C). We established a further link between EMP3 CpG island hypermethylation and its gene silencing by the treatment of the methylated neuroblastoma and glioma cell lines with a DNA demethylating agent. The treatment of the IMR-32, LAN-1, and U-87 cell lines with the demethylating drug, 5-aza-2'-deoxycytidine, restored expression of the EMP3 RNA transcript (Fig. 1C).

Reintroduction of EMP3 in deficient neuroblastoma cell lines has tumor suppressor-like properties in colony formation assays and mouse tumor xenografts. Although the potential features of EMP3 in cell proliferation have been

proposed before, we assayed the ability of EMP3 to function as a suppressor of tumor growth in our model, using IMR-32 and LAN-1, two neuroblastoma cell lines with EMP3 methylation-associated silencing.

We first tested the inhibitory abilities of EMP3 in IMR-32 cells using a colony-focus assay with G418 selection after transfection with the EMP3 gene (pCMV-EMP3) or the empty vector, as described in Materials and Methods. EMP3 expression was monitored by RT-PCR. EMP3 reexpression in IMR-32 cells showed tumor-suppressing activity with markedly less colony formation than with the empty vector (Fig. 2A). An average of 11 colonies formed when the gene EMP3 was transfected, compared with an average of 78 cell colonies formed in the control empty vector-transfected cells (Mann-Whitney test, $P < 0.001$; Fig. 2B). Additionally, as internal controls, we used vectors for the bona fide tumor suppressor gene p16^{INK4a} and an inactive, mutant form of this gene in the transfection assays. An average of five colonies grew after transfection of the tumor suppressor gene p16^{INK4a}, whereas 60 colonies appeared when IMR-32 cells were transfected with the mutant form of the gene (Fig. 2B). This implies that the growth inhibitory effect of EMP3 transfection is similar to that of p16^{INK4a} transfection.

We next tested the ability of the other EMP3-methylated neuroblastoma cell line, LAN-1, to form tumors in nude mice

comparing EMP3-transfected LAN-1 cells with empty vector-transfected LAN-1 cells. The same mice were s.c. injected with 10^6 EMP3 (right flank) and empty vector-transfected (left flank) LAN-1 cells (Fig. 2C). All mice were killed 30 days after injection and the tumors were dissected and weighed. LAN-1 cells transfected with the empty vector formed tumors rapidly, but cells transfected with the EMP3 expression vector had much lower tumorigenicity (Fig. 2D). At the time of sacrifice, tumors were 20 times larger in those mice with the empty vector, 481.7 ± 176.4 mg, than in xenografts arising in mice transfected with EMP3, 21.8 ± 18.4 mg (Mann-Whitney test, $P < 0.001$; Fig. 2E).

EMP3 is hypermethylated in primary neuroblastomas and gliomas and is a predictor of poor outcome. Once the functional consequences of EMP3 CpG island hypermethylation had been determined, we considered the relevance of EMP3 methylation in human primary tumors by studying a large set of human primary neuroblastomas and gliomas. EMP3 CpG island hypermethylation was found in 24.1% of neuroblastomas (28 of 116) and in 39% of gliomas (16 of 41; Fig. 3A). For gliomas, EMP3 hypermethylation was independent of the age of onset and sex of the patient and the histologic type, being present in glioblastomas and anaplastic astrocytomas. We had previously characterized neuroblastoma tumors for loss of heterozygosity at 19q13, 1p36, 1p22, and 11q, gain of 17q and MYCN amplification (9, 22–24), all of which are putative molecular prognostic factors for this tumor type. Most importantly, the only genetic defect associated with EMP3 hypermethylation was the loss of heterozygosity at 19q13.3 (Fisher's exact test, $P = 0.004$), which is the exact chromosomal region where EMP3 is located, once again suggesting a role for EMP3 as the putative tumor suppressor gene confined to this locus.

We next determined whether or not there was a relationship between the hypermethylation status of the gene EMP3 and the outcome of neuroblastoma patients (this clinical information was not available for the gliomas). First, we confirmed that our studied cases were representative of the general population of neuroblastic tumors. Indeed, noninfant patients of the cohort had poorer survival than infant patients (Kaplan-Meier log-rank, $P = 0.006$; Fig. 3B) and patients with MYCN-amplified tumors had poorer survival than patients without MYCN amplification (Kaplan-Meier log-rank, $P < 0.001$; Fig. 3B), as expected (1, 5, 25, 26). With respect to EMP3, we found that EMP3 promoter-associated CpG island hypermethylation was significantly associated with death of disease (Kendall τ , $P = 0.030$; $r = 0.190$; Fig. 3B). In this context, mortality was higher in the group of tumors with methylated EMP3 than in the group with the unmethylated gene (53.6% deceased cases when EMP3 was methylated versus 31.8% when the gene was unmethylated). This association was also found when the cases were stratified by stage: for both local-regional and metastatic neuroblastomas, the percentage of deceased patients was higher in tumors with methylated EMP3 (33.3% for local-regional and 78.6% for stage IV) than in tumors with unmethylated EMP3 (13.3% for local-regional and 46.1% for stage IV). Furthermore, EMP3 promoter hypermethylation was significantly associated with poor survival in patients that remained alive after 2 years follow-up (Kaplan-Meier, $P = 0.030$) for all stages (Fig. 3B), and for all stage IV patients (Kaplan-Meier, $P = 0.030$; Fig. 3B). Thus, EMP3 CpG island hypermethylation is a likely predictor of poor outcome in neuroblastoma patients.

Discussion

Loss of 19q13 is commonly found in human malignant gliomas (1, 3, 11–16) and neuroblastomas (9, 23, 27) associated with a specific clinical behavior and survival rate for both tumor types. Indeed, our own previous data indicated an association between specific 19q13.3 loss of heterozygosity and progressing neuroblastoma tumors with poor survival and lack of response to standard cytotoxic therapy (9). Thus, it has been of considerable interest to identify the putative tumor suppressor gene (or genes) from this candidate region of the long arm of chromosome 19 (27–29). So far, the numerous studies based on classic genetic techniques have failed to localize the tumor suppressor gene of the 19q13 region. In the present study, we adopted a double strategy to address this matter, combining the use of genetic expression approaches using microarrays and epigenetic analysis of CpG island hypermethylation. A comprehensive expression analysis in a large cohort of neuroblastic tumors revealed that only one gene located at the critical region 19q13.3 was consistently down-regulated in neuroblastomas, the myelin-related gene EMP3.

EMP3 belongs to the peripheral myelin protein 22-kDa (PMP22) gene family (also known as the TMP gene family), which includes four closely related members, PMP22, EMP3, EMP2, and EMP1, and an additional, more distant, member, MP20 (19, 20). The EMP3 gene encodes a 163-amino acid protein of 18 kDa containing four transmembrane domains and two N-linked glycosylation sites in the first extracellular loop. The EMP3 protein sequence is similar to that of PMP22, EMP1, and EMP2 in 33% to 43% of amino acids, with the greatest homology found in the transmembrane domains. PMP22 is the best-characterized member of the family. It is a major component of myelin and is produced predominantly by Schwann cells (30). PMP22 is most highly expressed in peripheral nerves, where it plays a crucial role in physiologic and pathologic processes in the peripheral nervous system. Genetic alterations in the PMP22 gene, including duplications, deletions, and point mutations, are responsible for several forms of hereditary peripheral neuropathies, including Charcot-Marie-Tooth disease type 1A, Dejerine-Sottas syndrome, and hereditary neuropathy with liability to pressure palsies (30). In contrast, the functions of the product of the gene EMP3 are not fully known. However, based on the homology with PMP22, which is strongly expressed during growth arrest (20), EMP3 is thought to be involved in cell proliferation and cell-cell interactions (19, 20). Our demonstration that EMP3 reintroduction in deficient cancer cells reduces colony formation and tumor growth in xenografts also implies a tumor suppressor function for the EMP3 gene.

Transcriptional inactivation of tumor suppressor genes by associated promoter CpG island hypermethylation is now recognized as a common feature of human tumors (31–33). Hypermethylation of these loci is known to give rise to particular profiles according to the tumor type (34, 35). For gliomas, several genes are known to undergo this epigenetic alteration, including the DNA repair gene, MGMT, and the cell cycle inhibitor, p16^{INK4a} (36–38), whereas for neuroblastoma CpG island hypermethylation, among others, have been described for the tumor necrosis factor receptors (39) and the developmental gene HOXA9 (7). In the particular case of neuroblastic tumors, a particular clustering of CpG island hypermethylation may allow

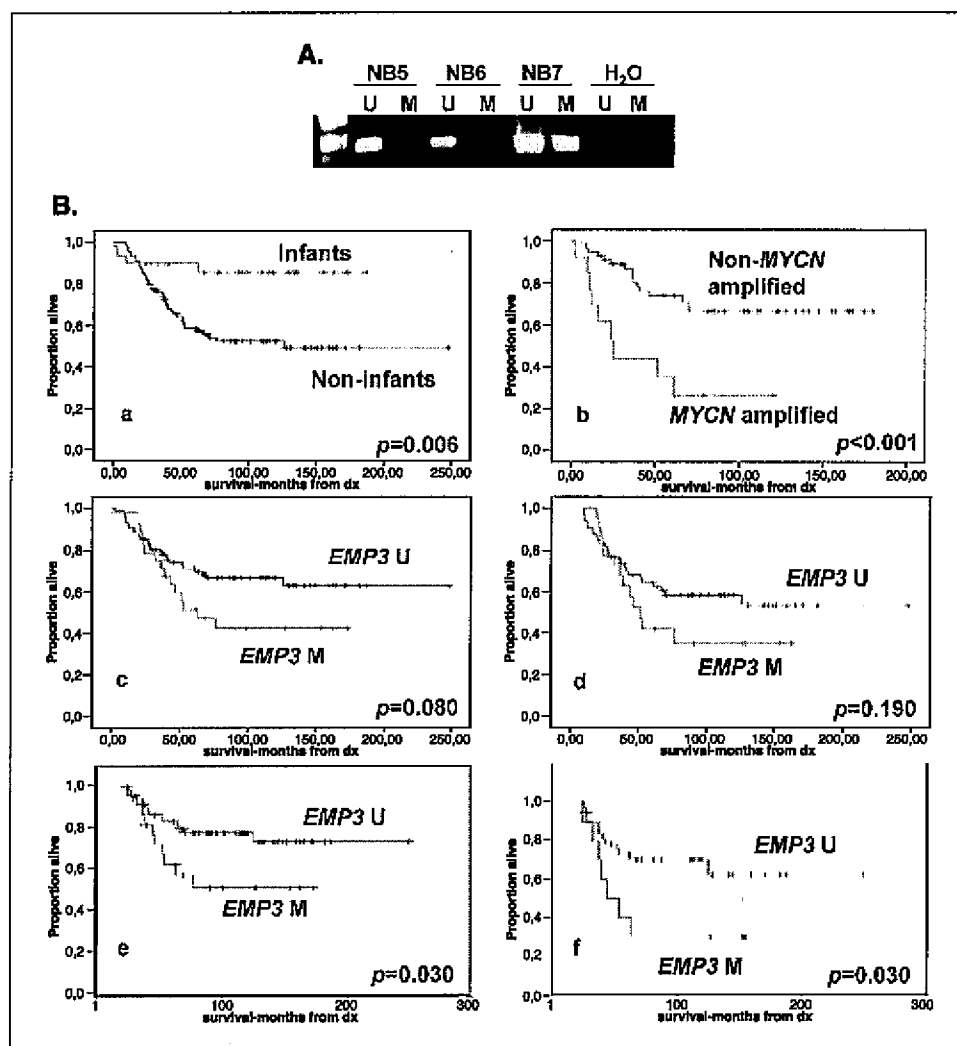


Figure 3. Clinical effect of EMP3 CpG island hypermethylation in neuroblastomas. **A**, methylation-specific PCR analysis of the *EMP3* gene in primary neuroblastomas. Lane M, methylated genes; lane U, unmethylated genes. **B**, bottom, Kaplan-Meier survival curves for the different comparisons described in the article: (a) comparison of infant (<12 months old at diagnosis) versus noninfant patients (>12 months old at diagnosis); (b) MYCN-amplified versus MYCN-unamplified tumors; (c) cases with EMP3 hypermethylation versus cases with unmethylated EMP3 for all 116 patients included in the study; (d) patients with EMP3 promoter hypermethylation versus patients with unmethylated EMP3 for noninfant patients only; (e) patients with methylated EMP3 versus patients with unmethylated EMP3 for all children that survived after 24 months of follow-up; (f) patients with methylated EMP3 versus patients with unmethylated EMP3 for stage IV neuroblastoma cases that survived after 24 months of follow-up. U, unmethylated EMP3; M, methylated EMP3.

the classification of these patients into clinically relevant subgroups (7). However, only one other gene located at 19q13 has been reported to have methylation-associated silencing in a subtype of glioma (oligodendroglioma), the *ZNF342* gene that encodes a putative zinc finger protein (40). This is a very interesting observation and suggests that the high rate of loss of heterozygosity observed in these tumors could be related to the presence not only of one putative tumor suppressor gene but at least two: *ZNF342* and *EMP3*.

Finally, from a clinical standpoint, it is worth emphasizing the relevance of *EMP3* hypermethylation as a marker of poor outcome in neuroblastoma patients. The analysis of the cell lines provided the first indication of this: *EMP3* hypermethylation was restricted to those neuroblastoma cell lines of great malignant potential, with a high proliferation rate, *MYCN* gene amplification and belonging to the undifferentiated (I) or neuroblastic (N) cell types, whereas none of the less malignant cell lines with the Schwannian cell-type phenotype (S) or without *MYCN* amplification had *EMP3* hypermethylation. Most importantly, in the primary neuroblastoma tumors, *EMP3* hypermethylation is one of the first markers to predict poor prognosis after the first 2 years of onset of the disease. This finding is especially significant

because most of the currently available clinical factors and molecular markers of poor prognosis in neuroblastoma (such as *MYCN* amplification, advanced age or stage, and diploidy), are associated with a rapid tumor progression (2) and an increased short-term mortality, and currently it is difficult to predict the outcome of patients lacking these markers of poor prognosis after 2 years of the diagnosis.

In conclusion, our findings indicate a role for CpG island hypermethylation-silencing of the myelin-related gene *EMP3* in the development of neuroblastomas and gliomas. *EMP3* also exhibits tumor suppressor features and is located in the 19q13 critical region of loss of heterozygosity in both tumor types. Furthermore, for neuroblastomas, the presence of *EMP3* hypermethylation is a prognostic factor of poor outcome in these patients. These observations warrant further research to elucidate *EMP3* function in normal cells and dysfunction in cancer cells.

Acknowledgments

Received 11/30/2004; revised 1/17/2005; accepted 1/27/2005.

The costs of publication of this article were defrayed in part by the payment of page charges. This article must therefore be hereby marked advertisement in accordance with 18 U.S.C. Section 1734 solely to indicate this fact.

References

1. Castleberry RP. Neuroblastoma. *Eur J Cancer* 1997;33:1430-7.
2. Schwab M, Westermann F, Hero B, Berthold F. Neuroblastoma: biology and molecular and chromosomal pathology. *Lancet Oncol* 2003;4:472-80.
3. Cairncross JG, Ueki K, Zlatescu MC, et al. Specific genetic predictors of chemotherapeutic response and survival in patients with anaplastic oligodendrogliomas. *J Natl Cancer Inst* 1998;90:1473-9.
4. Ueki K, Ramaswamy S, Billings SJ, Mohrenweiser HW, Louis DN. ANOVA, a putative astrocytic RNA-binding protein gene that maps to chromosome 19q13.3. *Neurogenetics* 1997;1:31-6.
5. Brodeur GM, Maris JM. Neuroblastoma. In: Pizzo PA, Poplack DG, editors. *Principles and practice of pediatric oncology*. Philadelphia: Lippincott; 2002. p. 895-937.
6. Look AT, Hayes FA, Shuster JJ, et al. Clinical relevance of tumor cell ploidy and *N-myc* gene amplification in childhood neuroblastoma: a Pediatric Oncology Group study. *J Clin Oncol* 1991;9:581-91.
7. Alaminos M, Davalos V, Cheung NK, Gerald WL, Esteller M. Clustering of gene hypermethylation associated with clinical risk groups in neuroblastoma. *J Natl Cancer Inst* 2004;96:1208-19.
8. Brodeur GM, Pritchard J, Berthold F, et al. Revisions of the international criteria for neuroblastoma diagnosis, staging, and response to treatment. *J Clin Oncol* 1993;11:1466-77.
9. Mora J, Cheung NK, Chen L, Qin J, Gerald W. Loss of heterozygosity at 19q13.3 is associated with locally aggressive neuroblastoma. *Clin Cancer Res* 2001;7:1358-61.
10. Levin VA, Gutin PH, Leibel S. Neoplasms of the central nervous system. In: DeVita VT Jr, Hellman S, Rosenberg SA, editors. *Cancer principles and practice of oncology*. Philadelphia: Lippincott; 1993. p. 1679-737.
11. Bello MJ, Leone PE, Vaquero J, et al. Allelic loss at 1p and 19q frequently occurs in association and may represent early oncogenic events in oligodendroglial tumors. *Int J Cancer* 1995;64:207-10.
12. Fallon KB, Palmer CA, Roth KA, et al. Prognostic value of 1p, 19q, 9p, 10q, and EGFR-FISH analyses in recurrent oligodendrogliomas. *J Neuropathol Exp Neurol* 2004;63:314-22.
13. Maintz D, Fiedler K, Koopmann J, et al. Molecular genetic evidence for subtypes of oligoastrocytomas. *J Neuropathol Exp Neurol* 1997;56:1098-104.
14. Ohgaki H, Schauble B, zur Hausen A, von Ammon K, Kleihues P. Genetic alterations associated with the evolution and progression of astrocytic brain tumours. *Virechows Arch* 1995;427:113-8.
15. Smith JS, Alderete B, Minn Y, et al. Localization of common deletion regions on 1p and 19q in human gliomas and their association with histological subtype. *Oncogene* 1999;18:4144-52.
16. Smith JS, Tachibana I, Lee HK, et al. Mapping of the chromosome 19 q-arm glioma tumor suppressor gene using fluorescence *in situ* hybridization and novel microsatellite markers. *Genes Chromosomes Cancer* 2000;29:16-25.
17. Herman JG, Graff JR, Myohanen S, Nelkin BD, Baylin SB. Methylation-specific PCR: a novel PCR assay for methylation status of CpG islands. *Proc Natl Acad Sci U S A* 1996;93:9821-6.
18. Esteller M, Tortola S, Toyota M, et al. Hypermethylation-associated inactivation of p14(ARF) is independent of p16(INK4a) methylation and p53 mutational status. *Cancer Res* 2000;60:129-33.
19. Taylor V, Suter U. Epithelial membrane protein-2 and epithelial membrane protein-3: two novel members of the peripheral myelin protein 22 gene family. *Gene* 1996;175:115-20.
20. Ben-Porath I, Benvenisty N. Characterization of a tumor-associated gene, a member of a novel family of genes encoding membrane glycoproteins. *Gene* 1996;183:69-75.
21. Liehr T, Kühlenbaumer G, Wulf R, et al. Regional localization of the human epithelial membrane protein genes 1, 2, and 3 (EMP1, EMP2, EMP3) to 12p12.3, 16p13.2, and 19q13.3. *Genomics* 1999;58:106-8.
22. Mora J, Cheung NK, Kushner BH, et al. Clinical categories of neuroblastoma are associated with different patterns of loss of heterozygosity on chromosome arm 1p. *J Mol Diagn* 2000;2:37-46.
23. Mora J, Gerald WL, Cheung NK. Evolving significance of prognostic markers associated with new treatment strategies in neuroblastoma. *Cancer Lett* 2003;197:119-24.
24. Alaminos M, Mora J, Cheung NK, et al. Genome-wide analysis of gene expression associated with MYCN in human neuroblastoma. *Cancer Res* 2003;63:4538-46.
25. Seeger RC, Brodeur GM, Sather H, et al. Association of multiple copies of the *N-myc* oncogene with rapid progression of neuroblastomas. *N Engl J Med* 1985;313:1111-6.
26. Schwab M. MYCN in neuronal tumours. *Cancer Lett* 2004;204:179-87.
27. Hartmann C, Johnk L, Kitange G, et al. Transcript map of the 3.7-Mb D19S112-D19S246 candidate tumor suppressor region on the long arm of chromosome 19. *Cancer Res* 2002;62:4100-8.
28. Rubio MP, Correa KM, Ueki K, et al. The putative glioma tumor suppressor gene on chromosome 19q maps between APOC2 and HRC. *Cancer Res* 1994;54:4760-3.
29. Rosenberg JE, Lisle DK, Burwick JA, et al. Refined deletion mapping of the chromosome 19q glioma tumor suppressor gene to the D19S412-STD interval. *Oncogene* 1996;13:2483-5.
30. Jettan AM, Suter U. The peripheral myelin protein 22 and epithelial membrane protein family. *Prog Nucleic Acid Res Mol Biol* 2000;64:97-129.
31. Jones PA, Laird PW. Cancer epigenetics comes of age. *Nat Genet* 1999;21:163-7.
32. Esteller M. CpG island hypermethylation and tumor suppressor genes: a booming present, a brighter future. *Oncogene* 2002;21:5427-40.
33. Herman JG, Baylin SB. Gene silencing in cancer in association with promoter hypermethylation. *N Engl J Med* 2003;349:2042-54.
34. Costello JF, Fruhwald MC, Smiraglia DJ, et al. Aberrant CpG-island methylation has non-random and tumour-type-specific patterns. *Nat Genet* 2000;24:132-8.
35. Esteller M, Corn PG, Baylin SB, Herman JG. A gene hypermethylation profile of human cancer. *Cancer Res* 2001;61:3225-9.
36. Esteller M, Garcia-Foncillas J, Andion E, et al. Inactivation of the DNA-repair gene MGMT and the clinical response of gliomas to alkylating agents. *N Engl J Med* 2000;343:1350-4.
37. Merlo A, Herman JG, Mao L, et al. 5' CpG island methylation is associated with transcriptional silencing of the tumour suppressor p16/CDKN2/MTS1 in human cancers. *Nat Med* 1995;1:686-92.
38. Costello JF, Berger MS, Huang HS, Cavenee WK. Silencing of p16/CDKN2 expression in human gliomas by methylation and chromatin condensation. *Cancer Res* 1996;56:2405-10.
39. van Noesel MM, van Bezouw S, Salomons GS, et al. Tumor-specific down-regulation of the tumor necrosis factor-related apoptosis-inducing ligand decoy receptors DCR1 and DCR2 is associated with dense promoter hypermethylation. *Cancer Res* 2002;62:2157-61.
40. Hong C, Bollen AW, Costello JF. The contribution of genetic and epigenetic mechanisms to gene silencing in oligodendrogliomas. *Cancer Res* 2003;63:7600-5.

EXHIBIT 4

Polymorphisms in *GLTSCR1* and *ERCC2* Are Associated with the Development of Oligodendrogliomas

Ping Yang, M.D., Ph.D.¹

Thomas M. Kolmeyer, M.S., M.B.A.²

Kristin Buckner²

William Bamlet, M.S.¹

Karla V. Ballman, Ph.D.¹

Robert B. Jenkins, M.D., Ph.D.²

¹ Department of Health Sciences Research, Mayo Clinic and Foundation, Rochester, Minnesota.

² Department of Laboratory Medicine and Pathology, Mayo Clinic and Foundation, Rochester, Minnesota.

Supported by Grants CA85779 (to Robert B. Jenkins), CA80127 (to Ping Yang), and CA15083 (to Robert B. Jenkins) from the National Cancer Institute.

The consensus pathologic diagnosis of the cases was determined by Caterina Giannini, Bernd Scheithauer, Peter Burger, Allan Yates, Andrew Bollen, and Kenneth Aldape—neuropathologists who are active participants in the program project Grant CA85779. The authors thank them for their careful review of the cases.

Secretarial assistance was provided by Ms. Heidi Bollum and Miss Susan Ernst.

Address for reprints: Ping Yang, M.D., Ph.D., Department of Health Sciences Research, Mayo Clinic College of Medicine, 200 First Street SW, Rochester, MN 55905; Fax: (507) 266-2478; E-mail: yang.ping@mayo.edu

Received August 5, 2004; revision received January 6, 2005; accepted January 13, 2005.

BACKGROUND. Deletions of 19q have been associated with gliomas, especially oligodendrogliomas. In addition, cases with oligodendrogliomas with the 19q deletion have been observed to have a better survival compared with cases without the 19q deletion. The authors have previously described a 150-kilobase minimal deletion region in gliomas that maps to 19q13.33 and contains 3 novel candidate genes (*GLTSCR1*, *EHD2*, and *GLTSCR2*).

METHODS. The authors performed an association study using 141 cases with gliomas (61 cases with astrocytomas, 40 cases with oligodendrogliomas, 40 cases with mixed oligoastrocytomas) and 108 general controls. They evaluated 7 single nucleotide polymorphisms (SNPs) in 6 genes within and nearby the minimal 19q deletion region (*ERCC2*, *RAI*, *ASE-1*, *ERCC1*, *GLTSCR1*, and *LIG1*).

RESULTS. The prevalence of a germline *GLTSCR1*-exon-1 T allele (SNP rs1035938) was 40% in cases with oligodendrogliomas compared with 27% in controls ($P = 0.029$), and the prevalence of an *ERCC2*-exon-22 T allele (SNP rs1052555) was 35% in cases with oligodendrogliomas compared with 18% in controls ($P = 0.043$). One high-risk and 1 low-risk haplotype were associated with oligodendroglioma development ($P = 0.003$ and 0.026 , respectively). Cases with oligodendrogliomas with the 19q deletion had a significantly higher frequency of the *GLTSCR1*-exon-1 T allele compared with cases without the 19q deletion ($P = 0.01$). It was noteworthy that cases with gliomas who were homozygous for the *GLTSCR1*-exon-1 T allele had a significantly better survival: 77% and 68% survival at 2 and 5 years compared with 56% and 34% for other genotypes ($P = 0.02$, log-rank test). Multivariable analysis identified grade, age, and the *GLTSCR1*-exon-1 and *ERCC2*-exon-22 genotypes as independent predictors for survival.

CONCLUSIONS. These results suggested that alterations in *GLTSCR1* (or a closely linked gene) were associated with the development and progression of oligodendroglioma. *Cancer* 2005;103:2363–72. © 2005 American Cancer Society.

KEYWORDS: glioma, oligodendroglioma, astrocytoma, single nucleotide polymorphisms, chromosome 19q deletion, linkage disequilibrium.

Malignant gliomas are the most common primary central nervous system tumors affecting adults, with nearly 18,500 diagnosed annually in the U.S. and a mortality rate approaching 80% in the first year after diagnosis.¹ Despite this poor prognosis, our understanding of glioma development and progression remains modest, and our abilities to effectively stratify and treat these malignancies continue to be limited.

Previous molecular analyses have demonstrated different genetic alterations associated with gliomas. Briefly, tumors of astrocytic lineage often demonstrate anomalies of chromosome arms 9p, 10p, 10q,

11p, 13q, 17p, 17q, 19q, and 22q, whereas oligodendrogliomas and mixed oligoastrocytomas (MOAs) commonly have alterations of 1p and 19q.² A number of tumor suppressor genes have been cloned from these regions, including the *CDKN2A/p16/p14^{ARF}* and *CDKN2B/p15* gene cluster mapped to 9p, the *p53* gene mapped to 17p, the *RB* gene mapped to 13q, and most recently, the *PTEN*^{6,4} and *DMBT5* genes mapped to 10q. However, the genes on 1p and 19q remain to be identified.

Chromosome 19 q-arm alterations are of particular interest because they have not been found to play a role in other common malignancies⁶ and because they are the only known genetic abnormalities shared by all 3 glioma subtypes.⁷⁻⁹ These observations, coupled with the high frequency of 19q alterations,¹⁰ strongly suggest that 19q harbors ≥ 1 gene important for the pathogenesis of gliomas, and further suggest that this gene may be of fundamental importance for glial development and growth regulation. Furthermore, a recent report by Cairncross, et al.¹¹ suggested that combined loss of chromosome arms 1p and 19q in high-grade oligodendrogliomas was highly associated with chemotherapeutic response and longer disease recurrence-free survival after chemotherapy, whereas *CDKN2A* deletions conferred a worse prognosis. Recently, we have extended these observations to oligodendrogliomas of all grades. For example, tumors with both 1p and 19q deletions have a statistically significant prolonged survival compared with tumors without these alterations.¹² We have also found that genetic alterations of 1p and 19q may predict chemotherapeutic response in a set of low-grade oligodendrogliomas and astrocytomas.¹³

We have previously described a 150-kilobase (kb) minimal deletion region in gliomas that maps to 19q13.33.¹⁴ This region contains 3 novel transcripts (*EHD2*, *GLTSCR1*, and *GLTSCR2*; *GLTSCR* stands for glioma tumor suppressor candidate region) and 2 known genes (*SEPWI* and *CRX*).¹⁵ Although no tumor-specific alterations were observed in any of the putative transcripts, several recent observations suggest that genes in or near this region may be involved in tumor development. Polymorphisms in loci near this deletion region (*ERCC1*, *ERCC2*, *RAI*, *ASE-1*, and *D19S246*) have been associated with basal cell, breast, and lung carcinoma and MOAs.¹⁶⁻²² Specifically, individuals carrying the *ERCC2* variant, *R156R*, have been shown to be at a higher risk for gliomas with the strongest association with MOAs.²² A polymorphism within *GLTSCR1* has recently been associated with prostate carcinoma aggressiveness.^{23, 24} Based on this preliminary evidence, we conducted an association study in gliomas using these and other markers that

map within and nearby the 150-kb minimally deleted region observed in gliomas.

MATERIALS AND METHODS

Case-Control Populations

Blood specimens were collected from 249 study subjects: 141 cases with glioma and 108 general controls. The 141 gliomas were surgically resected at Mayo Clinic (Rochester, MN) between December 1987 and December 2001. This existing resource was initiated in 1987 and stored tissue samples of every patient whose surgically resected glioma was large enough to spare for research purposes. Tissue samples were obtained for 35% of all surgical cases. For the cases for whom we had tissue samples, we actively sought patients' consent to donate a blood sample, and the time from surgery to blood draw was within 30 days for > 95% of the patients.

The controls were selected from a pool of Olmsted County residents enrolled as general controls in the Mayo Clinic Cancer Center between 1997 and 2001, who had a blood sample remaining after their clinical tests were performed.^{25,26} This design was chosen because the Mayo Clinic is a major primary care provider for the local population, and > 90% of Olmsted County residents visit the Mayo Clinic ≥ 1 time in any 3-year period.²⁷ Eligible control subjects had no current or previously diagnosed malignancy (except non-melanoma skin carcinoma) as of the date of phlebotomy. Controls received a self-administered questionnaire and a request for permission to use their blood samples.

In accordance with the institutional review board of Mayo Clinic, clinical information was collected and is regularly updated for the patients with glioma through follow-up and questionnaires. These data include date of birth, gender, date of diagnosis of primary tumor, date of surgical resection or biopsy and pathology of the specimen, treatment with chemotherapy and/or radiotherapy for primary and/or recurrent lesions, date of last follow-up, and status of patient (living/deceased) at the time of last follow-up.

Tumors were classified morphologically and graded according to the World Health Organization system²⁸ by three independent neuropathologists. Consensus morphology and grade were established for each glioma, as previously described.¹⁰ Table 1 summarizes the morphology of the cases and other basic characteristics of cases and controls. There were 61 cases with astrocytomas, 40 cases with oligodendrogliomas, and 40 cases with mixed oligodendrogliomas. The 19q deletion status of the gliomas was determined by fluorescence in situ hybridization anal-

TABLE 1
Basic Description of 141 Glioma Cases and 108 Controls

| Characteristics | General controls (n = 108) (%) | All gliomas (n = 141) (%) | Astrocytomas (n = 61) (%) | Mixed oligoastrocytomas (n = 40) (%) | Oligodendrogliomas (n = 40) (%) |
|--|-----------------------------------|------------------------------|------------------------------|---|------------------------------------|
| Gender | | | | | |
| Men | 67 (62) | 94 (67) | 42 (69) | 28 (70) | 24 (60) |
| Women | 41 (36) | 47 (33) | 19 (31) | 12 (30) | 16 (40) |
| Race/ethnic background | | | | | |
| Non-Hispanic white | 103 (95) | 128 (94) | 57 (97) | 36 (92) | 35 (92) |
| Hispanic white | 1 (1) | 1 (1) | 0— | 0— | 1 (3) |
| Non-U.S. white | 4 (4) | 7 (5) | 2 (3) | 3 (8) | 2 (5) |
| Unknown | 0— | 5— | 2— | 1— | 2— |
| Age group (yrs) ^a | | | | | |
| < 50 | 10 (9) | 91 (64) | 26 (43) | 29 (72) | 36 (90) |
| ≥ 50 | 97 (91) | 50 (36) | 35 (58) | 11 (28) | 4 (10) |
| Geographic region of residence | | | | | |
| Midwest states ^c | 108 (100) | 97 (70) | 42 (69) | 34 (85) | 21 (55) |
| Non-Midwest states | — | 32 (23) | 12 (20) | 5 (13) | 15 (40) |
| Outside U.S. ^d | — | 10 (7) | 7 (11) | 1 (2) | 2 (5) |
| Tumor grade ^b | | | | | |
| II | — | 42 (30) | 4 (7) | 13 (32) | 25 (62) |
| III | — | 33 (28) | 5 (8) | 21 (52) | 13 (33) |
| IV | — | 60 (42) | 52 (85) | 6 (15) | 2 (5) |
| Primary vs. recurrent brain tumor ^b | | | | | |
| Primary | — | 110 (78) | 54 (89) | 26 (65) | 30 (75) |
| Recurrent | — | 31 (22) | 7 (11) | 14 (35) | 10 (25) |
| Initial diagnosis ^b | | | | | |
| Mayo Clinic | — | 96 (71) | 49 (83) | 22 (56) | 25 (66) |
| Elsewhere | — | 40 (29) | 10 (17) | 17 (44) | 13 (34) |
| Unknown | — | 5— | 2— | 1— | 2— |

^a $P < 0.05$ determined by the Pearson's chi-square test, comparing with the general control group.

^b $P < 0.05$ determined by the Pearson's chi-square test, comparison among three tumor subgroups.

^c Includes: Iowa, Illinois, Indiana, Michigan, Minnesota, North Dakota, South Dakota, and Wisconsin.

^d Includes: Brazil, Greece, Hungary, Mexico, Peru, Saudi Arabia, Spain, and Yugoslavia.

ysis of paraffin-embedded material using previously described methods.¹²

DNA Extraction, Polymerase Chain Reaction Amplification, and Genotype Determination

Table 2 summarizes the 7 single nucleotide polymorphisms (SNPs) in 6 genes that were analyzed. These 7 SNPs previously had been shown to be associated with basal cell carcinomas (BCC), breast carcinomas, or MOAs.^{16–22} The ASE-1-exon-3 SNP was previously identified as an ERCC1-3' untranslated region (UTR) SNP.²¹ The July 2003 assembly of the University of California Santa Cruz's (Santa Cruz, CA) human genome database (available from URL: <http://genome.ucsc.edu/>) shows that this SNP lies outside of ERCC1 and within the coding region of ASE-1.

Genomic DNA was extracted from blood specimens using the phenol-chloroform method. Polymerase chain reaction (PCR) primers (Table 3) were purchased from Integrated DNA Technologies (Coralville, IA). PCR reactions were performed in a 25-μL reaction

volume containing 2.50 μL GeneAmp10X PCR Gold Buffer (Applied Biosystems, Foster City, CA), 1.5 mM MgCl₂, 200 μM each deoxynucleotide triphosphate, 7 pmol of each PCR primer, 0.625 U of AmpliTaq Gold (Applied Biosystems), and 25 ng of genomic DNA. The PCR reactions to amplify the GLTSCR1-exon-1 fragment included 4% dimethylsulfoxide and an additional 0.125 U of AmpliTaq Gold. PCR amplification was performed using a PTC-225 Peltier thermal cycler (MJ Research, Waltham, MA). Cycling conditions for all sequences except GLTSCR1-exon-1 were 50 cycles of denaturation at 95 °C for 30 seconds, annealing for 30 seconds, and extension at 72 °C for 30 seconds followed by a final extension at 72 °C for 10 minutes. Annealing was performed at 61.5 °C for ERCC2-exon-6, RAI-exon-6, ASE-1-exon-3, and Lig1-exon-6. ERCC2-exon-22 was annealed at 53.8 °C, and ERCC1-exon-4 was annealed at 59.0 °C. GLTSCR1-exon-1 was amplified using the following cycling conditions: initial denaturation at 95 °C for 10 minutes, 40 cycles of denaturation at 95 °C for 30 seconds, annealing at 60 °C for

TABLE 2
SNPs Analyzed

| RS no. | Gene ^a | Location ^a | Chromosome 19 position ^b | Function of change | Alleles (frequencies) ^c |
|-----------|-------------------|-----------------------|-------------------------------------|---------------------|------------------------------------|
| rs1052555 | <i>ERCC2</i> | Exon 22 | 50547364 | D711D | C(0.69), T(0.31) |
| rs230406 | <i>ERCC2</i> | Exon 6 | 50560149 | R156R | C(0.53), A(0.47) |
| rs6966 | <i>RAI</i> | Exon 6 | 50574802 | Untranslated region | A(0.83), T(0.17) |
| rs3212986 | <i>ASE-1</i> | Exon 3 | 50604576 | K504Q | C(0.76), A(0.24) |
| rs3177700 | <i>ERCC1</i> | Exon 4 | 50615493 | N118N | T(0.63), C(0.37) |
| rs1035938 | <i>GLTSCR1</i> | Exon 1 | 52075583 | S397S | C(0.75), T(0.25) |
| rs20580 | <i>Lig1</i> | Exon 6 | 53346365 | A170A | C(0.52), A(0.48) |

SNP: single nucleotide polymorphism; RS no.: accession number in the National Center for Biotechnology Information (NCBI) SNP database.

^a Gene and location are from the NCBI SNP database. Available from URL: <http://www.ncbi.nlm.nih.gov/SNP/> [accessed].

^b In Mb, from July 2003 freeze of the University of California Santa Cruz (UCSC) human genome database. Available from URL: <http://genome.ucsc.edu/> [accessed].

^c Found among general controls in our pilot study.

TABLE 3
Primers Used for PCR and Pyrosequencing

| Locus | Primers | | |
|----------------|-----------------------------|----------------------------|------------------------|
| | 5'-BlotIn labeled for PCR | Unlabeled for PCR | Pyrosequencing |
| ERCC2-exon-22 | 5'-GAGCACCTCACAGATGCCA | 5'-CCATCTGCCGCAGGAAGTA | 5'-CCACCTGGACACCCT |
| ERCC2-exon-6 | 5'-CACAGCCTCACAGCCTCCTA | 5'-CCATCAAATTCCTGGACAAGAGT | 5'-CCAGTAACCTCATAG |
| RAI-exon-6 | 5'-CATAACCACAATGATGAGCATGTA | 5'-CTCTCCCAATTAAGTGCCT | 5'-ATTAAGTGCCCTCACACAG |
| ASE-1-exon-3 | 5'-CTCTGGGGAGGCAATCTGG | 5'-AGGGCCACTGAATTCAGAGTC | 5'-GGACAAGAAGCGGAA |
| ERCC1-exon-4 | 5'-CAGAGCTCACCTGAGGAACA | 5'-CATCCCTATTGATGGCTTCTGC | 5'-GTACTGAAGTTCGTGGG |
| GLTSCR1-exon-1 | 5'-CAAGCGAACGTCCTCAAGCA | 5'-GGCAGTAGGAAGTGGTCTGG | 5'-TTGGTTCAGGAGGTGGA |
| Lig1-exon-6 | 5'-CGGAGGAGAGGACCAGAAACT | 5'-CCATCTGACCGTTCTGTATCGT | 5'-ACAGAGGCTGAAGTGG |

PCR: polymerase chain reaction.

30 seconds, and extension at 72 °C for 30 seconds followed by a final extension at 72 °C for 10 minutes.

Pyrosequencing was performed on a PSQ 96 (Biotage AB, Uppsala, Sweden) using streptavidin-labeled Dynabeads (Dynal Biotech, Oslo, Norway) according to the protocol provided.²⁹

Statistical Analysis

The frequency distribution at each SNP locus was tested against the Hardy-Weinberg equilibrium under the allele Mendelian biallelic expectation using the chi-square test. No significant distortion was detected.

Data for both primary and recurrent tumors were used to evaluate the association between the seven candidate SNP markers and the risk of glioma in a case-control design. Pooled cases as well as each morphologic subgroup were compared with the control group. Univariable associations of allele (each chromosome as a unit) and genotype (a person as a unit) with disease were evaluated using contingency table methods in SAS software, version 8.2 (SAS Institute, Inc., Cary, NC). These associations were assessed us-

ing the Pearson chi-square and Fisher exact tests for dichotomous categorical variables, and the Cochran-Armitage trend tests for genotype associations. Genotype-specific odds ratios (ORs), as an assessment of relative risk and potential confounding effects from other loci, were estimated and adjusted, respectively, using logistic regression for the significant markers identified from the univariate analysis. The multiple SNP marker-disease association by estimated haplotype was evaluated using haplo.score (a Mayo-developed software), which accounts for ambiguous linkage phase.³⁰ Linkage disequilibrium (LD) was assessed using the Graphical Overview of Linkage Disequilibrium (GOLD) software package (Center for Statistical Genetics, University of Michigan, Ann Arbor, MI).³¹

Survival analyses were performed using cases with glioma, with survival defined as the time from surgical diagnosis of the primary tumor to death or time of last follow-up. Cases who were alive at their last follow-up were censored. Survival distributions were estimated with Kaplan-Meier curves³² and compared among patient subsets with log-rank tests.³³ Univariate associ-

TABLE 4
Allele-Based Analysis of Association of Selected 19q SNPs with Glioma Development

| Locus | General controls (n = 108) | All gliomas (n = 141) | | Astrocytomas (n = 61) | | Mixed oligoastrocytomas (n = 40) | | Oligodendrogliomas (n = 40) | |
|----------------|-------------------------------|-----------------------|----------------------|-----------------------|----------------------|-------------------------------------|----------------------|--------------------------------|----------------------|
| | (%) | No. (%) | P value ^a | No. (%) | P value ^a | No. (%) | P value ^a | No. (%) | P value ^a |
| ERCC2-exon-22 | 210 Chrs | 274 Chrs | 0.694 | 122 Chrs | 0.898 | 76 Chrs | 0.418 | 76 Chrs | 0.043 |
| Allele T | 64 (30.5) | 79 (28.8) | | 38 (31.1) | | 27 (35.5) | | 14 (18.4) | |
| Allele C | 146 (69.5) | 195 (71.2) | | 84 (68.9) | | 49 (64.5) | | 62 (81.6) | |
| ERCC2-exon-6 | 208 Chrs | 274 Chrs | 0.518 | 122 Chrs | 0.170 | 74 Chrs | 0.669 | 78 Chrs | 0.884 |
| Allele C | 110 (52.9) | 153 (55.8) | | 74 (60.7) | | 37 (50.0) | | 42 (53.9) | |
| Allele A | 98 (47.1) | 121 (44.2) | | 48 (39.3) | | 37 (50.0) | | 36 (46.1) | |
| RAF-exon-6 | 216 Chrs | 276 Chrs | 0.216 | 118 Chrs | 0.173 | 80 Chrs | 0.742 | 78 Chrs | 0.118 |
| Allele A | 183 (84.7) | 222 (80.4) | | 93 (78.8) | | 69 (86.2) | | 60 (76.9) | |
| Allele T | 33 (15.3) | 54 (19.6) | | 25 (21.2) | | 11 (13.8) | | 18 (23.1) | |
| ASE-1-exon-3 | 210 Chrs | 282 Chrs | 0.548 | 122 Chrs | 0.915 | 80 Chrs | 0.314 | 80 Chrs | 0.749 |
| Allele A | 51 (24.3) | 62 (22.0) | | 29 (23.8) | | 15 (18.8) | | 18 (22.5) | |
| Allele C | 159 (75.7) | 220 (78.0) | | 93 (76.2) | | 65 (81.2) | | 62 (77.5) | |
| ERCC1-exon-4 | 214 Chrs | 280 Chrs | 0.996 | 122 Chrs | 0.598 | 78 Chrs | 0.367 | 80 Chrs | 0.867 |
| Allele C | 78 (36.5) | 102 (36.4) | | 48 (39.3) | | 24 (30.8) | | 30 (37.5) | |
| Allele T | 136 (63.5) | 178 (63.6) | | 74 (60.7) | | 54 (69.2) | | 50 (62.5) | |
| GLTSCR1-exon-1 | 216 Chrs | 286 Chrs | 0.392 | 126 Chrs | 0.770 | 80 Chrs | 0.589 | 80 Chrs | 0.029 |
| Allele T | 58 (26.9) | 85 (30.4) | | 34 (28.3) | | 19 (23.8) | | 32 (40.0) | |
| Allele C | 158 (73.1) | 195 (69.6) | | 86 (71.7) | | 61 (76.2) | | 48 (60.0) | |
| LIG1-exon-6 | 216 Chrs | 282 Chrs | 0.807 | 122 Chrs | 0.905 | 80 Chrs | 0.585 | 80 Chrs | 0.323 |
| Allele A | 103 (47.7) | 133 (47.2) | | 59 (48.4) | | 41 (51.3) | | 33 (41.2) | |
| Allele C | 113 (52.3) | 149 (52.8) | | 63 (51.6) | | 39 (48.7) | | 47 (58.7) | |

SNP: single nucleotide polymorphism; Chrs: chromosome.

^aP value = Pearson's chi-square test (in comparison to the general control group).

ations of patient characteristics, tumor characteristics, and SNP markers with survival were ascertained with a Cox proportional hazards model. Multivariate analyses were performed with classification and regression tree (CART) models,^{34, 35} as well as with multivariate Cox proportional hazards models. The multivariate analyses were done on the pooled cases. Potential prognostic variables included tumor type (i.e., astrocytoma, oligodendroglioma, or MOA), the other variables in Table 1 (treating age as a continuous variable), and 7 SNP markers. The statistical tests were 2-sided tests and *P* values ≤ 0.05 were statistically significant.

RESULTS

Characteristics of Cases and Controls

Gender and ethnic background distributions were similar between pooled cases and controls and among tumor types (cases). However, because of the study design (i.e., both groups were selected from existing resources), there was a significant difference between cases and controls with regard to age at blood sample collection and geographic region of residence. Tumor grade, the proportion of primary tumors, and the proportion of patients with an initial diagnosis at Mayo

Clinic differed significantly among the tumor subgroups. These differences are not unexpected and reflect the nature of the tumors. Patients with astrocytomas tend to present with a higher grade than patients with oligodendrogliomas and mixed oligodendrogliomas.

An Association Study Using Candidate SNPs

We compared allele frequencies of each of the 7 SNPs between general controls and glioma cases by morphologic subtypes (Table 4). The presence of a germline *GLTSCR1*-exon-1 T allele was significantly associated with the development of oligodendroglioma (*P* = 0.029). The association between the *ERCC2*-exon-22 C allele and oligodendroglioma also achieved significance (*P* = 0.043). Similar results were observed when the data were analyzed using genotype-based methods. For example, *GLTSCR1*-exon-1 genotypes TT, TC, and CC were observed in 18%, 45%, and 37% of cases with oligodendrogliomas compared with 7%, 39%, and 54% of controls, respectively (*P* = 0.032). *ERCC2*-exon-22 genotypes TT, TC, and CC were observed in 0%, 37%, and 63% of cases with oligodendrogliomas, respectively, compared with 10%, 42%, and 49% of controls, respectively (*P* = 0.04). It is noteworthy that

TABLE 5
Haplotype-Based Analysis of Association of Selected 19q SNPs with Oligodendroglioma Development

| ERCC2- exon-22 | ERCC2- exon-6 | RAI- exon-6 | ASE-1- exon-3 | ERCC1- exon-4 | GLTSCR1- exon-1 | LIG1- exon-6 | Empirical P value | Simulated P value | Haplotype frequency | | |
|-------------------|------------------|----------------|------------------|------------------|--------------------|-----------------|----------------------|----------------------|---------------------|--------------|--------------|
| | | | | | | | | | Overall | Controls | Cases |
| T | C | A | A | C | T | C | 0.35 | 0.35 | 0.020 | 0.016 | 0.046 |
| T | C | A | A | C | C | A | 0.026 | 0.023 | 0.068 | 0.096 | 0.004 |
| C | A | A | A | C | T | C | 0.28 | 0.29 | 0.026 | 0.026 | 0.057 |
| C | A | A | A | C | C | C | 0.97 | 0.97 | 0.034 | 0.042 | 0.000 |
| T | C | A | C | C | T | A | 0.003 | 0.014 | 0.016 | 0.000 | 0.054 |
| C | C | A | C | C | C | C | 0.61 | 0.62 | 0.027 | 0.034 | 0.000 |
| T | C | A | C | T | C | A | 0.17 | 0.18 | 0.054 | 0.067 | 0.000 |
| T | C | A | C | T | C | C | 0.19 | 0.17 | 0.039 | 0.044 | 0.021 |
| C | A | A | A | C | C | A | 0.51 | 0.50 | 0.029 | 0.000 | 0.056 |
| C | C | T | C | T | T | C | 0.06 | 0.07 | 0.032 | 0.021 | 0.048 |
| C | C | T | C | T | C | A | 0.59 | 0.60 | 0.042 | 0.037 | 0.050 |
| C | C | T | C | T | C | C | 0.13 | 0.14 | 0.061 | 0.039 | 0.102 |
| C | A | A | C | T | T | A | 0.60 | 0.61 | 0.071 | 0.028 | 0.097 |
| C | A | A | C | T | T | C | 0.59 | 0.60 | 0.066 | 0.076 | 0.039 |
| C | A | A | C | T | C | A | 0.60 | 0.59 | 0.073 | 0.112 | 0.042 |
| C | A | A | C | T | C | C | 0.79 | 0.79 | 0.128 | 0.130 | 0.170 |

SNP: single nucleotide polymorphism.

of the 13 cases with glioma with the *GLTSCR1*-exon-1 TT genotype, 7 (53%), 2 (15%), and 4 (31%) developed oligodendrogliomas, MOAs, and astrocytomas, respectively. No other significant associations between SNP genotypes and oligodendrogliomas or other glioma subtypes were observed in our study.

Table 5 summarizes the haplotype-based analysis of oligodendrogliomas. Twenty-five haplotypes were identified and only haplotypes with a frequency of ≥ 0.03 in either cases or controls are shown. One high-risk (TCACCTA) and 1 low-risk (TCAACCA) haplotype were identified (simulated $P = 0.014$ and 0.023 , respectively). These 2 haplotypes differ only by the presence of an ASE-1-exon-3 allele (C or A) or a *GLTSCR1*-exon-1 allele (T or C). The high-risk haplotype was computationally identified by the DNA markers program in two cases with oligodendrogliomas and none with another glioma or in a control. No haplotypes were significantly associated with astrocytoma or MOA development in the current study.

LD analysis was performed using both D' (close to 1) and R^2 (> 0.3), to detect pairwise LD among all 7 loci. Significant LD was found between ASE-1-exon-3 and *ERCC1*-exon-4 in controls, astrocytomas, and MOAs. Borderline significant LD was found in oligodendrogliomas between *ERCC2*-exon-22 and *ERCC2*-exon-6 ($D' = 1.00$ and $R^2 = 0.20$) and between *ERCC2*-exon-6 and RAI-exon-6 ($D' = 1.00$ and $R^2 = 0.28$). No LD was detected between *GLTSCR1*-exon-1 and any of the other six 19q SNPs in the study populations.

To estimate the risk of developing oligodendrogl-

omas associated with the *GLTSCR1*-exon-1 genotype, we calculated the ORs of CT and TT using CC as the referent genotype (Table 6). The unadjusted OR for individuals with CT was 1.7 (95% confidence interval [95% CI], 0.7–3.7), and for those with the TT genotype, it was 3.4 (95% CI, 1.1–10.8). There was an indication that genotype CT may also increase the risk of oligodendrogliomas, but the OR was not statistically greater than unity with our current sample size.

We also attempted to estimate the risk of developing oligodendrogliomas associated with the *ERCC2*-exon-22 genotype. Based on our allele-based analysis (shown in Table 4), individuals with the CC and TT genotypes are expected to be at the highest and the lowest risk, respectively, for developing oligodendrogliomas. Because there were no cases with oligodendrogliomas in our study sample that had the TT genotype at the *ERCC2*-exon-22 locus, we used the CT and TT genotypes combined as the reference group to estimate the risk associated with the CC genotype. There was an increased OR (1.8, 95% CI, 0.9–3.9) for the development of oligodendrogliomas among cases with the CC genotype, but this did not quite achieve statistical significance.

We also performed a two-locus analysis as an attempt to control potential confounding effects from other loci on the observed association between *GLTSCR1* and oligodendroglioma risk. The risk for developing oligodendrogliomas among cases who were TT at the *GLTSCR1* locus did not change significantly after adjusting for the other 6 SNP genotypes, as dem-

TABLE 6
OR for GLTSCR1 Genotypes Using Multiple Logistic Models

| GLTSCR1-exon-1 genotype | Normal controls (n = 108) | Oligodendroglioma cases (n = 40) | OR (95% CI) | OR ^a (95% CI) | OR ^b (95% CI) |
|-------------------------|---------------------------|----------------------------------|--------------------|--------------------------|--------------------------|
| CC (reference) | 58 | 15 | — | — | — |
| CT | 42 | 18 | 1.65 (0.75, 3.65) | 1.63 (0.73, 3.62) | 1.44 (0.64, 3.24) |
| TT | 8 | 7 | 3.38 (1.06, 10.82) | 3.25 (1.01, 10.41) | 2.17 (0.61, 7.69) |
| TT/CT | 50 | 25 | 1.93 (0.92, 4.07) | 1.89 (0.89, 4.00) | 1.57 (0.73, 3.39) |

OR: odds ratio; 95% CI: 95% confidence interval.

^a GLTSCR1-exon-1 OR from a model adjusted for ERCC1-exon-1.

^b GLTSCR1-exon-1 OR from a model adjusted for ERCC2-exon-22.

onstrated by adjusting for *ERCC1*-exon-1 and *ERCC2*-exon-22 in Table 6.

Because the controls were selected from an existing resource (i.e., the Olmsted County normal control pool) and were not matched to the cases with glioma (Table 1), we conducted stratified analyses by age groups, gender, ethnic background, geographic region of residence, place of initial tumor diagnosis, tumor grade, and primary versus recurrent tumor (data not shown). The changes in allele and genotype frequencies did not substantially change our reported associations.

Correlations between Germline SNPs with Glioma 19q Deletion Status

We performed a stratified analysis to determine whether there were associations between the 7 SNPs and glioma 19q deletion status. The *GLTSCR1*-exon-1 T allele is associated with glioma 19q deletion status. *GLTSCR1*-exon-1 genotypes TT, TC, and CC were observed in 9%, 56%, and 34%, respectively, of cases whose glioma had 19q deletion, compared with 5%, 34%, and 63%, respectively, of cases whose glioma lacked 19q deletion ($P = 0.060$). *GLTSCR1*-exon-1 genotypes TT, TC, and CC were observed in 15%, 60%, and 25% of cases whose oligodendroglioma had 19q deletion compared with 11%, 11%, and 78%, respectively, of cases whose oligodendroglioma lacked 19q deletion ($P = 0.019$). No other significant associations were observed between SNP genotypes and cases whose tumors had 19q deletion.

Haplotype analysis was performed for cases with oligodendrogliomas, 20 with and 9 without 19q deletion. One new high-risk haplotype was observed (CCTCTTC, simulated $P = 0.01$) in the group with the 19q deletion, and none were observed in the group without deletion. This haplotype is similar to the high-risk haplotype identified for the oligodendrogliomas as a whole and shares the ASE-1-exon-3 C and the

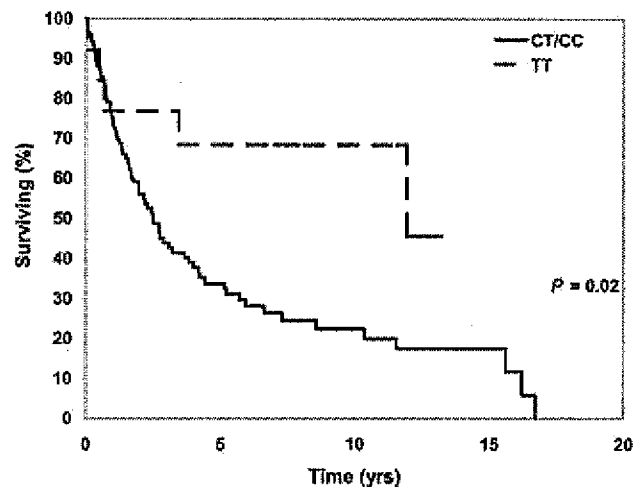


FIGURE 1. Kaplan-Meier curve comparing the survival of cases with glioma with the *GLTSCR1*-exon-1 TT genotype with cases with glioma with *GLTSCR1*-exon-1 CT or CC genotypes. Straight line: CT/CC; dashed line: TT.

GLTSCR1-exon-1 T alleles. Also this haplotype contains the high-risk *ERCC2*-exon-22 C allele. The number of mixed oligodendrogliomas and MOAs with 19q loss was too small for stratified analysis.

Glioma Survival and Candidate SNP Markers

Using the above case cohort, we have also compared the association of ASE-1-exon-3, *ERCC2*-exon-22, and *GLTSCR1*-exon-1 polymorphisms with case survival and other clinical variables. Importantly, the cases with gliomas with the *GLTSCR1*-exon-1 TT genotype had a better survival: 77% and 68% survival at 2 and 5 years for the TT genotype compared with 56% and 34% at 2 and 5 years for the CT/CC genotype ($P = 0.02$, log-rank test) (Fig. 1). This difference in survival was also observed for the cases with oligodendrogliomas alone but did not reach statistical significance ($P = 0.08$). The ASE-1 and *ERCC2* polymorphisms were not significantly associated with glioma 19q deletion

TABLE 7
Relative Survival Time of Glioma Case Sub-groups Partitioned by
CART Analysis

| CART group | No. in group (no. dead) | HR (95% CI) |
|----------------------------------|----------------------------|------------------------|
| Grade < 4 | | |
| Age < 57 yrs | | |
| <i>GLTSCR1</i> -exon-1: TT | 8 (1) | 0.11 (0.02-0.85) |
| <i>GLTSCR1</i> -exon-1: TC or CC | | |
| <i>ERCC2</i> -exon-22: TT or CT | 31 (10) | 0.45 (0.19-1.05) |
| <i>ERCC2</i> -exon-22: CC | 34 (16) | 1.00 (reference group) |
| Age ≥ 57 yrs | 8 (7) | 2.21 (0.90-5.42) |
| Grade = 4 | | |
| Age < 48 | 20 (14) | 1.95 (0.94-4.04) |
| Age ≥ 48 | 40 (35) | 8.67 (4.51-16.68) |

CART: classification and regression tree; HR: hazard ratio; 95% CI: 95% confidence interval.

status or with the morphologic grade of glioma. In addition, the *ASE-1* and *ERCC2* polymorphisms were not associated with survival after univariate analysis.

To identify subgroups with the longest and shortest survival, we used CART^{34,35} modeling to determine clinical and genetic variables that were independently associated with survival. The CART model selected tumor grade, age at diagnosis, *GLTSCR1*-exon-1 genotype, and *ERCC2*-exon-22 genotype as the informative variables for generating survival subgroups. Morphology type was not identified as an important predictive factor. Six subgroups of cases with glioma with different survivals were generated (Table 7). The survival reference group consisted of 34 cases who were < 57 years old at the time of a Grade < 4 glioma diagnosis and who were CT/CC at *GLTSCR1*-exon-1 and CC at *ERCC2*-exon-22. Eight cases with Grade < 4 glioma, who were < 57 years old at the time of diagnosis and who carried the TT genotype at *GLTSCR1*-exon-1, had the best survival (hazard ratio = 0.11; 95% CI, 0.02-0.85). The 40 Grade 4 cases with glioma, who were > 47 years old at diagnosis, had the worst survival (hazard ratio = 8.67; 95% CI, 4.51-16.68).

DISCUSSION

The current study data suggest that alterations in *GLTSCR1* (or a closely linked gene) and *ERCC2* are associated with the development of oligodendrogliomas and with glioma survival. Specifically, our results indicate a threefold increased risk of oligodendrogliomas among cases with a TT genotype compared with cases with a CC genotype at a *GLTSCR1*-exon-1 polymorphic locus. There is limited, but suggestive, evidence in the published literature that some individuals are predisposed to develop gliomas. For example, an inherited susceptibility to gliomas has been re-

ported to be present in 5-7% of families.³⁶⁻³⁹ Ten percent of these families (or approximately 1% of all patients with gliomas) carry germline high-penetrance mutations in the *p53*, *NF1*, *NF2*, *hMLH1*, *hPMS2*, or *p16* genes).³⁶ The genetic basis for the remainder of the families is unknown. Linkage studies have been limited mainly due to lack of informative pedigrees. One recent study reported a low-penetrance susceptibility locus for familial glioma at 15q23-q26.3.³⁷

The association of low-penetrance genetic alterations, particularly DNA sequence polymorphisms with glioma development, only has been assessed by a few studies. Candidate genes evaluated include polymorphisms in DNA repair pathways such as base-excision repair, nucleotide-excision repair, and double-strand-break repair genes,³⁸ and in metabolic pathways of carcinogens such as N-Nitroso compounds, pesticides, and polycyclic aromatic hydrocarbons.³⁹ Our finding of an *ERCC2* variant as a potential risk genotype is consistent with a previous study,²² although the precise nature of the variation needs to be further investigated.

Of specific relevance to our current study are association studies of 19q alleles with cancer (and glioma) development. Recent linkage studies have associated markers at 19q12 and 19q13.2 with aggressive prostate carcinoma.^{23,24} Polymorphisms in the *ERCC2* and the *RAI* genes have been associated with the development of BCC and postmenopausal breast carcinoma.¹⁶⁻¹⁹ A genome-wide survey recently reported the association of *D19S246* (mapped to 19q13.3) with the development of adenocarcinoma of the lung.²⁰

Two recent studies have suggested that polymorphisms in the *ASE-1* and *ERCC2* genes are associated with the development of MOAs.^{21,22} In these reports, oligodendrogliomas were grouped with the MOAs. Importantly, the *ERCC2*, *RAI*, and *ASE-1* genes map within 3 Mb of the 150-kb minimally deleted 19q region observed in primary gliomas.¹⁴ *GLTSCR1* is also mapped within this region. Nexø et al.¹⁹ have reported that a polymorphism in *GLTSCR1* is in LD with the *RAI* and *ERCC2* alleles associated with BCC. Furthermore, the marker with the peak LOD (Log-Odd) score for the association of aggressive prostate carcinoma (*D19S902*) lies within the *GLTSCR1* gene.²⁴

GLTSCR1 is highly conserved among humans, chimps, mice, and rats. The 5' flanking and UTR regions of *GLTSCR1* are GC rich. The *GLTSCR1* polymorphism we tested alters a CpG within this 5' CpG island. It is possible that germline alterations of CpGs may affect the transcription of *GLTSCR1* and other candidate genes in the region. Two recent reports have implicated 2 other 19q13.33 genes in the development of oligodendrogliomas. Both are located within 3 Mb

of the *GLTSCR1*-exon-1 polymorphism. In a platelet-derived growth factor/retrovirus mouse Model 1 of glioma, vector sequences were integrated with p190RhoGAP (also known as GRLF1) in a small proportion of tumors.⁴⁰ In addition, methylation of a CpG island 5' to the gene *ZNF342* was observed in a large proportion of oligodendrogliomas with the 19q deletion.⁴¹

Two loci in LD in our relatively small sample could have occurred by chance but could also indicate a tight linkage of a causal variant within or close to the markers being study. We did not observe LD between *GLTSCR1*-exon-1 and any of the other six 19q SNPs in the study populations, suggesting that this synonymous SNP is tightly linked to a causal variant that was not included in this study, or that the T allele at this locus may be causally related to oligodendrogliomas through a to-be-revealed mechanism. Conversely, we detected LD between *ASE-1* and *ERCC1* in our controls and cases with astrocytomas or MOAs, but not in cases with oligodendrogliomas. In addition, a borderline significant LD was detected in a 3-locus cluster of *ERCC2*-exon-2, *ERCC2*-exon-6, and *RAI*-exon-6 only among cases with oligodendrogliomas.

The associations of the *GLTSCR1*-exon-1 T allele with glioma development and survival are provocative. The data suggest that it is not simply the 1p and 19q deletion status that determines the prognosis of patients with gliomas. Rather, our data suggest that the 19q genotype, and putatively an associated alteration in a target gene, is an important biologic and clinical variable.

Two notable limitations of our study are potential referral bias of the cases and the choice of the control group. Bias due to referral cases is considered minimal because seeking care at our institution was not predetermined by genotype, and the allele distributions of the seven markers in our study are in agreement with data reported in the literature. Our choice of a control group was not ideal because it has been always difficult to find proper controls in a tertiary referral clinic where a large number of new cases can be rapidly enrolled. Because our cases with glioma are mainly referral based, ideal controls should be matched with cases by age, gender, race, geographic referral area, and duration of care at Mayo Clinic (i.e., equally referred). However, finding such ideal controls is not feasible mainly because approximately 60% of our cases are from outside of the tristate area (Minnesota, Wisconsin, and Iowa) in which a limited number of eligible controls can be found and enrolled. Moreover, this generates more concerns because these patients were typically referred for other disorders, which may be related to the conditions being study. Recognizing

the imperfection of our population-based control group, we were able to generate intriguing preliminary results, justifying further rigorous investigations with a proper design. Our control group could also provide estimates of the expected allele frequencies of the candidate markers in a defined population.

Our results require confirmation using a relatively large series of patients with gliomas and controls. Although *GLTSCR1* is a promising candidate gene underlying oligodendroglioma development, the data with this SNP in exon-1 need to be reproduced with independent study samples with closely matched cases and controls. In addition, other SNPs within *GLTSCR1* (or mutations in another gene(s) in LD with *GLTSCR1*) may underlie the associations we observed. Thus, additional SNPs at 19q13.33 must be investigated. Finally, 19q deletions have been associated with response to therapy as well as survival. It must be determined if 19q SNPs are associated with the response of gliomas to radiotherapy and/or chemotherapy.

REFERENCES

1. Levin VA, Gutin PH, Leibe S. Neoplasms of the central nervous system. In: De Vita VT, Hellman S, Rosenberg SA, editors. Cancer principles and practice of oncology. Philadelphia: Lippincott, 1993:1679-1737.
2. Kitange GJ, Templeton KL, Jenkins RB. Recent advances in the molecular genetics of primary gliomas. *Curr Opin Oncol*. 2003;15:197-203.
3. Li J, Yen C, Liaw D, et al. PTEN, a putative tyrosine phosphatase gene mutated in human brain, breast, and prostate cancer. *Science*. 1997;275:1943-1947.
4. Steck PA, Pershouse MA, Jasser SA, et al. Identification of a candidate tumour suppressor gene, *MMAC1*, at chromosome 10q23.3 that is mutated in multiple advanced cancers. *Nat Genet*. 1997;15:256-362.
5. Mollenhauer J, Wiemann S, Scheurle W, et al. DMBT1, a new of the SRCR superfamily, on chromosome 10q25.3-26.1 is deleted in malignant brain tumours. *Nat Genet*. 1997;17:32-39.
6. Seizinger BR, Klinger HP, Junien C, et al. Report of the committee on chromosome and gene loss in human neoplasia. *Cytogenet Cell Genet*. 1991;58:1080-1096.
7. Reifenger J, Reifenger G, Liu L, James CD, Wechsler W, Collins VP. Molecular genetic analysis of oligodendroglial tumors show preferential allelic deletions of 19q and 1p. *Am J Pathol*. 1994;145:1175-1190.
8. von Deimling A, Louis DN, von Ammon K, Petersen I, Wieslter OD, Seizinger BR. Evidence for a tumor suppressor gene on chromosome 19q associated with human astrocytomas, oligodendrogliomas, and mixed gliomas. *Cancer Res*. 1992;52:4277-4279.
9. Kraus JA, Koopman J, Kaskel P, et al. Shared allelic losses on chromosome 1p and 19q suggest a common origin of oligodendroglioma and oligoastrocytoma. *J Neuropathol Exp Neurol*. 1995;54:91-95.

10. Smith JS, Alderete B, Minn Y, et al. Localization of common deletion regions on 1p and 19q in human gliomas and their association with histological subtype. *Oncogene*. 1999;18:4144-4152.
11. Cairncross JG, Ueki K, Zlatescu MC, et al. Specific genetic predictors of chemotherapeutic response and survival in patients with anaplastic oligodendrogliomas. *J Natl Cancer Inst*. 1998;90:1473-1479.
12. Smith JS, Borell TJ, Lee HK, et al. Alterations of chromosome arms 1p and 19q as predictors of survival in oligodendrogliomas, astrocytomas, and mixed oligoastrocytomas. *J Clin Oncol*. 2000;18:636-645.
13. Smith JS, Borell TJ, O'Fallon JR, et al. Deletions of chromosome arms 1p and 19q in low-grade gliomas and the association of these alterations with response to PCV chemotherapy as initial therapy [abstract]. *Neurooncol*. 1999;1:S57.
14. Smith JS, Tachibana I, Lee HK, et al. Mapping of the chromosome 19 q-arm glioma tumor suppressor gene using fluorescence in situ hybridization and novel microsatellite markers. *Genes Chromosomes Cancer*. 2000;29:16-25.
15. Smith JS, Tachibana I, Pohl U, et al. A transcript map of the chromosome 19q-arm glioma tumor suppressor region. *Genomics*. 2000;64:44-55.
16. Dybdahl M, Vogel U, Frentz G, Wallin H, Nexø BA. Polymorphisms in the DNA repair gene XPD: correlations with risk and age at onset of basal cell carcinoma. *Cancer Epidemiol Biomarkers Prev*. 1999;8:77-81.
17. Rockenbauer E, Bendixen MH, Bukowy Z, et al. Association of chromosome 19q13.2-3 haplotypes with basal cell carcinoma: tentative delineation of an involved region using data for single nucleotide polymorphisms in two cohorts. *Carcinogenesis*. 2002;23:1149-1153.
18. Yin J, Rockenbauer E, Hedayati M, et al. Multiple single nucleotide polymorphisms on human chromosome 19q13.2-3 associate with risk of basal cell carcinoma. *Cancer Epidemiol Biomarkers Prev*. 2002;11:1449-1453.
19. Rockenbauer E, Bendixen MH, Bukowy Z, et al. Association of chromosome 19q13.2-3 with basal cell carcinoma: tentative delineation of an involved region using data for single nucleotide polymorphisms in two cohorts. *Carcinogenesis*. 2002;23:1149-1150.
20. Yanagitani N, Kohno T, Kim JG, et al. Identification of D19S246 as a novel lung adenocarcinoma susceptibility locus by genome survey with 10-cM resolution microsatellite markers. *Cancer Epidemiol Biomarkers Prev*. 2003;12:366-371.
21. Chen P, Wiencke J, Aldape K, et al. Association of an ERCC1 polymorphism with adult-onset glioma. *Cancer Epidemiol Biomarkers Prev*. 2000;9:843-847.
22. Caggana M, Kilgallen J, Conroy JM, et al. Associations between ERCC2 polymorphisms and gliomas. *Cancer Epidemiol Biomarkers Prev*. 2001;10:355-360.
23. Neville PJ, Conti DV, Krumroy LM, et al. Prostate cancer aggressiveness locus on chromosome segment 19q12-q13.1 identified by linkage and allelic imbalance studies. *Genes Chromosomes Cancer*. 2003;36:332-339.
24. Slager SL, Schaid DJ, Cunningham JM, et al. Confirmation of linkage of prostate cancer aggressiveness with chromosome 19q. *Am J Hum Genet*. 2003;72:759-762.
25. Taniguchi K, Yang P, Jett J, et al. Polymorphisms in the promoter region of the neutrophil elastase gene are associated with lung cancer development. *Clin Cancer Res*. 2002;8:1115-1120.
26. Yang P, Bamlet WR, Ebbert JO, Taylor WR, de Andrade M. Glutathione pathway genes and lung cancer risk in young and old age populations. *Carcinogenesis*. 2004;25:1935-1944.
27. Melton LJ III. History of the Rochester Epidemiology Project. *Mayo Clin Proc*. 1996;71:266-274.
28. Kleihues P, Louis DN, Scheithauer BW, et al. The WHO classification of tumors of the nervous system. *J Neuro-pathol Exp Neurol*. 2002;61:215-225.
29. Ingemarsson B, Sylvan A, Aldeborn A. Accurate allele frequency estimation of SNPs using Pryosequencing™ [abstract]. *Am J Hum Genet*. 2000;67:319(Suppl 2):1770.
30. Schaid DJ, Rowland CM, Tines DE, Jacobson RM, Poland GA. Score tests for association between traits and haplotypes when linkage phase is ambiguous. *Am J Hum Genet*. 2001;70:425-434.
31. Abecasis GR, Cookson WOC. GOLD-graphical overview of linkage disequilibrium. *Bioinformatics*. 2000;16:182-183.
32. Kaplan EL, Meier P. Nonparametric estimation from incomplete observations. *J Am Stat Assoc*. 1958;53:457-481.
33. Mantel N. Evaluation of survival data and two new rank order statistics arising in its consideration. *Cancer Chemother Rep*. 1966;50:163-170.
34. LeBlanc M, Crowley J. Relative risk trees for censored survival data. *Biometrics*. 1992;48:411-425.
35. Therneau TM, Atkinson EJ. An introduction to recursive partitioning using the RPART routines. Technical Report no. 61. Mayo Clinic, 1997.
36. de Andrade M, Barnholtz JS, Amos CI, Adatto P, Spencer C, Bondy M. Segregation analysis of cancer in families of glioma patients. *Genet Epidemiol*. 2001;20:258-270.
37. Paunu N, Lahermo P, Onkamo P, et al. A novel low-penetrance locus for familial glioma at 15q23-q26.3. *Cancer Res*. 2002;62:3798-3802.
38. Goode EL, Ulrich CM, Potter JD. Polymorphisms in DNA repair genes and associations with cancer risk. *Cancer Epidemiol Biomarkers Prev*. 2002;11:1513-1530.
39. Peters ES, Kelsey KT, Wiencke JK, et al. NAT2 and NQO1 polymorphisms are not associated with adult glioma. *Cancer Epidemiol Biomarkers Prev*. 2001;10:151-152.
40. Wolfe RM, Draghi N, Dai C, et al. p190RhoGAP can act to inhibit PDGF-induced gliomas in mice: a putative tumor suppressor encoded on human chromosome 19q13.3. *Genes Dev*. 2003;17:476-487.
41. Hong C, Bollen AW, Costello JF. The contribution of genetic and epigenetic mechanisms to gene silencing in oligodendrogliomas. *Cancer Res*. 2003;63:7600-7605.